

Republic of Iraq

Ministry of Higher Education and Scientific Research

University of Babylon

College of Materials Engineering

Department of Engineering of Polymers and Petrochemical Industries



Developed Polymer Nanocomposites for Bone Tissue Reparations Applications

A Thesis

Submitted to the Council College of Materials Engineering /
University of Babylon in Partial Fulfillment of the Requirements for the
Master Degree in Materials Engineering / Polymer.

Submitted by

Zahraa Kareem Mashi Hadi

B.Sc. Materials Engineering in 2019

Supervised by

Prof. Dr. Massar Najim Obaid

2022 A.D.

1444 H.A.

بِسْمِ اللَّهِ الرَّحْمَنِ الرَّحِيمِ
(ثُمَّ خَلَقْنَا النُّطْفَةَ عَلَاقَةً فَخَلَقْنَا
الْعَلَاقَةَ مُضْغَةً فَخَلَقْنَا الْمُضْغَةَ
عِظَامًا فَكَسَوْنَا الْعِظَامَ لَحْمًا ثُمَّ
أَنْشَأْنَاهُ خَلْقًا آخَرَ ۚ فَتَبَارَكَ اللَّهُ
أَحْسَنُ الْخَالِقِينَ)

صَدَقَ إِلَهُ الْعَظِيمِ

{الآية ١٤ من سورة المؤمنون}

Supervisors Certification

We certify that this thesis entitled (**Developed Polymer Nanocomposites for Bone Tissue Reparatons Applications**) was prepared by (**Zahraa Kareem Mashi**) under our supervision at Babylon University / College of Materials Engineering/Department of polymer and petrochemical industries, in Partial Fulfillment of the Requirements for the Award Master Degree of Science in Materials Engineering / Polymers Engineering.

Signature:

Name: **Prof. Dr.Massar Najim Obaid**

(Supervisor)

Date: / 12 / 2022

Dedication

To my supervisor Prof. Dr. Massar Najim Obaid ,

I appreciate you for the time you spent making the great effort for me, and I assure you that I will live up to your expectations

To my mother,

the source of giving and love, the reason of what I become today

To my father,

Thank you for your encouragement and support

To my dear sister Zainab,

who provided moral support

To all the members of my family

To everyone who gave me help and advice

ACKNOWLEDGEMENT

Praise, thank, and gratitude to the Singlehanded **ALLAH** who enabled and helped me to achieve this work.

I would like to express my deepest sense of gratitude to my supervisor, **Prof. Dr. Massar Najim Obaid**

I would like to thank Department of Polymer and all Teaching laboratories staff.

I would like to thank my Mom and Dad for their prayer and support for me.

Finally, I would like to thank everyone help me in any way in achieving the present work

Zahraa Kareem

2022

Abstract

Bone tissue defects affect millions of people worldwide. Although they are common treatment modalities, they are subjective allogeneic bone grafting that did not achieve the ideal therapeutic effect. This has prompted researchers to explore new ways of bone regeneration to overcome various clinical diseases such as bone infections, bone tumors, and bone loss by trauma. In recent decades, bone tissue engineering (BTE) has been developing. Scaffolding has been a pioneer in this field and highlights the design of BTE scaffolds according to bone biology and provides a rationale for the design of next-generation BTE scaffolds correspond to natural bone healing and regeneration. Therefore, researchers have been devoted to bone tissue engineering, and the interest has been focused on the development of composite materials for biomedical applications to address the above-mentioned problems. Though both synthetic and natural polymer composites have been used, natural polymers have replaced synthetic polymers due to the improved biocompatibility and non-toxic nature of their degradable products. Thus, a Biodegradable polymeric scaffold is used to promote tissues growth and remodeling as the new bone is formed, the temporary scaffold will degrade and be absorbed by the body.

In the current study, It improved the biological, morphological, and mechanical properties of chitosan (CS) by the synergetic effect of hydroxyapatite (HA) and zinc oxide (ZnO) nanoparticles. Thus, These were achieved in three steps, The first step included the used of nature polymer (Chitosan) and blended with synthetic polymer polyethylene glycol (PEG) as a plasticizer at different ratios (CS: PEG) (90:10, 80:20, 70:30)% respectively which prepared by casting method. Based on its flexibility, the (70:30) % blend is chosen and reinforced with three different weight fractions of hydroxyapatite nanoparticles (HA) (1, 2, and 3) w.t%. These nanocomposites were evaluated using Fourier Transform Infrared Spectroscopy (FTIR) , Differential Scanning Calorimetry (DSC), Field-Emission Scanning Electron Microscopy (FE-SEM), Atomic Force Microscopy (AFM), wettability, swelling, and degradation tests. It was found that the 3% w.t of HA was the best one due to its higher properties from mechanical, physical, and biological properties. The second step included three different percent of Nano zinc oxide (ZnO) (0.3,0.5 and 0.7) w.t % are added to the nanocomposite (CS/PEG/ 3% HA) to prepare hybrid nanocomposite and then described for morphological, mechanical, wettability, swelling, degradation, antibacterial activity, and cytotoxicity.

FTIR results for nanocomposite film indicated good interactions and created hydrogen bonding between the two polymers and also with nanoparticles of HA and ZnO. FE-SEM for (CS/PEG/HA), and (CS/PEG/HA/ZnO) showed a well-integrated blend of CS and PEG with good dispersion and embedding of nanoparticles (HA and ZnO) within the matrix. The results of the wettability test revealed to the addition of the PEG and nanoparticles of HA and ZnO to CS increased the wettability of CS. The contact angle decreased from 94° of neat CS to 38° at (CS/PEG/3%HA) and 26° at ((CS/PEG/3%HA/0.7% ZnO)) made the nature of the hybrid nanocomposite surface more hydrophilic which supports the biocompatibility and the ingrowth of living cells on it.

Based on the results of swelling studies, The swelling ratio of CS/PEG-blend has been increased in the culture medium, allowing nutrients to flow more easily through it while the swelling rate for nanocomposite was slightly decreased with increased percent of HA% and also, the hybrid nanocomposite slightly decrease and the rate of decrementation is (3) % with the addition 0.5 % ZnO due to nanoparticles are getting in between the polymer chains and occupying more spaces. Moreover, The Degradation rate of composite scaffolds increased with the addition of PEG, however, it slightly decreased with the addition of nanoparticles of (HA and ZnO w.t%) due to the presence of nanoparticles enhanced the stability of the scaffolds but remain in acceptance value.

The AFM results showed the surface roughness of CS increased by adding 30%PEG, But the surface roughness decreased with increased the percent of nanoparticles (HA and ZnO) however it stilled sharp surfaces which detected from the value of Kurtosis (S_{ku}) (S_{ku} is above 3,) that enhanced the adhesion of living cells. Another parameter of roughness is the surface bearing index (S_{bi}) which is a function of the mechanical properties and is increased with blend CS with PEG and reinforced with nanoparticles (HA, ZnO) w.t% that supported the results of the tensile test that referred to improve the mechanical properties of CS

The mechanical properties (Tensile strength and elastic of modulus) increased with increased percent of (HA% and ZnO%), The tensile strength increased by 84%, and the Elastic of modulus increased by (62) % with the addition of nanoparticles of 0.5% ZnO which support the bone defect regeneration. Furthermore, from the antibacterial test, the hybrid nanocomposite had antibacterial properties which were enhanced with increased weight fraction of HA and ZnO. MTT test indicates that the scaffold promotes cell viability (MG-63, HdFn) and proliferation in the scaffolds

Thus, this hybrid nanocomposite could serve as a potential candidate to be used for bone tissue engineering.

The third step was adding glutaraldehyde (0.02% GA) as a cross-linker to the best ratio of the polymeric blend (70%CS/30%PEG), nanocomposite reinforced withHA (CS/PEG/3%HA), and hybrid nanocomposite (CS/PEG/3%HA/0.5%ZnO) to find out the effect of the cross-linker on the properties of prepared nanocomposites.

Moreover, the polymeric blend cross-linked with GA showed higher wettability compared to nanocomposite and hybrid nanocomposite which demonstrates the contact angle increased due to the use of GA as a cross-linker. Moreover, the tensile strength, Elastic modulus and Elongation decrease with the addition of GA compare with non-cross-linked films due to bonds that form getting more compact with the addition of glutaraldehyde leading to reducing the mechanical properties.

Table of Contents

Abstract	I
Table of Content	III
List of Figures	VI
List of Tables	VIII
List of Symbols	IX
List of Abbreviations	X
Chapter One: Introduction	
1.1 General Introduction	1
1.2 Aims of the Study	3
1.3 Scope of current work	3
1.4 Thesis Layout	4
Chapter Two: Theoretical Part	
2.1 Introduction	5
2.2 Bone	5
2.2.1 The Structure of Bone	6
2.2.2 Bone – Mechanical Properties	8
2.2.3 Bone Defects and Fractures	10
2.3 Bone Tissue Engineering	11
2.4 Biomaterials for Bone Tissue Engineering	13
2.5 Bone Scaffold Concepts and Design	14
2.6 Types of Bone Scaffold	16
2.6.1 Ceramic-Based Scaffolds	17
2.6.2 Polymer-based scaffolds	20
2.6.2.1 Natural Polymers and Synthetic Polymers for Scaffolds	21
2.6.2.2 Biodegradable and Non-Biodegradable Polymer Scaffold for Tissue Engineering	22
2.6.3 Composite-based scaffolds	24
2.7 Scaffold features for bone regeneration	27
2.7.1 Biological requirements	27
2.7.3 Composition	28
2.7.4 Fabrication Techniques	30
2.8 Materials used in this research	35
2.8.2 Polyethylene glycol	37

2.8.3 Hydroxyapatite (HA)	38
2.8.3.1 Chemical, Physical Properties of Hydroxyapatite	39
2.8.3.2 Biological Properties of Hydroxyapatite	40
2.8.4 Nano Zinc oxide	41
2.8.4.1 Zinc oxide as antibacterial	42
2.8.5 Glutaraldehyde	43
2.9 Literatures Review	44-50
Chapter Three: Experimental Part	
3.1 Introduction	52
3.2 Materials	54
3.2.1 Chitosan	54
3.2.2 Polyethylene glycol	55
3.2.3 Glacial acetic acid	55
3.2.4 Nano Hydroxyapatite	56
3.2.5 Nano Zinc Oxide	56
3.2.5 Glutaraldehyde	56
3.3 Film formation	57
3.4 Tests	59
3.4.1 Infrared Fourier transform spectrometer (FTIR) test	60
3.4.2 Field Emission SEM (FESEM)	61
3.4.3 Contact Angle Test	61
3.4.4 Degree Of Swelling	62
3.4.5 In Vitro Degradation test:	62
3.4.6 Differential Scanning Calorimetry Test (DSC)	63
3.4.7 Anti-bacterial test	63
3.4.8 X-Ray Diffraction Analysis	64
3.4.9 Tensile test	64
3.4.10 Atomic Force Microscope (AFM) test	65
3.4.11 MTT assay	66
Chapter Four: Results & Discussion	
4.1 Introduction	69
4.2 Characteristics of Materials Used in This Study	70
4.2.1 FTIR Results of Neat Chitosan and Neat PEG	71
4.2.2 FTIR for Blend and Nano Composite	71
4.2.2.1 FTIR for Blend (CS/PEG) and Nanocomposite (CS/PEG)+HA w.t %	72

4.2.2.2 FTIR for Hybrid Nanocomposite (CS/PEG/3%HA) +ZnO w.t%	72
4.3 X-Ray Diffraction Test	74
4.3.1 X-Ray Diffraction of HA- Nanoparticles	75
4.3.2 The X-Ray Diffraction of ZnO- Nanoparticles	76
4-4 Wettability test	77
4.5 Degree of Swelling Test	79
4.6 DSC Analysis	80
4.7Tensile test	83
4.7.1 Effect Addition PEG and Different Percent of Nano-Hydroxyapatite on Tensile Strength and Elastic Modulus of CS	84
4.7.2 Effect Addition PEG and Different Percent of Nano-Hydroxyapatite on elongation of CS	85
4.7.3 Effect Addition Different Percent of Nano- ZnO on Tensile Strength and Elastic Modulus of Nanocomposite (CS/PEG/3%HA)	87
4.7.4 Effect Addition Different Percent of Nano- ZnO on Elongation of Nanocomposite (CS/PEG/3%HA)	88
4.8 Morphology Test	88
4.9 AFM Test	90
4.10 Degradation test	93
4.11 Antibacterial Test	95
4.11.1 Antibacterial for Neat Chitosan, CS/PEG Blend and Nanocomposite	96
4.11.2 Antibacterial for Hybrid Nanocomposite	97
4.12 MTT assay	97
4.3 Tests for Cross-linked Blend ,Nanocomposite ,Hybrid Nanocpmposite Film	100
4.3.1 FTIR for Cross-linked Blend ,Nanocomposite,Hybrid with Glutaraldehyde (GA)	100
4.3.2 Wettability for Cross-linked Blend, Nanocomposite with HA, Hybrid film	104
4.3.3 Tensile test for cross-linked with GA	106
4.3.3.1 Effect Addition GA on Tensile strength of Blend, Nanocomposite and Hybrid Nanocomposite	107
4.3.3.2 Effect Addition GA on Elastic Modulus of Blend, Nanocomposite and Hybrid Nanocomposite	107
4.3.3.3 Effect Addition of GA on Elongation of Blend ,Nanocomposite and Hybrid Nanocomposite	108
Chapter Five: Conclusions and Recommendations	

5.1 Conclusions	109
5.2 Recommendations	110
References	111

List of Figures

Figure No.	Subject	Page No.
Chapter one	Introduction	
1.1	Polymeric Biomaterial Application	2
Chapter tow	Theoretical Part and Literature Review	
2.1	The Human Skeleton and Bone Structure	6
2.2	Main Mineral and Protein Components of Bone	7
2.3	Bone Tissue Component	8
2.4	Various Types of Loading Subjected to Bone	16
2.5	Depicts the Distinctions between Normal and Osteoporotic Bones	10
2.6	History of Significant Achievements in the Development of Biomaterials for Bone-tissue Engineering	13
2.7	Bone Scaffolding Process	15
2.8	Polymeric scaffold	21
2.9	Classification of bio-degradable Polymer	24
2.10	Chemical Structure of Chitosan (CS)	27
2.11	a) Implantation PCL composite b) Implantation of PCL–TCP–Col scaffolds into the defects	28
2.12	Properties that an ideal scaffold should display for Bone Tissue Engineering applications	30
2.13	Various Porous Scaffold Fabrication Techniques	32
2.14	Chemical Structure of Chitosan	36
2.15	Chitosan Biomedical application	38
2.16	Chemical Structure of Polyethylene glycol (PEG)	39
2.17	Chemical Structure of HA	42
2.18	Chemical Structure of ZnO Nanoparticle	43
2.19	Chemical Structure of Glutaraldehyde	44
Chapter Three	Experimental part	
3.1	Flow Chart of Experimental Part	52-53

3.2	Schematic diagram of Film Preparation Process a) CS/PEG film b) Hybrid film	58
3.3	FTIR device	59
3.4	SEM device	59
3.5	Contact angle device	57
3.7	DSC device	62
3.8	X-Ray device	63
3.9	Tensile test device	64
3.10	AFM device	65
3.11	MTT assay procedure	66
Chapter Four	Result and discussion	
4.1	FTIR for Neat Chitosan	70
4.2	FTIR for Neat PEG	70
4.3	FTIR for Blend(CS/PEG) and (CS/PEG) + HA% Nano Composite	72
4.4	FTIR of Hybrid Nanocomposite	73
4.5	X-Ray Diffraction for HA-Nanoparticles	74
4.6	X-Ray Diffraction for ZnO-Nanoparticles	75
4.7	Swelling Rate for CS, (CS/PEG) Blend, Hybrid Nanocomposite in PBS	80
4.8	DSC for Melting Endotherm and in Nitrogen Atmosphere of Neat CS, PEG, and Blend CS/PEG	82
4.9	DSC for Melting Endotherm at Nitrogen Atmosphere of Blend CS/PEG and Nanocomposite as a Function of HA w.t%	82
4.10	DSC for Melting Endotherm at Nitrogen Atmosphere of Hybrid Nanocomposite as a Function of ZnO w.t%	83
4.11	Tensile Strength for CS, Blend (CS/PEG) and Nanocomposite as a Function of Different Percent of HA Nanoparticles	84
4.12	Elastic modulus for CS, Blend (CS/PEG) and Nanocomposite as a Function of Different Percent of HA Nanoparticle	85

4.13	Elongation for CS, Blend (CS/PEG) and Nanocomposite as a Function of Different Percent of HA Nanoparticle	86
4.14	Tensile Strength for Hybrid Nanocomposite as a Function of Different Percent of ZnO Nanoparticles	87
4.15	Elastic Modulus for Hybrid Nanocomposite as a Function of Different Percent of ZnO Nanoparticles	87
4.16	Elongation for Hybrid Nanocomposite as a Function of Different Percent of ZnO Nanoparticles	88
4.17	FE-SEM of Blend 0.7CS/0.3PEG at Magnification a- 5kx b- 50kx c- 100kx d- 200kx	89
4.18	FE-SEM of Nanocomposite CS/PEG/3% HA at Magnification a- 50kx b- 100kx c- 200kx	89
4.19	FE-SEM of Hybrid Nanocomposite CS/PEG/3%HA/0.5%ZnO at Magnification a- 30kx b- 50kx c- 100kx	90
4.20	3D AFM Image	92
4.21	Degradation rate for CS,CS/PEG Blend, nanocomposite with Ha w.t.% and Hybrid nanocomposite	94
4.22	Illustrated The Inhibition Area of Neat CS, CS/PEG Blend, and Polymer Blend Nano Composites for E. coli and Staphylococcus Colony.	95
4.23	Inhibition Diameter of Neat CS, CS/PEG Blend, and Nanocomposites as a Function of HA-Nanoparticles Content in Composite	96
4.24	Illustrated The Inhibition Area of Hybrid Nanocomposites for E. coli and Staphylococcus Colony.	97
4.25	Inhibition Diameter of Hybrid Nanocomposites as a Function of ZnO-Nanoparticles Content in Composite.	97
4.26	Inverted Cell viability of MG-63 ,HdFn cells grown	99
4.28	FTIR for Cross linked and Uncross linked CS/PEG Blend	101
4.29	FTIR for Cross linked and Uncross linked Nanocomposite CS/PEG /3%HA	102
4.30	FTIR for Cross-linked and Uncross-linked Hybrid Nanocomposite	103
4.31	Tensile Strength for Cross-linked Blend(CS/PEG),(CS/PEG(HA+ZnO w.t.))	104
4.32	Elongation for crosslinked Blend(CS/PEG),(CS/PEG(HA,ZnO w.t.))	107

4.33	Elongation for crosslinked Blend(CS/PEG),(CS/PEG(HA,ZnO w.t.))	108
------	--	-----

List of Tables

Table No.	Subject	page No.
Chapter tow	Theoretical Part and Literature Review	
2.1	Mechanical Properties of Spongy(Cancellous) Bone	9
2.2	Natural and Synthetic polymer	23
Chapter three	Experimental Part	
3.1	Chitosan properties	53
3.2	PEG properties	54
3.3	Glacial acetic acid properties	54
3.4	Nano Hydroxyapatite properties	55
3.5	Nano ZnO properties	55
3.6	Glutaraldehyde properties	56
3.7	Images for Solution and Dry film	57
Chapter four	Result and Discussion	
4.1	Show FTIR for Neat CS and PEG	71
4.2	FTI+R Bands for Hybrid Nanocomposite	73
4.3	XRD for Nano-HA	74
4.4	the XRD for ZnO-Nanoparticles	75
4.5	Contact angle image for Blend and Nanocomposite	78
4.6	Contact Angle for Hybrid Nanocomposite	79
4.7	DSC for Melting Endotherm at Nitrogen Atmosphere for CS/PEG,Nanocomposite film and Hybird nanocomposite film	83
4.8	Shows the Parameters of Roughness of AFM Test	93
4.9	FTIR for CS/PEG Blend, Nanocomposite, Hybrid Cross-linked with GA	100
4.10	Contact angle for CS/PEG blend, nanocomposite (HA,ZnO w.t.%) cross-linked with GA	102

4.11	Image of Contact angle for CS/PEG blend, nanocomposite (3%HA)film ,Hybrid film(3%HA,0.5%ZnO) cross-linked with GA	104
------	---	-----

List of English Symbols

Symbol	Title	Unit
Ca	Calcium	
Pa	Phosphate	
T _g	Glass Transition Temperature	°C
T _m	Melting Temperature	°C
ΔH	the apparent enthalpy of fusion per gram of composite	Jg ⁻¹
ΔH _o	the heat of fusion of a 100% crystalline PEG	Jg ⁻¹
R _a	Roughness average	nm
R _q	Root Mean square	nm
S _{Ku}	Kurtosis	
Sb _i	Surface bearing index	
X _c	percentage of crystallinity	%
W ₁	Mass of Specimen before Degradation	g
W ₂	Mass of Dry Specimen after Degradation	g

List of Abbreviations

Abbreviate	Meaning
ASTM	American Standard for Testing Materials
AFM	Atomic Force Microscopy
BMP	Bone Morphogenetic Protein
BTE	Bone Tissue Engineering
BHK21	Baby hamster kidney cell
CS	Chitosan
DSC	Differential Scanning Calorimetry
FDA	US Food and Drug Administration
FE-SEM	Field Emission-Scanning Electron Microscopy
FTIR	Fourier Transform Infrared

GA	Glutaraldehyde
HA	Hydroxyapatite
LED	Light-emitting diode
PLA	Poly(lactic acid)
PGA	Polyglycolic acid
PLGA	Poly(lactic-co-glycolic acid)
PEG	Polyethylene glycol
PHA	Polyhydroxyalkanoates
PBSA	Poly(butylene succinate-co-butylene adipate)
PBS	Phosphate buffer saline solution
RGD	arginine–glycine–aspartic acid
TE	Tissue Engineering
XRD	X-Ray Diffraction
ZnO	Zinc oxide

Chapter One

Chapter One

1.1 General Introduction

Bone play an important role in the body by supporting mechanical stress and maintaining ionic balance while trauma or diseases such as tumor and osteoporosis may lead to bone damage. When bones fail to repair themselves due to severe injury or disease, a replacement surgery can be performed to replace the bone defect with a bone substitute [1].

Fractures in Europe increased at an annual rate of 28%, With an additional economic burden of 25%, which attracted great attention from bone repair research. Current clinical approaches to treating large-sized bone defects .It mainly includes autologous bone grafts and allogeneic bone grafts. Autologous bone grafts are the gold standard for bone histology Repair and regeneration because autogenous bone is good bone conduction, bone conduction, which can form a balanced structure and ensure the mechanical strength at the site of the bone defect [2].

However, allogeneic bone transplantation remains has unavoidable defects such as neurovascular injury at the donor site and infections. To address weaknesses and limitations, allogeneic bone scaffolding widely used due to its accessibility. However, the allograft bone The implant has problems such as poor osseointegration and immunosuppression rejection, and transmission of blood diseases. faced with this situation, researchers began to explore artificial alternatives to natural grafts derived from bone [3].

Recent advances in BTE have allowed researchers to use multiple methods to combine cells, polymeric biomaterials and biological materials to create Synthetic tissue-forming agents to repair bone defects [4]. This is The method has the advantages of high modifiability, low risk of infection, it has excellent biocompatibility, and does not result in obvious complications [5].

A biomaterial is any material that is used to create devices that replace a part or function of the body in a relatively safe, reliable, cost-effective, and biologically acceptable manner. A wide range of devices and materials are used to treat disease or injury such as sutures, Medical implants, including heart valves, and grafts, artificial joints, hearing loss implants, dental implants and other common examples [4].

In the improvement field of tissue engineering the main hindrance is that not all materials at the same time had a good biocompatibility and suitable mechanical properties. Frequently, the materials had strong mechanical strength were bio inert, at the same time as the materials which had high bioactivity leaning to have weak mechanical strength with high porosity. Therefore, in order to assemble a high mechanical strength with bioactivity, hybrid and nanocomposite materials have been advanced [5].

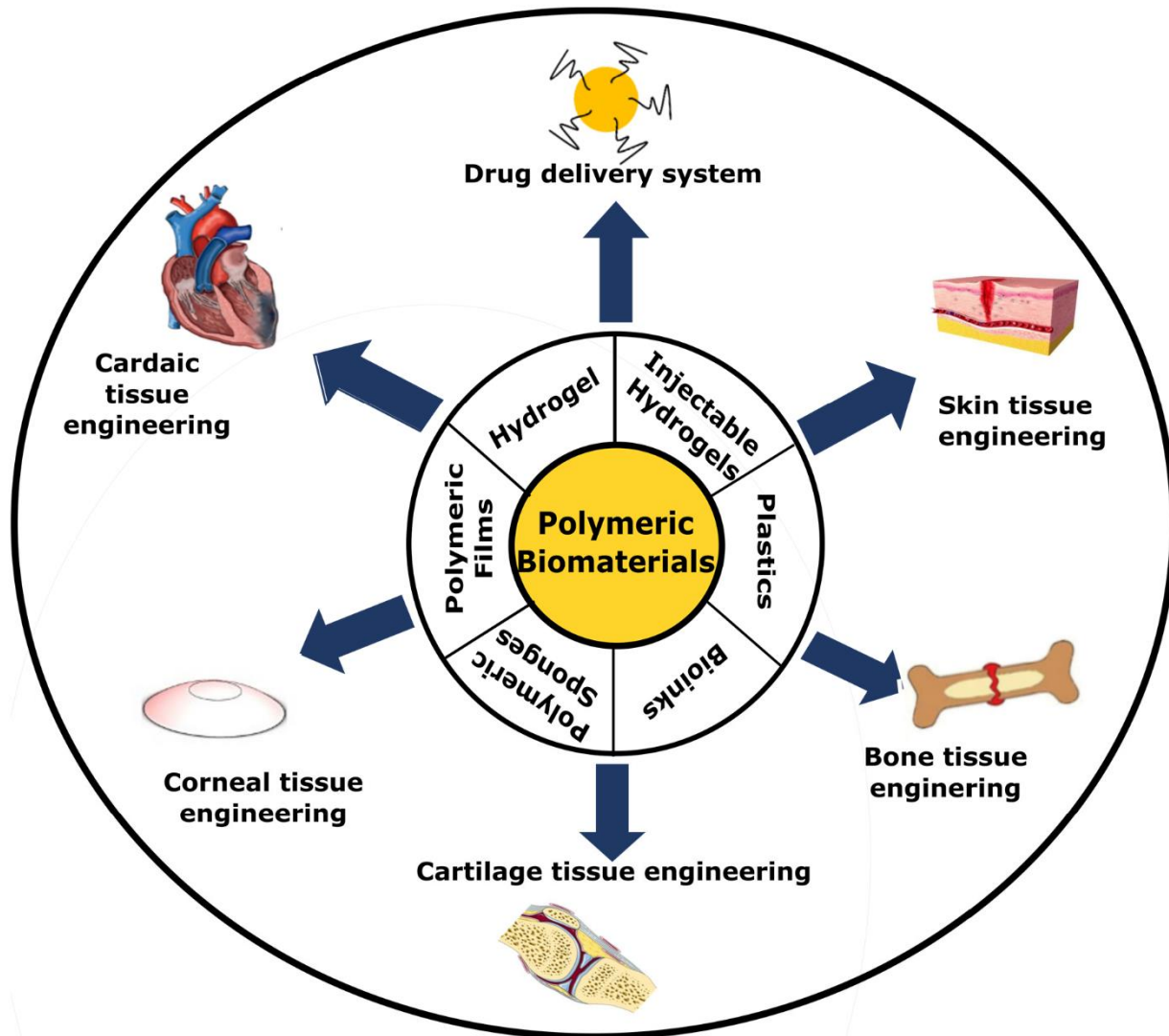


Figure (1-1) Polymeric Biomaterial Application [4].

In regenerative medicine approaches, or scaffolding Implants are often used to support regeneration bone tissue. Where its role is important in the treatment of

"segmental bone defects" where the size of the defect is so large that the natural healing process The gap cannot be closed without such support scaffolding. It is important in the treatment of large pieces' disadvantages is the reach of a biomaterials system that guarantees rapid and complete regeneration of functional bone tissue in segmental dysfunction [6].

The system may include not only vital substances the scaffold but also the potential drug delivery devices that come up with a scaffold and release of growth factors, or other biological factors that can stimulate and direct bone regeneration process. The stimulation process also includes the scaffold itself. It must be optimally designed not only to "support" the unhindered progression of the bone regeneration process including angiogenesis, but also to "stimulate" the process. In order to "support" the process of bone tissue regeneration, the porous scaffold must be made of a biocompatible material, be able to provide adequate mechanical support, and provide it a wide interconnected pore space for tissue invasion and cell nutrition and oxygen especially before completion Angiogenesis [6].

1.1 Aims of the study

develop a hybrid nanocomposite polymeric material to be used to compensate for damage to the bone by improving mechanical properties, structural, morphological and biological properties

1.2 Scope of the Current Work

To achieve the above aim, the following activities have been done:

1. Literature survey on the relating topics.
2. Samples of degradable system preparation includes:
 - a) Blend CS+X%PEG.
 - b) Nano composite CS+PEG+ X %NPs(HA).
 - c) Hybrid Nano composite CS+X%PEG +X%NPs(HA+ZnO).
 - d)Cross-linked sample (the best samples of Blend, Nanocomposite, Hybrid)
3. Sample mechanical tests, such as tensile strength; sample morphological characterization tests, such as SEM, XRD, FTIR, and AFM; degradation and swelling tests; and in vitro tests, such as (antibacterial activity and Cytoixity) to detect biocompatibility.

1.4 Thesis Layout

This thesis includes five chapters, as follows:

Chapter One: The general introduction and the aim of this study.

Chapter Two: This chapter will provide a detailed on general structure for bone and bone tissue, biomaterial that used in scaffold, natural and synthetic biodegradable polymer for bone tissue regeneration, fabrication techniques and considered literature review.

Chapter Three: describes the used materials, film preparation and test equipment.

Chapter Four: covers the results and discussion of the experimental work.

Chapter Five: Summarizes the work conclusions and gives some suggestions for future work.

Additionally, references as well as Arabic abstract are included.

Chapter Tow

Chapter Two

Theoretical Part and Literature Review

2.1 Introduction

The World Health Organization and the United Nations are calling the years 2000–2010 the bone and joint decade, because rheumatic diseases cause more pain and disability than any other disease group. It can be seen that about 650 people out of every 100,000 live with musculoskeletal diseases on average. They have found that osteoarthritis, rheumatoid arthritis, osteoporosis, and low back pain are the four major musculoskeletal conditions that cause the most trouble. Musculoskeletal system injuries, like sports injuries, are also included in this group. How bad these diseases are is shown by how much pain and disability they cause. Musculoskeletal conditions are the most common cause of long-term disability around the world, and their number has grown by 25% in the last 10 years [7].

Recently, biomedical approaches that have involved in repairing and restoring the functions of damaged tissues are categorized under tissue engineering field. Of all bone, tissue engineering is one of the promising fields that aim to create biological replacements that have the ability to restore, repair, maintain or improve tissue functions. The steps often start with manipulating and manufacturing of an appropriate porous scaffold suitable for bone tissue regeneration. However, scaffold modifications may be the best way to accelerate degradation, for instances, adding ceramic particles to increase the surface area that is available for hydrolysis to enhance functional repair of segmental defects [8].

2.2 Bone

Bones are living, dynamic tissues that undergo ongoing modification by the body. Their roles include strengthening the body's structure, protecting important organs, and enabling movement. In addition, they offer an environment for bone marrow, where the body generates blood cells and serves as a mineral storage region, notably for calcium. The skeleton accounts for around 15% of total body mass as shown in figure (2-1). Approximately 270 ,soft bones are present in newborn humans some merge as they mature.

Between 206 and 213 bones are present in adults. Some individuals have more or fewer ribs, vertebrae, fingers, and toe bones than others [9-10].

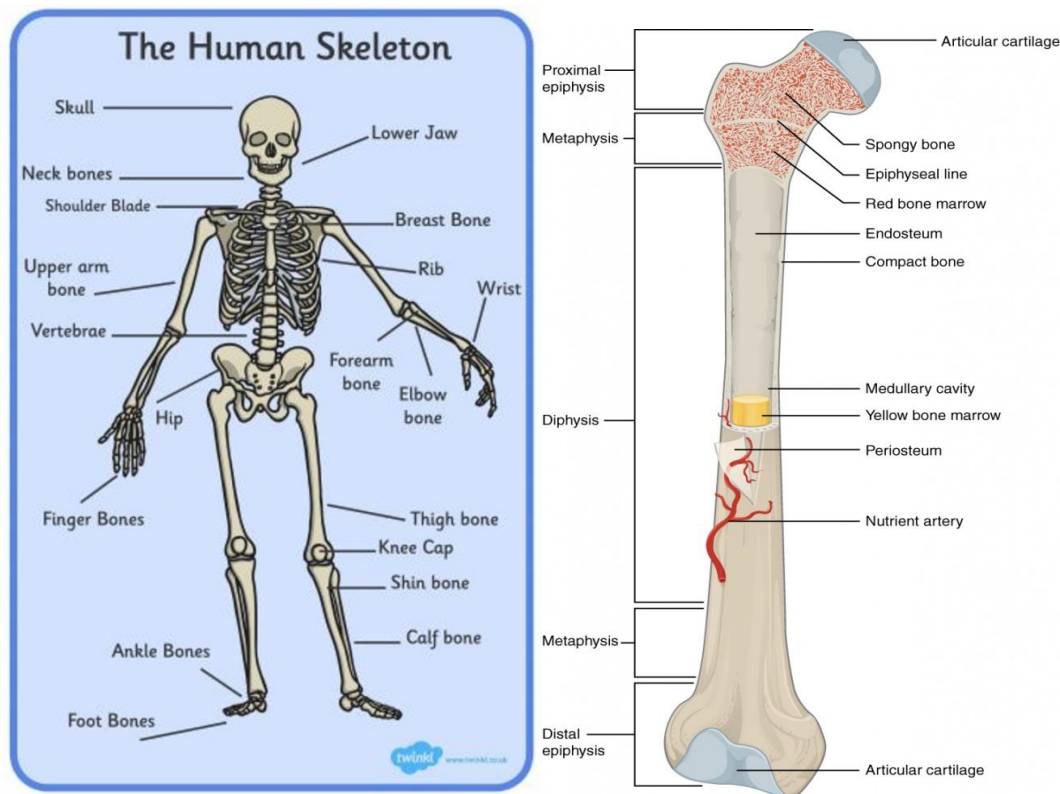


Figure (2-1): The Human Skeleton and Bone Structure[10].

2.2.1 The Structure of Bone

Bones are complex, living tissues that undergo ongoing remodeling. To be more precise, bone is a form of connective tissue that serves vital purposes in the body, including movement, support, and protection of internal organs and soft tissues. Also, bones store minerals like calcium and phosphate and are home to the bone marrow [11]. The number of people who experience age-related tissue loss or damage is rising as a result of increased life expectancy brought on by technical advancements and advances in medical knowledge. These occurrences result in a lower quality of life because they may make it more difficult for them to walk or possibly cause social and psychological issues. Finding new and improved solutions to this issue is therefore crucial [12]. Bone graft is the second most commonly transplanted tissue globally, 2.2 million bone grafting operations are performed each year [13].

Given the significance of this tissue, it is necessary to grasp its structural, molecular, and functional biology in order to recognize bone as a multicellular unit with a dynamic structure [11].

Bone has been studied for more than 300 years. With all new advances in technology have been deeper there understand the complex structure of this connective tissue. Even today, new discoveries are being made microstructure at the microscopic level and beyond. Bone is a natural composite material consisting primarily of a collagen-containing organic phase as a matrix and a mineral phase composed of hydroxyapatite as shown in Figure (2-2) [14].

This complex hierarchical structure of bones is directly related for their mechanical and biological functions, bones consist mostly of the protein collagen, which forms a soft framework. The mineral calcium phosphate hardens this framework, giving it strength. The bones contain 99% (of the body's calcium).

Bones have an internal structure similar to a honeycomb, which makes them rigid yet relatively light. Bones are composed of two type of tissue: Compact (cortical) bone is a hard outer layer that is dense, strong, and durable. It makes up around 80% of adult bone mass and forms the outer layer of bone. Cancellous (trabecular or spongy) bone makes up the remaining 20% of bone and consists of a network of trabeculae, or rod-like, structures. It is lighter, less dense, and more flexible than compact bone as clear in figure (2-3) [13-16].

Bones in the human body classified into five types: **i) long, ii) short, iii) flat, iv) irregular and v) sesamoid** [15].

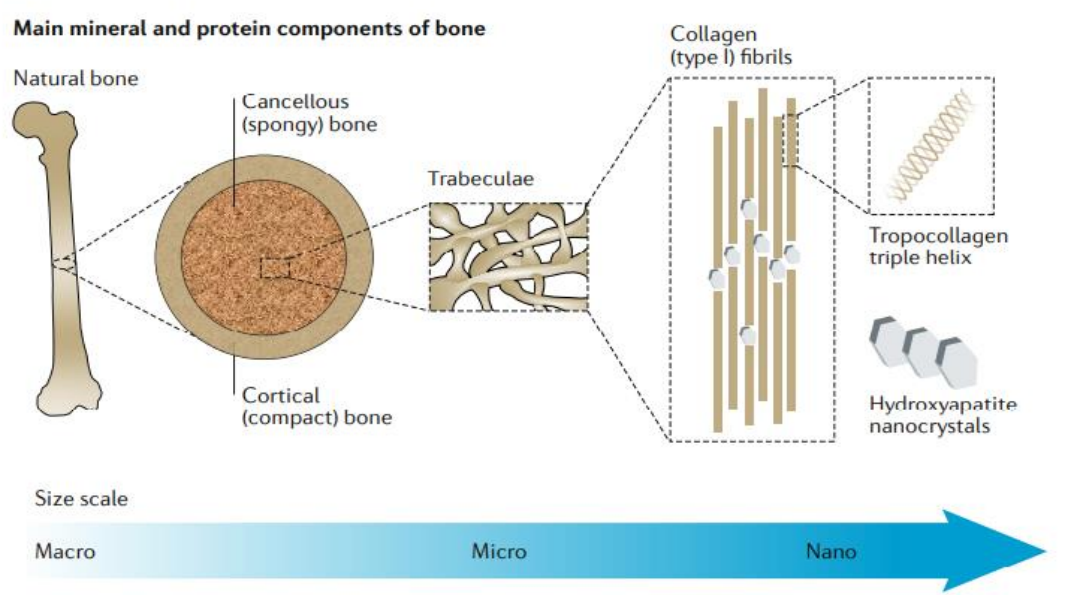


Figure (2-2): Main Mineral and Protein Components of Bone [16].

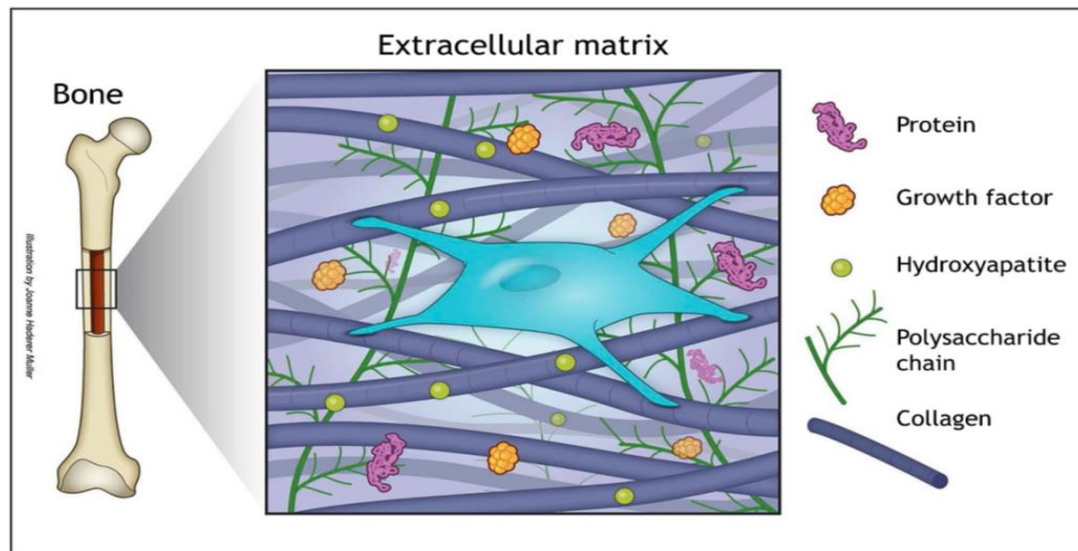


Figure (2-3): Bone Tissue Component [16].

2.2.2 Bone – Mechanical Properties

The multitude of mechanical, chemical and haematological functions makes bone a highly specialized form of connective tissue which undergoes subtle and continuous remodeling to conform to its functions. A good understanding of the structure and cellular components of bone is hence a prerequisite in bone tissue engineering [17].

The hardness of bone is attributed to the deposition of complex mineral substances, calcium hydroxyapatite composed of calcium, phosphorus, sodium, magnesium, fluoride and other ions in trace amounts, within the soft organic matrix of collagen, which is responsible for the toughness and visco-elasticity. Being a composite in several senses (porous, polymer-ceramic, lamellar, fibre-matrix), the mechanical properties of bone will therefore depend on each of these aspects of composition and structure [18].

The compact bone consists of closely packed Haversian systems with a central Haversian canal surrounded by concentric rings (lamellae) of matrix, whereas the cancellous bone has a loosely organized porous matrix where collagen fibrils form concentric lamellae. The mechanical properties of the cancellous bone, which have different structural features, are listed in Table (2-1). The mechanical properties of cancellous bone have been reported to be dependent on age, related to the changes in bone density. However, from a material science point of view it is important to also define the mechanical properties at the microstructural levels which listed in Table (2-2). Although the cancellous and cortical bone may be composed of similar materials, the maturation of the cortical bone material

may alter the mechanical properties at the microstructural level [17]. More often, a broad range of values are obtained while testing the mechanical properties. The composition of bone tissue, where the two-phase composite in which the mineral and collagen are bound in a complex manner, is more complicated than most engineering composites, a lot cannot yet be explained by commonly measured physical characteristics. The complex architecture and microstructural features of bone have hence made it an elusive structure in terms of mechanical characterization [17-18].

Table (2-1) Mechanical Properties of Spongy (Cancellous) Bone [18]

Property	Cancellous bone
Compressive strength (MPa)	2-12
Flexural, tensile strength (MPa)	10-20
Strain to failure (%)	5-7
Fracture toughness (MPam ^{1/2})	-
Young's modulus (GPa)	0.5-0.05

However, there are various forces acting on the bone during its working period. These forces or loads act in different directions and include body weight and forces induced by muscle contraction and ligament tension. A force is a vector. Thus, muscle forces can be resolved into two components: one force along the axis of the bone and other force perpendicular to the axis of the bone. The forces to which the bone is usually exposed include compression, tension, torsion, bending and shear stress. The resultant force acting on the bone can be found as shown in Figure (2-3) [19].

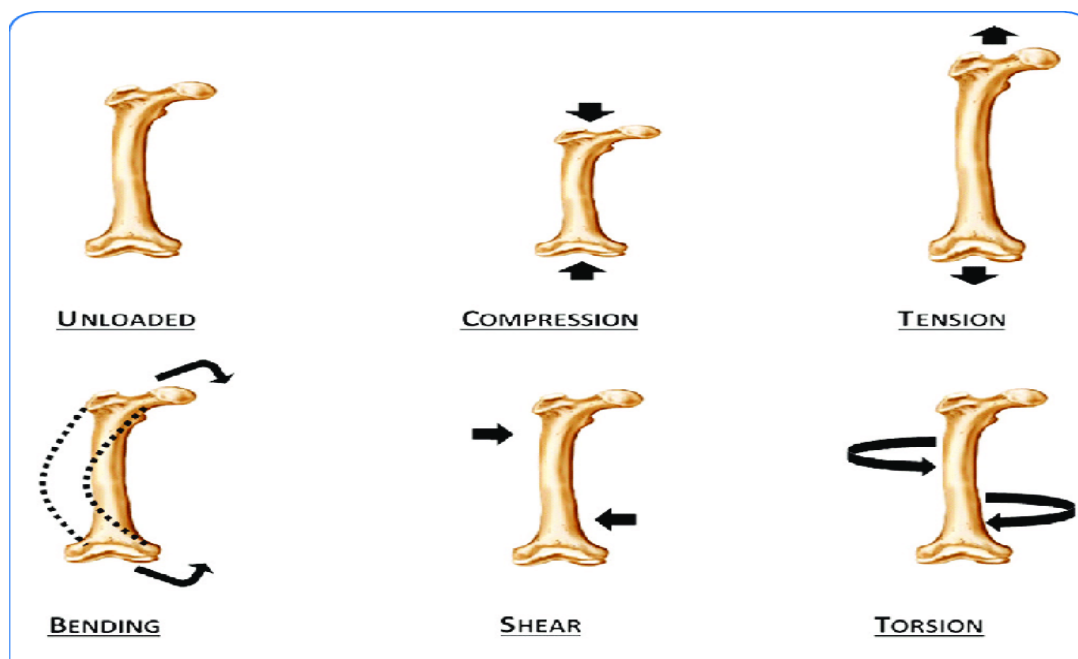


Figure (2-4): Various Types of Loading Subjected to Bone [19].

2.2.3 Bone Defects and Fractures

When a force is applied to a bone that is greater than the bone's capacity, it breaks or fractures. There are various forms of bone fractures (depending on the degree and direction of the impact, the particular bone involved, and the patient's age and its overall health) that can be caused by a variety of factors, including traumatic episodes such as sports injuries, automobile accidents, and falls, as well as illnesses such as osteoporosis and some types of cancer that predispose bones to fracture readily. Osteoporosis is largely acknowledged to be the most common bone disease in the world. It is a condition marked by diminished bone strength and density, as well as altered microgeometry and microscopic architecture (Figure 2-4), which increases the risk of fracture. Bone fracture repair is a regenerative process that mimics many of the biological events of embryonic skeletal development [20].

In case of long-bone injuries, a significant loss in bone tissue results when the natural healing potential of the bone falls far below the required regeneration. Hormonal imbalance caused as a result of aging is also a significant cause of bone loss. Studies showed that the hormone estrogen suppresses osteoclast activation and parathyroid hormone regulates bone remodeling [21].

Diabetes is yet another major disorder that contributes sizably to the loss of bone tissue. This occurs as a result of elevated levels of free radicals in the surrounding tissues causing an acidic environment, thereby activating the osteoclasts that resorb the bone matrix. Allografts and autografts are being employed for replacement of lost bone tissue. However,

these options pose major disadvantages such as lack of donors and immunogenic rejection of the graft by the host's body. To overcome these disadvantages, bone tissue engineering (BTE) is now being employed in the treatment of bone defect/loss [22].

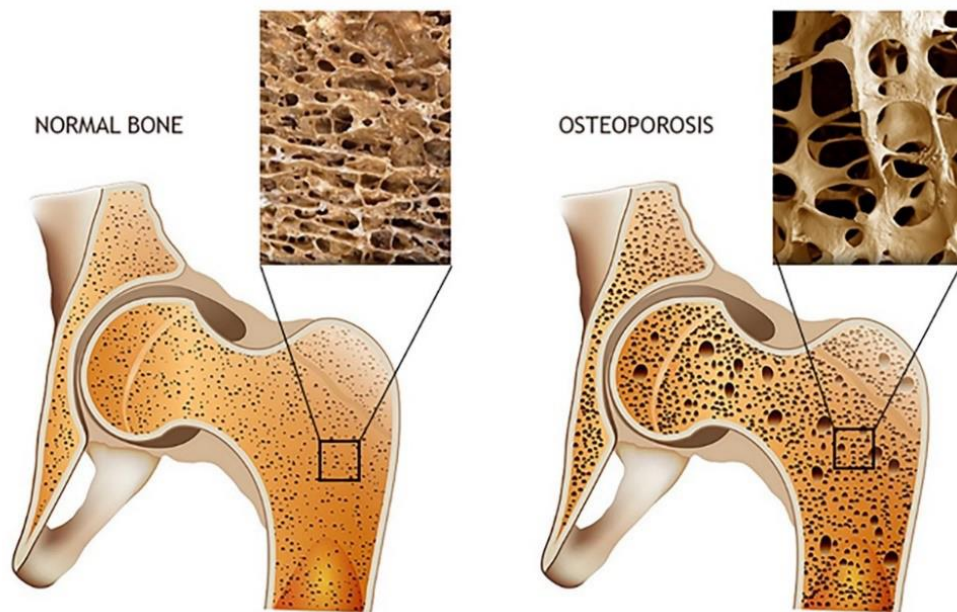


Figure (2-5) Depicts the Distinctions between Normal and Osteoporotic Bones [23].

A typical bone is a honeycomb-like structure with microscopic, densely packed voids inside. This trait enables bones to be both strong enough to provide bodily structure and light enough to allow movement. The loss of the honeycomb structure where the spaces become wider and the bone density is lost, indicates the decreased bone strength and increased fragility of an osteoporotic bone [23].

2.3 Bone Tissue Engineering

Tissue engineering (TE) is an interdisciplinary field of science where modern technologies have been developed. Tissue engineering represents an emerging interdisciplinary field that applies the principles of biological, chemical, and engineering sciences towards the goal of tissue regeneration. It is considered as a highly multidisciplinary field as it draws experts from various fields like clinical medicine, mechanical engineering, material science, genetics, and life sciences. Cell scaffold and growth factors are the three key materials for tissue engineering. Cells are often implanted or 'seeded' into an artificial structure capable of supporting three-dimensional tissue formation. These structures are basically called as scaffolds [24].

Tissue engineering is another application of nanotechnology to medicine. It helps to reproduce or replace damaged tissues by using suitable scaffolds made of nanomaterials and growth factors. Thus, tissue engineering is an area of nanotechnology where we focus on the construction of new tissues or organs for replacement. The developing scaffolds with the optimal characteristics, such as their strength, rate of degradation, porosity, and microstructure, as well as their shapes and sizes, are more readily and reproducibly controlled in polymeric scaffolds. Biological scaffolds are derived from human, animal tissues and synthetic scaffolds [25].

After an early empirical phase of biomaterials selection based on availability, design attempts were primarily focused on either achieving structural/mechanical performance or on rendering biomaterials inert and thus unrecognizable as foreign bodies by the immune system. Biomaterials used as implants in the form of sutures, bone plates, joint replacements, ligaments, vascular grafts, heart valves, intraocular lenses, dental implants, and medical devices like pacemakers, biosensors, and so forth [26].

Broadly speaking, the main demands on biomaterials for TE scaffolds are that they serve the bulk mechanical and structural requirements of the target tissue, and enable molecular interactions with cells that promote tissue healing. In the first respect, synthetic polymers are very attractive candidates as their material properties are typically more flexible than those of natural materials. It is reasonably straightforward to control the mechanical and chemical properties of synthetic polymers; they can be non-toxic, readily available and relatively inexpensive to produce, and in many cases can be processed under mild conditions that are compatible with cells. For these reasons, they have found widespread application in TE [26].

The initial attempts at bone regeneration included calcium phosphates and bioresorbable metals. This was followed by studies of bone formation in polymeric materials and the development of bioglass, the first material created by humans that could adhere to living tissues. After more research identified bioactive substances including proteins and peptides, bone tissue engineering became a distinct area of study. Later, scaffolds were created utilizing various material kinds and altered to cause particular biological reactions. Regulatory agencies have assessed goods incorporating different biomaterials during the development of biomaterials for use in bone-tissue engineering applications and have approved a number of commercial items

for use in clinics as shown in Figure (2-6). FDA, (US Food and Drug Administration); BMP, (bone morphogenetic protein).

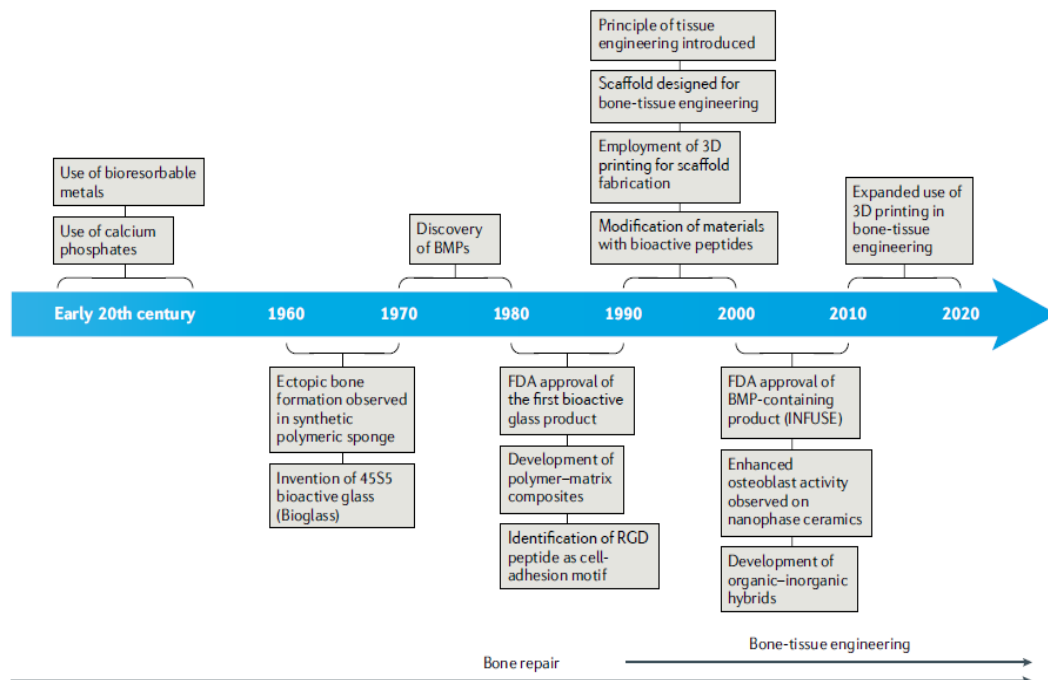


Figure (2-6): History of Significant Achievements in the Development of Biomaterials for Bone-tissue Engineering [27].

2.4 Biomaterials in Bone Tissue Engineering

Biomaterial is used to create devices that replace a body part or function in a safe, dependable, cost-effective, and physiologically acceptable way. The common equipment and materials used today in the treatment of illness and damage include sutures, needles, catheters, plates, dental fillings, etc. A biomaterial is now understood to be a synthetic material that is used to replace a portion of a living system or to perform a function in close proximity to live tissue [28].

Biomaterials play a critical role in this technology by acting as synthetic frameworks referred as scaffolds, matrices, or constructs. The state of the art in biomaterials design has continuously evolved over the past few decades. In recent years, there has been increasing importance on materials that could be used in biomedical areas. Biomaterials intended for biomedical applications target to develop artificial materials that can be

used to renovate or restore function of diseased or traumatized tissues in the human body and thus improve the quality of life [26].

Biomaterials can broadly be classified as: **1) Biological biomaterials; and 2) Synthetic biomaterials.** Biological materials can be further classified into soft tissue such as (Skin, Tendon, Pericardium and Cornea) and hard tissue types such as (Bone, Dentine and Cuticle). In the case of synthetic materials, it is further classified into: a) Metallic; b) Polymeric; c) Ceramic; and d) Composite biomaterials. The spectrum of materials available for use in medicine is made up of main classes, each with its own characteristic range of properties [28].

2.4.1 Classification of Natural Biomaterials

Natural biomaterials include substances which are natural in origin or certain chemical modifications of the substances to be used for development of scaffolds or any other implants. Based on the nature of their origin, natural biomaterials can be broadly classified under two main categories, protein based and polysaccharide based natural biomaterials [29].

2.4.1.1 Protein based natural biomaterials

Protein based biomaterials consists of certain recombinant proteins with amino acids as the major constituent. They involve certain mechanical and biological motifs derived from natural proteins that provide structural support, as well as guide to cell and tissue behavior. Silk, collagen and fibrin are the most explored protein based natural biomaterial [29]

a) Silk is a protein based polymer that is spun into fibers by some lepidoptera larvae such as silkworms, spider, scorpions, mites and flies. The most widely used silks are from the domesticated silkworm-*Bombyx mori*, and from spiders-*Nephila clavipes* and *Araneus diadematus*. Silk proteins have proved to be a promising biomaterial due to their unique combination of biocompatibility, biodegradability, self-assembly, mechanical stability and ability to tailor its structure and morphology. Silk protein in combination with some organic/in-organic solvents and water soluble gelatin materials have been extensively used for fabrication of 3D porous composite scaffolds for regeneration of bone, ligament and skin tissues [30].

b) Collagen is the most abundant protein in the body that provides strength and structural stability to tissues including skin, blood vessels, tendons, cartilage and bone. Apart from its favorable mechanical strength and cell-binding properties, collagen has good biocompatible and biodegradable features [31]. 89% of the organic matrix of bone is composed of Collagen-I combined with hydroxyapatite (HA). Collagen crosslinked with HA, chitosan fibres and mesenchymal stem cells have been used to generate porous scaffolds for bone tissue engineering. Cross-linked collagen based composite scaffolds have been found to exhibit minimal inflammatory and non-fibrotic cellular growth [32].

c) Fibrin is a protein based natural polymer produced from fibrinogen that supports numerous living tissues and wound healing by inducing angiogenesis and promoting cell attachment and proliferation. Due to the strong adhesive properties of fibrin to biological surfaces, it is often used as a biological sealant to fill sub-critical defects in bone with clot and generation of new bone tissues. Studies report addition of fibrin with cells seeded into biodegradable scaffolds which have poor cell adhesion properties for cell delivery and tissue engineering applications. Fibrin coating on PLLA based scaffold have been found to improve scaffold adhesion properties thereby promoting early tissue regeneration [33-34].

2.4.1.2 Polysaccharide based natural biomaterials

Natural polymers mimic the natural macromolecular environment of cells and display excellent biocompatibility with favorable mechanical properties and ability to be loaded with growth factors necessary for bone formation. Polysaccharide based biomaterials are natural polymers consisting of sugar monomers. Polysaccharides are derived from plant or animal sources and known to be highly bioactive with regards to tissue engineering applications. **Chitosan, alginate, hyaluronan and agarose** are some of the potential polysaccharide biomaterials used for developing scaffolds for tissue engineering.

a) Alginate or Alginic acids are biopolymers composed of non-repeating unbranched exopolysaccharides derived from certain seaweeds, bacteria and brown algae [35]. Alginate is highly hydrophilic, biocompatible, relatively economical and biodegradable under normal physiological conditions [36]. Owing to its unique physiological properties, composite scaffolds have been found successful with alginate combined with different

other biomaterials like HA [35], chitosan [37] and collagen for bone regeneration.

b) Hyaluronic acid or Hyaluronan is a polysaccharide which is a major glycosaminoglycan present in the extracellular matrix of tissues that promotes early inflammation critical for wound healing. Hyaluronan has unique visco-elastic properties with good biocompatibility, biodegradability and ability to maintain a hydrated environment conducive for cell infiltration, because of which they are widely used in synthesis of composite bone scaffolds. Hyaluronan -coated scaffolds were also prepared to enhance the bioactivity of scaffolds prepared from synthetic polymers such as PLA, PVP, PLGA, etc [38-39]. Therefore, Hyaluronic acid offers great potential as a scaffolding material.

c) Agarose is a marine algal polysaccharide obtained by isolation of red algae and seaweed. Agarose has the ability to form into hydrogel thereby providing a three dimensional environment for cell proliferation and retention of their phenotype. Moreover, the physical structure of the gels can be altered by varying the agarose concentration which results in desired pore sizes. Therefore, agarose based hydrogel scaffolds and composite scaffolds made of agarose combined with HA finds its applications in bone tissue engineering [40].

Other algae based polysaccharide: **Algae** is a rich source of plenty of different varieties of sulphated polysaccharides, which have antioxidant, anti-allergic, anti-inflammatory and anti-coagulant properties ideal for tissue engineering applications. Sulphated polysaccharides like Ulvan extracted from green algae *Ulva*, Carrageenans from red algae *Rhodophyceae* and Fucoidan from brown algae *Phaeophycophyta* have been extensively utilized for synthesis of composite bone scaffolds [41].

2.5 Bone Scaffold Concepts and Design

Scaffolds are fundamental to the concept and traditional approach of tissue engineering, because they provide an architectural framework into which cells can be seeded and then directed in vitro to produce the necessary tissues and organs before being transplanted in the patient. The biomaterial scaffolds can provide the first biomechanical profile till the seeded cells generate their own natural extracellular matrix. During the development, deposition, and organization of the newly created tissue

matrix, the original scaffold is either eliminated or metabolized, leaving behind a viable organ or tissue. that restores, maintains, or enhances tissue function [42].

As a result, it is critical that the scaffold create an environment that promotes cell proliferation and differentiation. According to technical criteria, the scaffold should be biocompatible, mechanically strong, and stable. These three features are heavily influenced by the material used and the design of the matrix's architecture. A wide range of material kinds and combinations have been shown to be viable choices for bone-tissue engineering applications. Multiple factors influence the material used in bone tissue engineering in general, including the intended fabrication and implementation methods [43]. Nonetheless, in view of the organic and inorganic composition of natural bone tissue, the most common biomaterials used for bone-tissue-engineering applications are polymers, bioceramics and composite materials as shown in Figure (2-7) the polymeric scaffold. Polymers are organic materials composed of long chains of atoms joined by covalent bonds. Both naturally derived and synthetic polymers are valuable material types for bone-tissue engineering. For instance, several bone-tissue-engineering products currently on [44].

Scaffolds can be made out of either natural polymers or synthetic polymers. Commonly used scaffolds include synthetic biodegradable. The advantage of synthetic scaffolds is the ability to control their properties (e.g. mechanical properties and degradation rate), while natural scaffolds are more efficient at fostering cell adherence. One of the benefits of using natural polymers is that they are naturally biocompatible and can be broken down by enzymes. Scaffolds can be made from a number of different polymers, including agarose, collagen, alginate, gelatin, hyaluronic acid, and chitosan [45].

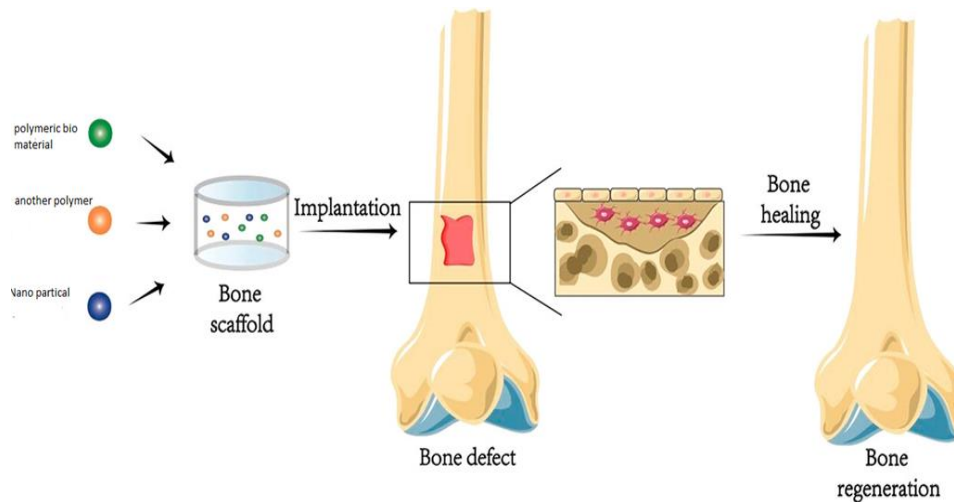


Figure (2-7) bone scaffolding process [51]

Scaffolds usually serve at least one of the following purposes [46]

1. Allow cell attachment and migration
2. Deliver and retain cells and biochemical factors
3. Enable diffusion of vital cell nutrients and expressed products
4. Exert certain mechanical and biological influences to modify the behavior of the cell phase
5. Biodegrade at a controllable rate that approximates the rate of tissue regeneration under the culture conditions of interest.

2.6 Types of Bone Scaffold

A nonviable substance used in a medical device with the intention of interacting with biological systems is another definition given for it. Numerous material kinds and combinations have shown to be excellent candidates for use in bone- and tissue-engineering applications. In general, a variety of parameters, such as the desired production and implementation methods, influence the material selection for bone-tissue engineering. However, taking both organic and inorganic into account Nonetheless, given the organic and inorganic makeup of natural bone tissue, polymers, bio ceramics, and composite materials are the most often employed biomaterials for bone-tissue engineering applications. Along with the biomaterials, cells and/or biologically active chemicals may be added in bone-tissue engineering material systems [47].

2.6.1 Ceramic-Based Scaffolds

The similarity to the biological environment, and hence the reduced likelihood of toxicity and inflammatory reactions, gives materials of natural origin a distinct advantage over synthetic materials. Natural materials are more rapidly degraded by enzymes, leading to eventual metabolization by physiological mechanisms. Apart from the disadvantages of natural variability in structure and incompatibility with various processing methods, naturally occurring biomaterials have provided novel solutions in the area of bone tissue engineering. Bioceramics are considered biocompatible, hard, brittle materials with relatively poor tensile properties but with excellent compressive strength, high resistance to wear, and with favorable, low frictional properties in articulation. Bio ceramics, natural or synthetic, used alone or with additional organic or polymeric materials, are amongst the most promising of all biomaterials for hard and soft tissue replacement applications. Natural bio ceramics, such as animal skeletons (hydroxyapatite or calcium carbonate), are known to be designed through natural optimization methods to physically support and maintain a range of tissues for variety of functions [48].

2.6.1.2 Coral

Naturally produced ceramic organic composites can combine good mechanical properties with an open porosity, which makes them candidates for use as delivery vehicles for cells. Due to their interconnected porous architecture, high compressive breaking stress good biocompatibility and resorb ability, corals used as scaffolds for bone tissue engineering [49].

2.6.1.3 Bio glass

One of the disadvantages of using synthetic calcium phosphate materials is their low mechanical strength, partly due to the porosity of the scaffold. Certain ceramic materials, such as HA, β -TCP and selected compositions of silicate and phosphate glasses and glass ceramics, for example the commercially available Bioglass, react with physiological fluids and form tenacious bonds to hard and soft tissues through cellular activity. These materials are therefore known as 'bioactive'. If biodegradability and bioactivity are to be combined in an optimized tissue-engineering scaffold, then the design of composite materials offers an exceptional opportunity.

Composites allow for the creation of bioresorbable and bioactive scaffolds with tailored physical and mechanical properties [48].

2.6.2 Polymer-based scaffolds

Polymers are organic compounds made up of long chains of atoms held together by covalent bonds [47]. Polymer-based scaffolds can be distinguished as synthetic or natural, and both have been widely used as biodegradable scaffolds in bone tissue engineering. These polymers and their composites are seen as the most promising candidates for bone regeneration, due to their biocompatibility and biodegradability. Beyond that, they are very versatile, which allow them to be easily tailored to accomplish specific and desired requirements, by manipulating them in terms of chemical composition and structures as shown in Figure (2-8) [46].

For example, some bone-tissue-engineering products are already on the market that include amino-acid sequences (particularly, the adhesion ligand arginine-glycine-aspartic acid (RGD) to which cells readily adhere. The enzymes and cells of the receiving patient are used to degrade and remodeling these materials, respectively, and they can be converted into microparticles or nanoparticles capable of transporting additional biological components [48]

Both natural and synthetic polymers have advantages and disadvantages. The former is bioactive, have biomimetic surfaces that contain particular properties that facilitate cell adhesion and cell differentiation, and they can trigger degradation and natural remodeling. However, their limitations include inappropriate immunogenic responses, microbial contamination, weak mechanical strength and they can undergo an uncontrollable degradation [50].

Polymer-based scaffolds can be classified according to its origins (Natural and Synthetic Polymers) or can be classified to (Biodegradable and Non-Biodegradable Polymers):

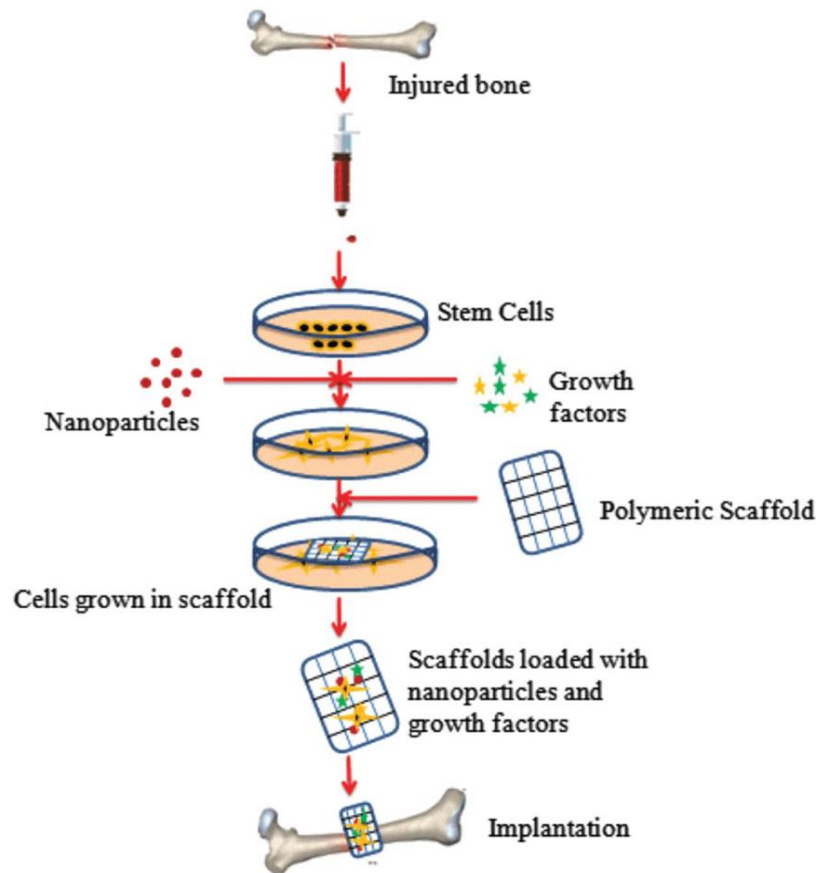


Figure (2-8): Polymeric scaffold [45]

2.6.2.1 Natural Polymers and Synthetic Polymers for Scaffolds

Polymers have been widely used as biomaterials for the fabrication of medical device and tissue-engineering scaffolds. In biomedical applications, the criteria for selecting the materials as biomaterials are based on their material chemistry, molecular weight, solubility, shape and structure, hydrophilicity/hydrophobicity, lubricity, surface energy, water absorption degradation, and erosion mechanism. Polymeric scaffolds are drawing a great attention due to their unique properties such as high surface-to-volume ratio, high porosity with very small pore size, biodegradation, and mechanical property. They offer distinct advantages of biocompatibility, versatility of chemistry, and the biological properties which are significant in the application of tissue engineering and organ substitution. Researchers have attempted to grow skin and cartilage, bone and cartilage, liver, heart valves and arteries, bladder, pancreas, nerves, corneas, and various other soft tissues [51].

Scaffold materials can be synthetic or biologic, degradable or nondegradable, depending on the intended use. The properties of polymers

depend on the composition, structure, and arrangement of their constituent macromolecules. It can be categorized into different types in terms of their structural, chemical, and biological characteristics, for example, ceramics, glasses, polymers, and so forth. Naturally occurring polymers, synthetic biodegradable, and synthetic nonbiodegradable polymers are the main types of polymers used as biomaterials [52].

Natural polymers can be considered as the first biodegradable biomaterials used clinically. Natural materials owing to the bioactive properties have better interactions with the cells which allow them to enhance the cells' performance in biological system. Natural polymers can be classified as proteins (silk, collagen, gelatin, fibrinogen, elastin, keratin, actin, and myosin), polysaccharides (cellulose, amylose, dextran, chitin, and glycosaminoglycans), or polynucleotides (DNA, RNA) as shown in Table (2-2) [53].

Synthetic biomaterial guidance provided by biomaterials may facilitate restoration of structure and function of damaged or diseased tissues. Synthetic polymers are highly useful in biomedical field since their properties (e.g., porosity, degradation time, and mechanical characteristics) can be tailored for specific applications in addition, they feature more reproducibility and long shelf life, when compared with natural polymers [48].

Synthetic polymers are often cheaper than biologic scaffolds; it can be produced in large uniform quantities and have a long shelf time. Many commercially available synthetic polymers show physicochemical and mechanical properties comparable to those of biological tissues. Synthetic polymers represent the largest group of biodegradable polymers, and they can be produced under controlled conditions. They exhibit, in general, predictable and reproducible mechanical and physical properties such as tensile strength, elastic modulus, and degradation rate. PLA, PGA, and PLGA copolymers are among the most commonly used synthetic polymers in tissue engineering. PHA belongs to a class of microbial polyesters and is being increasingly considered for applications in tissue engineering [54].

However, their biocompatibility and biodegradability are often insufficient, limiting their potential use in the clinical side. We can overcome these issues by blending synthetic and natural polymers or by

using composite materials that improve the scaffold properties and thereby allowing controlled degradation and improving the biocompatibility in tissue engineering applications. The combination of degradable polymers and inorganic bioactive particles represents the approach in terms of achievable mechanical and biological performance in hard tissue [55].

Table (2-2): Natural and Synthetic polymer [53]

Natural	Synthetic
Collagen	Poly(esters) Most common: poly (-hydroxy acids) such as poly(lactic acid) and poly(glycolic acid)
Component of the extra cellular matrix	Poly(-caprolactones)
Fibrin	Poly(anhydrides)
Gelatin	Poly(orthoesters)
Poly(hydroxybutyrate)	Polyethylene
Polysaccharides	Poly(methyl methacrylate)

2.6.2.2 Biodegradable and Non-Biodegradable Polymer Scaffold for Tissue Engineering

Biodegradable materials that could be broken down by nature either through hydrolytic mechanisms without the help of enzymes and/or enzymatic mechanism. Other terms like absorbable, erodible, and resorbable have also been used in the literature to indicate biodegradation [56].

The interests in biodegradable polymeric biomaterials for biomedical engineering use have increased dramatically during the past decade. This is because this class of biomaterials has two major advantages that non-biodegradable biomaterials do not have. First, they do not elicit permanent chronic foreign-body reactions due to the fact that they are gradually absorbed by the human body and do not permanently leave traces of residual in the implantation sites. Second, some of them have recently been found to be able to regenerate tissues [57].

Biodegradability is primarily dependent on hydrolyzable and oxidizable chemical structures chain coupling (ester > ether > amide > urethane), balance of hydrophobicity (hydrophilic is faster than hydrophobic), and molecular weights (lower is faster than higher). Physical properties such as crystallinity (amorphous is faster than crystalline), orientation, T_m or T_g , and morphological properties such as surface area or thickness affect the rate of degradation and hardness [58].

Applications of biodegradable polymers include implantable large devices, such as bone screws, bone plates, contraceptive reservoirs, stents, balloons and small implants such as sutures, staples, drug delivery vehicles, membranes, films, tissue engineering scaffolds and regenerate tissues [59].

There's two types of biodegradable polymer based on origin as shown in Figure (2-9).

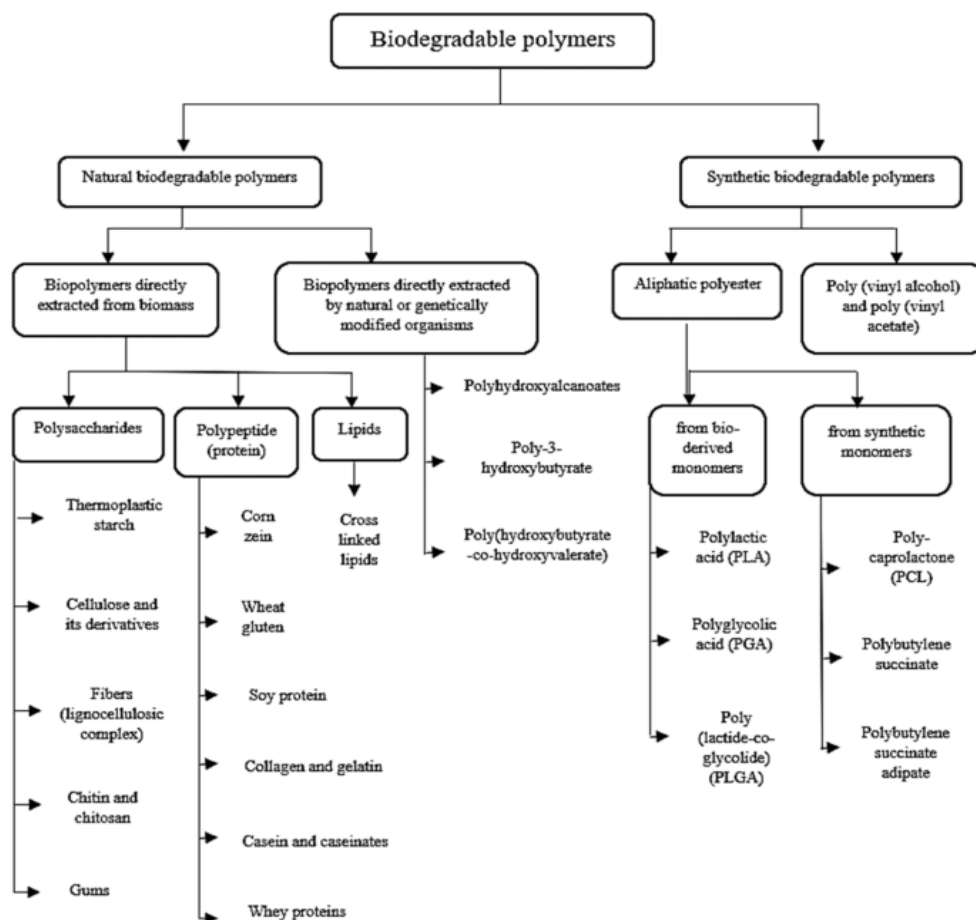


Figure (2-9): Classification of Bio-Degradable Polymer [58]

Biodegradation is one of the key factors to determine the time-dependent performance of scaffolds. It has been recognized that there are two categories of polymeric degradation. The first is named as ‘surface’ erosion, in which the degradation occurs mainly on the surface in contact with surrounding liquid, while the second is named ‘bulk’ degradation that takes place throughout the whole material domain [59-60]

Non-Biodegradable Polymer: The term describes polymers that do not break down to a natural, environmentally safe condition over time by biological processes. They consist of long chains of carbon and hydrogen atoms. These molecules form an interatomic type of bonding and is adamant meaning it is tough for microbes to break the bonds and digest them. Thus a long period is required to decompose them. These include Polyethylene (PE), ultra-high molecular weight polyethylene (UHMWPE), high-density polyethylene (HDPE), Polycarbonate(PC), Polyurethane Polymethylmethacrylat (PMMA) and poly (ether-ether-ketone) PEEK. The main application of non-biodegradable biopolymers includes implantable of bone cement [59].

2.6.3 Composite-based scaffolds

The combination of bioactive ceramics such as calcium phosphates with polymers improves the mechanical properties of scaffolds. However, a major challenge is to get a good chemical and physical binding between the polymer and the ceramic phase. A composite matrix also enhances the osteoconductive properties of the scaffold. Natural polymers in combination with hydroxyapatite [collagen–hydroxyapatite composites] (Liao et al., 2005) [61]; chitosan–hydroxyapatite (Li et al.,2005) [62].

Potential problems of biocompatibility in tissue engineering, by applying degradable, erodable and resorbable polymer scaffolds, may also be related to biodegradability and bioresorbability. Therefore, it is important that the 3D scaffold–cell construct is exposed at all times to sufficient quantities of neutral culture medium, especially during the period where the mass loss of the polymer matrix occurs it has been reported that a high amount of degradation by-products leads to the death of an entire cell culture. The incorporation of TCP, HA and basic salts into fast polymer matrix systems, such as PGA and PGA/PLA, produces a hybrid/composite material. In addition, the basic resorption products of HA or TCP would

buffer the acidic resorption by-products of the aliphatic polyester and may thereby help to avoid the formation of an unfavourable environment for the cells due to decreased pH. An interdisciplinary group at the National University of Singapore has evaluated and patented the parameters necessary to process PCL and PCL composites (PCL–HA, PCL/TCP, etc.) by Fused Deposition Modelling (FDM) (Hutmacher, 2000) as shown in Figure (2-10) [63].

These so-called first-generation scaffolds have been studied for more than 5 years in a clinical setting, have been commercialized (and have gained Federal Drug Administration (FDA) approval. Schantz et al. (2006)[64] used FDM-fabricated PCL scaffolds as burr hole plugs in a pilot study for cranioplasty as shown in Figure (2-10 b). The clinical outcome after 12 months was positive, with all patients tolerating the implants, no adverse side-effects reported and good cosmetic and functionally stable cranioplasty observed in all cases. The second-generation scaffolds produced by FDM for bone engineering are based on composites a have been evaluated *in vitro* and *in vivo* (Zhou et al.,2007) [65].





Figure (2-10): a) Implantation of PCL Composites Scaffold (PCL–HA, PCL–TCP, etc.) by FDM (Hutmacher, 2000) [63]. b) Implantation of PCL–TCP–Coll Scaffolds into the Defects [65].

2.7 Scaffold features for bone regeneration

Despite the increasing number of researches, discoveries and innovations, there is often a gap between research and clinical application/commercialization which is commonly termed the “Valley of Death” due to the large number of ventures that “die” between the scientific technology development and its actual commercialization.

One of the key factors to bridge this gap is the possibility to modulate scaffold characteristics so that specific biological, clinical, manufacturing, economic and regulatory prerequisites can be met. An ideal scaffold suitable for BTE applications should allow or improve cell viability, attachment, proliferation and homing, osteogenic differentiation, vascularization, host integration and, where necessary, load bearing.

Moreover, it should enable easy handling without extensive preparatory procedures in the operation theatre and allow minimally invasive implantation. It should be sterilizable by industrial techniques and reproducible on a large scale with cost effective processes. Finally, all its properties should meet the applicable Agency or competent authority requirements. Scaffold characteristics that can be modulated, improved or changed to make a scaffold suitable for BTE applications can be grouped into four main types: biological requirements, structural features, biomaterial composition, and types of fabrication process [66].

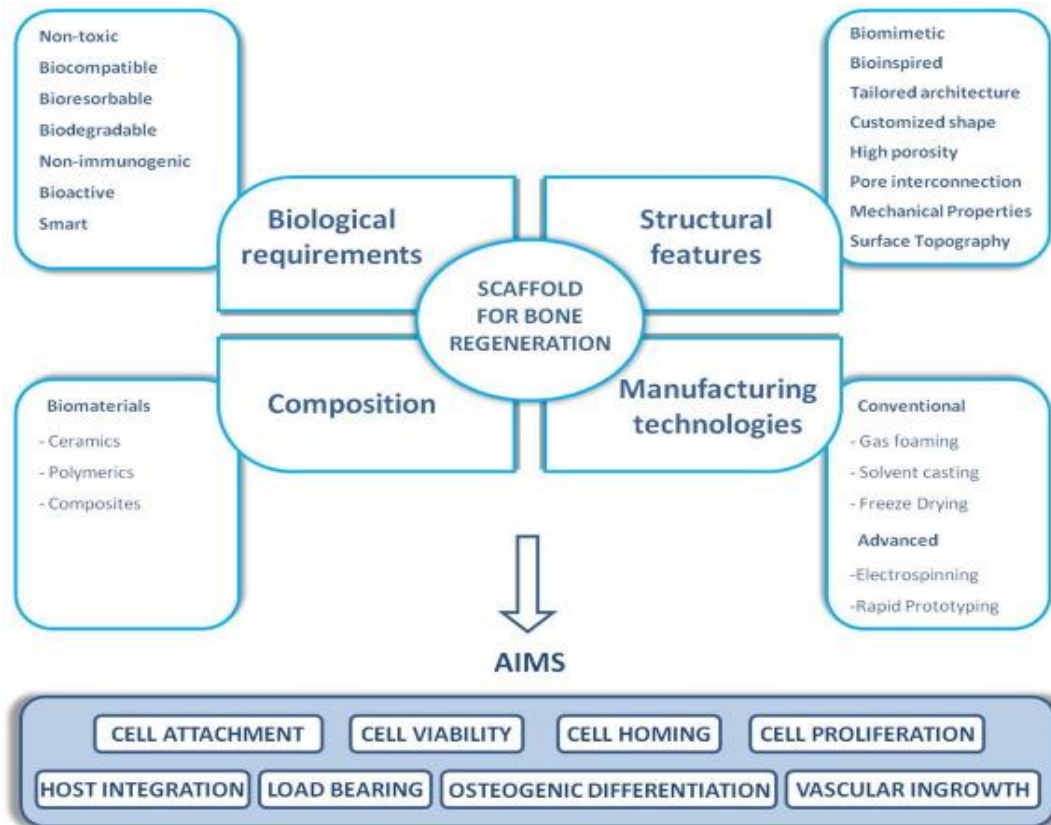


Figure (2-11): Properties that an ideal scaffold should display for Bone Tissue Engineering applications [67]

2.7.1 Biological requirements

First of all, a scaffold must be biocompatible and nontoxic. In particular, cells must adhere, function normally, proliferate, differentiate and produce new matrix [66]. Bioresorbable and biodegradable features are also important in order to allow tissue formation to occur in tandem with degradation. In addition, even degradation products should be non-toxic and able to be excreted by the body without or with negligible interference with other organs. Variation of mechanical strength during degradation is critical in load bearing implants, since the load should be gradually transferred to the regenerating tissue. Likewise, it is important for a scaffold to avoid the host immune response. Recently, the concept of immune-inert biomaterials has been implemented with that of immunomodulatory ones able to regulate the immune system [66].

Another key feature is scaffold bioactivity i.e. its ability to interact with the surrounding living tissues or organs. Conventional passive biomaterials display low or ineffective capacity to cross-talk with the

environment. Bioactive scaffolds are designed to promote proper cell migration or differentiation, tissue neoformation and integration in the host, avoiding undesirable processes such as scarring. More recently, attention has been directed towards “**osteoinductive or smart biomaterials**” that seem to hold great potential for bone tissue regeneration. In fact, they display the ability to instruct and respond to the surrounding in vivo environment to ectopically form bone. The biological mechanisms of this phenomenon have not been fully elucidated yet and two main hypotheses have been proposed [68].

2.7.2 Structural features

Recent advances in BTE have led to the development of novel biomaterials that allow to better mimic the 3D bone structure, in terms of mechanical properties as well as osteoinductive (Osteoinductive that is, able to stimulate cells to undergo phenotypic conversion to osteoprogenitor cell types capable of bone formation and the ability to attract immature cells to healing site to develop into bone forming cells.), osteoconductive (Osteoconduction means that bone grows on a surface. This phenomenon is regularly seen in the case of bone implants. Implant materials of low biocompatibility such as copper, silver and bone cement shows little or no osteoconduction.) and osteogenic features. In this perspective, the development of vascularized engineered scaffolds is one of the greatest challenges, since the lack of, or an inadequate vasculature, easily results in an ineffective osseointegration. Recently, nanomaterials have emerged as promising biomimetic candidates, since bone itself is a typical example of a nanocomposite. The commonly accepted definition of nanomaterials refers to materials with features between 1 and 100 nm, such as nanopatterns, nanofibers, nanotubes, nanopores, nanospheres and nanocomposites. They display excellent torsion and tensile modulus. In particular, nanoceramics appear to be promising to solve the brittleness of bioactive ceramics structure since bubbles and defects decrease with the size of crystalline grain into nanometer [69].

2.7.3 Composition

The majority of scaffolds that are currently used for BTE applications are polymers, bioactive ceramics (glasses) and hybrids (composites). Depending on composition and intended use, they may be injectable or

rigid. Polymers can be natural or synthetic. Naturally derived polymers, such as fibrin, hyaluronic acid, chitosan and collagen exhibit good biocompatibility, osteoconductivity and low immunogenicity [68]

However, disadvantages are represented by a degradation rate difficult to control and low mechanical stability. Synthetic polymers, like polyanhydride, polypropylene fumarate (PPF), Polycaprolactone (PCL), polyphosphazene, polylactic acid (PLA), polyether ether ketone (PEEK) and poly(glycolic acid) (PGA) display a controlled degradation rate, the possibility to design or tune bone mechanical properties and to fabricate complex shapes, cell attachment improvement (negatively-charged chemical groups) and the potential to deliver soluble molecules. Moreover, this type of polymers can be produced at reduced costs, in large uniform quantities and have a long shelf life. A critical drawback is its lower ability to interact with cells in comparison with natural polymers that, because of their intrinsic nature, show better bioactive properties [70].

2.7.4 Fabrication Techniques

The fabrication technique is the final criterion for designing scaffold for tissue engineering applications and all the criteria listed above depend on it. 3D fabrication available technologies can be divided into two main categories: **conventional and Rapid Prototyping (RP)** [71].

2.7.4.1 Freeze-drying Lyophilization or freeze-drying has evolved as a conventional fabrication technique for BTE. This technique has often been used for food products, biological materials, and drug delivery systems. The advantage of this technique is to fabricate a scaffold without the use of a high temperature or a separate leaching step and can produce a scaffold of various sizes and shape as required. It is a dehydration technique based on the removal of water/solvent from the frozen solution by sublimation under vacuum, at low pressure, leading to an anhydrous or almost anhydrous 3D-structure. The method consists of creating an emulsion by homogenization of a polymer solution (in an organic solvent) and water mixture, rapidly cooling the emulsion to lock in the liquid state structure, and removing the solvent and water by freeze-drying [72]. Over 90% of porosity can be expected from this technique with the pore size ranging from 20 to 200 μm . The pore size is mostly controlled by controlling the parameters such as rate of the freeze, pH, polymer concentration and

temperature. For this process, vacuum with high power is needed to come out with a scaffold which has high porosity and interconnectivity. Several natural biomolecules and synthetic polymers such as silk proteins, CS, Col, cellulose, Gel, PGA, PLLA, PLGA, PLGA/PPF blends, etc. are widely been used in the freeze-drying technique. But this technique is a slow and expensive method, since the cycle may be long, necessitating considerable energy consumption. Freeze-drying can be coupled with techniques such as solvent casting, particulate leaching, gas foaming, porogen leaching or by emulsion freeze-drying [72-73].

2.7.4.2 Solvent casting It is one of the easiest and inexpensive techniques for fabricating scaffold. It is completely based on the evaporation of the solvent present in the polymeric solution producing porous scaffolds. The scaffold can be prepared by two methods namely (i) The polymer solution is poured into the mold and allowed to rest for the evaporation of the solvent to obtain a porous 3D-scaffold. (ii) The mold is dipped into the polymeric solution and allowed to rest to obtain a polymeric membrane. Some of the solvents used for casting are methylene chloride, methanol, acetone, dichloromethane, chloroform, etc. The major drawback of this technique is that the solvent used may be toxic and might retain some toxicity thus they are either combined with freeze-drying or particulate leaching technique for better results [74-75].

2.7.4.3 Particulate leaching This method involves mixing water-soluble salt (e.g., sodium chloride, sodium citrate), sugar particles or a porogen into a biodegradable polymer solution. The polymeric solution is then cast into the mold of the desired shape. After the solvent is removed by lyophilization, the salt particles/porogen is leached out to obtain a porous structure. This method is highly advantageous because size of the pores can be controlled by salt/polymer ratio and also the size of the particle added. However, the pore shape is limited to the crystal shape of the salt. Another drawback is the difficulty in removing soluble salt/particles from the interior of a polymer matrix which makes it hard to fabricate very thick scaffolds. In fact, most of the porous materials prepared by solvent casting and particulate leaching method are restricted by thickness [76-77].

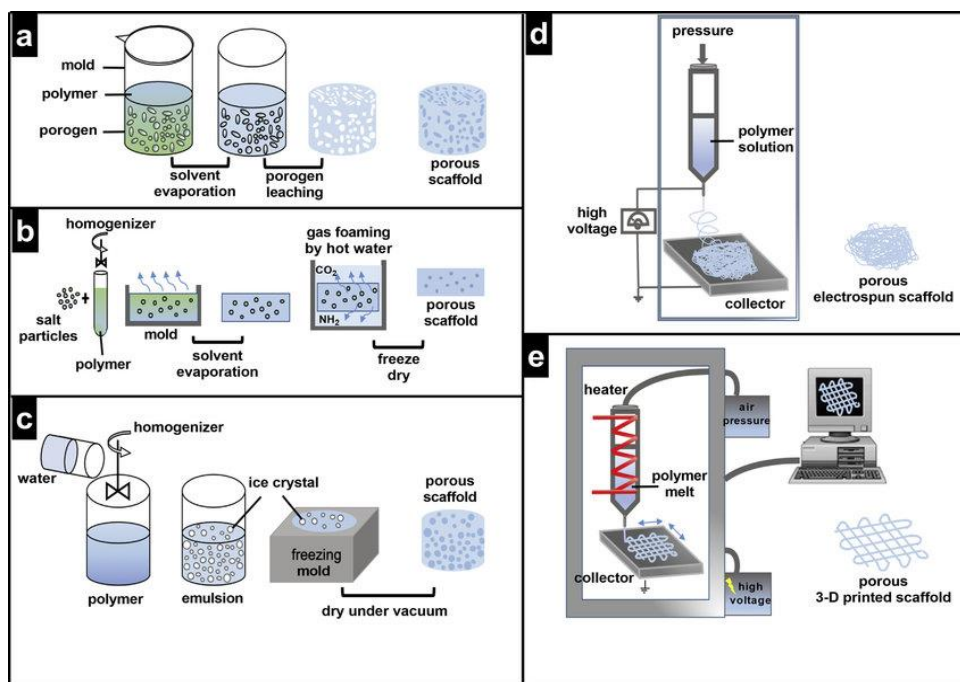


Figure (2-14) various porous scaffold fabrication techniques. (a) Porogen leaching, (b) Gas foaming, (c) Freeze-drying, (d) Solution electrospinning, (e) Melt electrowriting and 3-D printing.

2.7.4.4 Gas foaming process can be used to fabricate highly porous polymer foams without the use of any solvents. In this method, an inert gas usually carbon dioxide (CO₂) is used as an agent for the formation of polymer foam. Solid polymer disks are exposed to high-pressure gas which leads to the nucleation and growth of gas bubbles in the material. They are then freeze-dried to get a 3D-structure with a pore size of around 100 μm and porosity up to 93%. The disadvantage of this method is that it mostly yields a closed-pore structure, with less interconnectivity. This can further be combined with other methods to get a better scaffold architecture [77].

2.7.4.5 Thermally induced phase separation Thermally induced phase separation technique is based on changes in thermal energy to induce separation of a homogeneous polymer solution into a multi-phase system domain by a quench route. Firstly, the polymer is dissolved in a solvent (phenol or naphthalene) at a high temperature, followed by dispersion of biologically active molecule in these solutions. On declining the temperature, the separation is induced, the homogeneous solution separates into a polymer-rich phase and solvent-rich phase either by solid-liquid demixing or liquid-liquid phase separation mechanism. Then the solvent is removed by extraction, evaporation, and sublimation to give porous scaffold with bioactive molecules integrated into to that structure. The

factors that affect the pore morphology of the scaffold are the type of polymer, solvent, the concentration of the polymer solution and phase separation temperature. The advantage of this technique is that it can easily combine with other fabrication technology and have good mechanical properties to design three-dimensional structures with controlled pore morphology [78].

2.7.4.6 Sol-Gel Method is based on the inorganic polymerization of metal alkoxides. A sol is formed by the addition of a surfactant, followed by condensation and gelation reactions. This process allows the fabrication of ceramic or glass materials in the form of ultra-fine or spherical shape powders, thin-film coatings, ceramic fibers, microporous inorganic membranes, monolithic ceramics and glasses and highly porous aerogel materials. To overcome the disadvantage posed by the fact that these scaffolds do not possess high mechanical strength, researcher developed a modified sol-gel process to fabricate sodiumoxide-containing BG ceramics. The structures showed improved mechanical strength, without losing biodegradability [79].

2.7.4.7 Electrospinning Electrospinning technique is a unique approach where the scaffold is prepared using electrostatic forces to produce fine fibers from polymer solutions or melts, and the fibers thus produced have a thickness ranging from nanometer to micrometer and a larger surface area than those obtained from conventional spinning processes. More than 200 different polymers and composites are used in the electrospinning such as silk fibroin, chitosan, gelatin, collagen, etc. and many synthetic polymers (PCL, PVP, PLLA, etc.) are also used in this technique. A high DC voltage in the range of 10-15 kV is necessary to generate the electrospun fibers, and it is conducted at room temperature with atmospheric conditions. Presently, there are two standard electrospinning setups, vertical and horizontal. Chiefly, an electrospinning set up consists of three major components: a high voltage power supply, a spinneret (e.g., a pipette tip) and a grounded collecting plate (usually a metal screen, plate, or rotating mandrel). Most of the polymers are dissolved in a solvent to form a homogeneous solution. Then the polymer fluid is introduced into the capillary tube and in the presence of a high voltage source, a certain polarity is introduced into the polymer solution or melt, which is then accelerated towards a collector of opposite polarity at a constant flow rate.

However, some polymers may emit an unpleasant or even harmful smell, so the processes should be conducted within chambers having a ventilation system [80].

2.7.4.8 3D-printing: The 3DP technique has been primarily used to create engineering prototypes, but recent advances have enabled the fabrication of printers able to make products comparable with traditionally manufactured items. To date, a large number of files containing information about the object to be printed, such as color, texture, layer thickness, etc., advantages of this printing technology in terms of costs, time and set up involve not only the possibility to enable mass customization of goods on a large scale, but also competitiveness for smaller production runs. Moreover, a high degree of customization is allowed since the cost of the first item is the same as the last [81-82].

Invented at the Massachusetts Institute of Technology, 3DP techniques able to ink-jet print a liquid binder solution onto a powdered at room temperature conditions. The process begins with a binder jetting machine distributing a layer of powder onto a platform. Liquid droplets of a bonding agent are deposited onto the powder layer through inkjet print heads, bonding the particles together. The platform is then lowered and a next layer of powder is laid out on top. By repeating the process of laying out powder and bonding, the parts are built up in the powder bed. Removal of the unbound powder reveals the fabricated part. The 3DP process can be direct or indirect by printing the actual part or a mold, respectively [82].

Other advantages of 3DP are represented by the feasibility to fabricate internal channels and by the multi- “color” printing option that allows to simultaneously arrange multiple types of cells, deposit multiple ECM materials, and exert controvert bioactive agents. Drawbacks are the difficulty in removing unbound powder from small or curved channels and the use of print head that can make finer features but are more prone to clogging [82].

2.8 Materials for Bone Regeneration

2.8.1 Chitosan (CS)

Chitosan, a naturally polymer, is a highly very adaptable biomaterial. Unlike natural polymers made from expensive mammalian proteins,

chitosan causes a small amount of encapsulation and a foreign-body reaction. It is derived from marine sources, a natural and renewable source. Chitin and Chitosan is the second most abundant long chain amino polysaccharide polymer occurring in nature after cellulose and was first identified in mushrooms. Although chitin provides strength to the cell wall of some fungi, it is present in the cuticles or exoskeletons of insects, arthropods, mollusks and is mainly isolated from crustaceans, including crab, lobster, crayfish, king crab, and shrimp for biomedical applications, chitin in the solid-state can be converted Mar[83].

Chitin requires deacetylation in order to acquire CS. When at least 60% of the chitin is deacetylates, CS is produced. Homopolymeric CS consists of randomly placed N-acetyl-D-glucosamine and D-glucosamine repeating units linked by β -(1-4) glycoside bonds. Physicochemical characteristics of CS, including its biodegradability, viscosity, solubility, and crystallinity, are inversely influenced by the molecular mass and degree of deacetylation. CS is biodegradable and acts as a powerful agent in wound healing by controlling inflammatory components [83-84].

The biocompatible and non-toxic nature Because of how closely CS matches glycosaminoglycans (GAGs) in terms of both structure and composition CS scaffolds have been shown to Cell adhesion and growth, vascularization, calcification, and osteogenic transformation for bone rejuvenation [85].

The empirical functionalization of CS was discovered to increase its bioactivity, with a significant role in BTE. Because of its wide availability, simplicity of processing, and low price, it is a useful biopolymer for scaffold fabrication and design in BTE. Reactive amine groups participate in electrolytic conduction, which is altered by protonation and deprotonation. This modulation of CS as a polycationic polymer is attributed to interactions with lipids, proteins, DNA, or negative charge synthetic polymers [86].

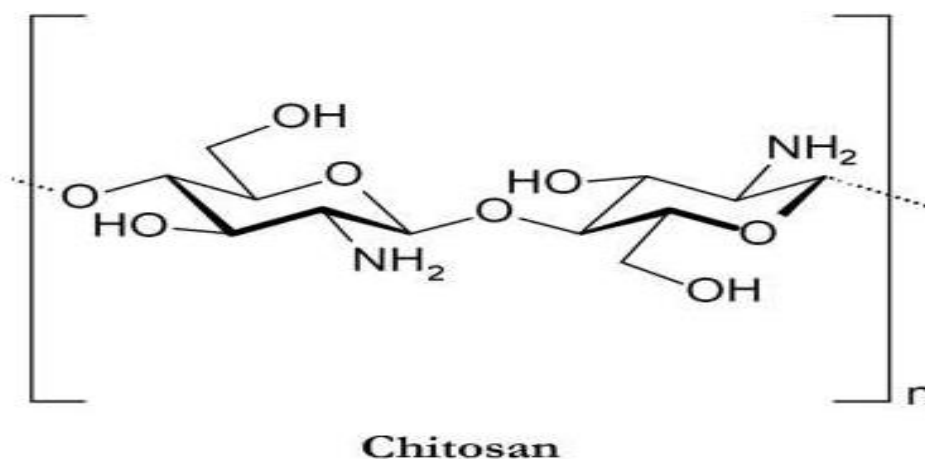


Figure (2-15) Chemical Structure of Chitosan (CS) [83]

As a natural multifunctional polysaccharide, chitosan has been widely studied for biomedical, surgical, and tissue engineering and pharmaceutical application, thanks to its biocompatibility, biodegradability, and muco-adhesiveness. Chitosan is reported to be increasingly used in the United States as an over-the-counter cholesterol-lowering agent. Positively-charged deacetylated chitosan could bind negatively charged molecules, such as fatty acids, lipids, and bile acids, in the intestinal tract, excreting these molecules from the body. Chitosan is thus considered as a promising candidate for obesity and hypercholesterolemia treatment. Chitosan could be also used for wastewater treatment and beverage clarification because of its good chelating or binding capacity of protonable amino groups for various species, such as metal ions. However, the most important medical and pharmaceutical applications of chitosan are drug delivery, wound dressings, and biocomposite scaffolds for tissue engineering [86].

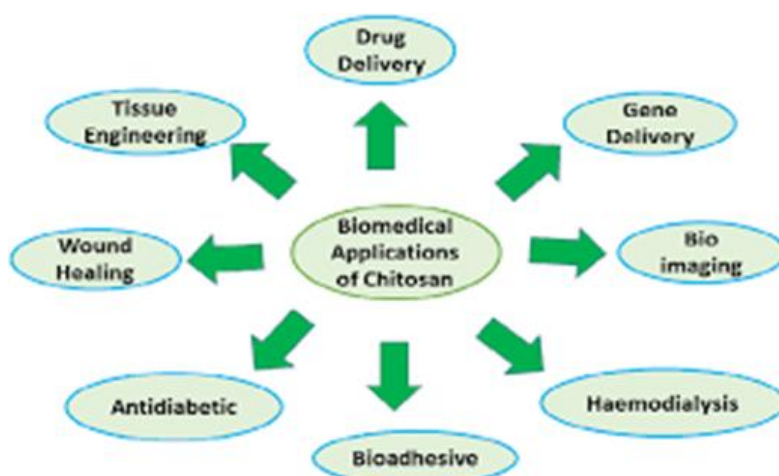


Figure (2-16) Chitosan Biomedical application [86]

2.8.2 Polyethylene glycol

polyethylene glycol (PEG) is one of the widely used polymer applied for medical implants. PEG is commonly used in polymer blend as it has several advantages such as its wide range of molecular weights, excellent solubility in water, low toxicity, chain flexibility, and biocompatibility. However, with the overwhelming applications of PEG, the shortcomings of PEG have also gradually emerged. It's reported that PEG can trigger complement activation and cause subsequent hyper sensitivity reactions [87].

Furthermore, anti-PEG antibodies have occurred in some clinical cases and led to the accelerated blood clearance for PEG or PEGylated products with repeated injection (so called ABC phenomenon) [87-88].

In addition, chronic use of PEG with high molecular can lead to accumulation in tissues due to its non-biodegradability, and whether it has adverse effect on the tissues is uncertain. Thus, development of alternative biocompatible polymers is urgently needed. Thus far, the molecular mechanisms underlying the biocompatibility of biomedical polymers remain unclear understanding of which will be of fundamental importance for developing novel safer biomedical polymeric materials [89].

Numerous studies on the biocompatibility of PEG focus on the pathological effects and pharmacokinetics of PEG, which mostly traced back to the middle of last century (from the 1950s to 1970s), and fail to define the molecular mechanism underlying its biocompatibility. With the rapid development of biology knowledge and techniques, there is an immediate need to update the researches by fundamental systemic evaluation on the interactions between PEG with biological system particularly at the cellular or molecular levels to clarify the molecular mechanism inherent to its excellent performance [89].

Indeed, the investigations that systematically study the interactions between polymers and cells are just beginning and urgently needed for the design and development of therapeutic polymeric materials [103]. Despite of the large number of studies involving PEG biocompatibility, the molecular mechanism underlying its good biocompatibility remains unclear. Moreover, few studies have been taken into consideration for the interaction between PEG and cells from the perspective of systems

biology. It's widely accepted that the low nonspecific interactions between PEG and body, namely stealth effect, largely contribute to the excellent performance of PEG, such as low immunogenicity [90].

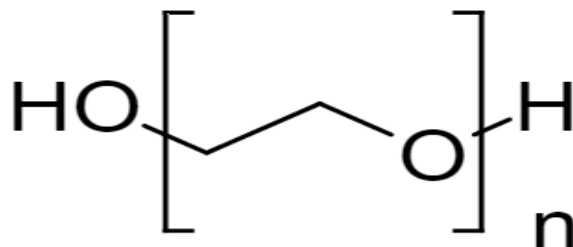


Figure (2-17) Chemical Structure of Polyethylene Glycol (PEG) [87]

2.8.3 Hydroxyapatite (HA)

HA is the most ubiquitous material present in bones and they are called as bioceramics. The stoichiometric Hap has a chemical composition of $\text{Ca}_{10}(\text{PO}_4)_6(\text{OH})_2$ with a calcium to phosphate (Ca/P) ratio of 1.67. Hydroxyapatite is the most stable calcium phosphate in fluids and humid conditions under neutral to alkaline conditions. Synthetic HAp has significant interest and importance because of its structural and compositional similarity to the predominant inorganic compounds of bones and teeth [91].

Synthetic nano-hydroxyapatite (n-HA) materials are well known to be bioactive, biocompatible, and osteoconductive. HA plays a unique role in regeneration of damaged bone because of its bioactivity and osteoconductivity. It has been incorporated in a wide variety of biomedical devices, including dental implants, coatings on Ti-based hip implants, biodegradable scaffolds for tissue engineering and drug delivery, and in other types of orthopedic implants. As a result, HAp has been extensively studied for biomedical applications in the form of powders, composites or even coatings in abundance, at microscale size [92]

Furthermore, it has also been studied for other non-medical applications; for example, as packing media for column chromatography, gas sensors and catalysts. Because of its diverse applications, the properties of the materials need to be tailored accordingly for real-world application [106]. The composition and structure of artificial nano-hydroxyapatite are like inorganic components in human bone tissues. It has non-toxicity, non-

irritant property, and is also non-allergenic, non-mutagenic and carcinogenic, and can generate a chemical reaction with bone to change bone conduction [93].

Therefore, nano hydroxyapatite could be Widely used in biological hard tissues, such as human bones, teeth and vascular stents, as repair and replacement materials, such as in oral implant ology for increasing dental spine, ear bone or spinerep[94].

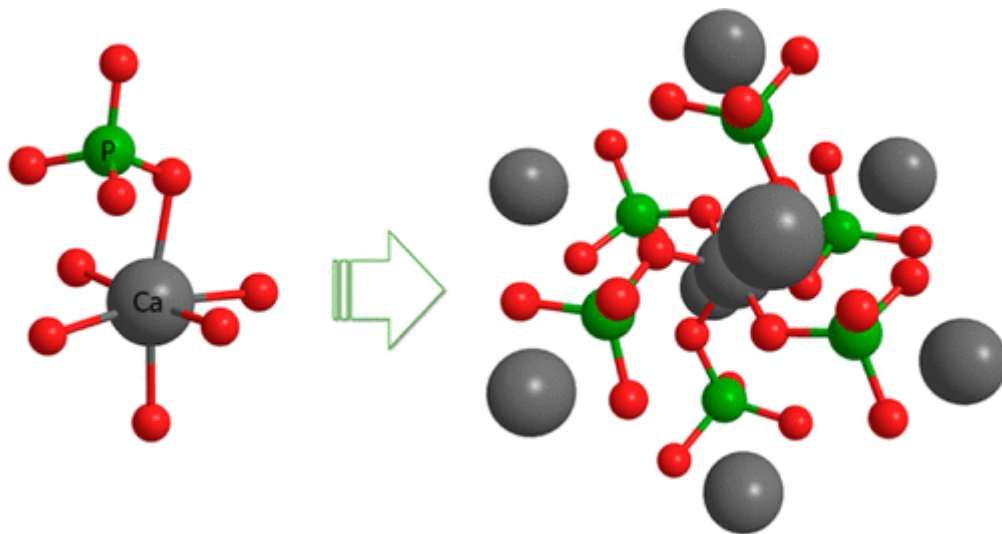


Figure (2-18) Chemical Structure of HA [91]

2.8.3.1 Chemical, Physical and Biological Properties of HA

HA is used as a bone substitute because of its chemical similarities with the natural bone. The major composition of bone is a mineral phase (69 wt%), an organic matrix (22 wt%), and water (9 wt%) [91]. Bone is the major calcified tissue present in mammals and is a ceramic–organic bionanocomposite that has a complex structure. HA with a general formula of $\text{Ca}_{10}(\text{OH})_2(\text{PO}_4)_6$ is much similar to an inorganic component of bone matrix [94]

Because of this close similarity, extensive research is ongoing to use HA as a bone substitute. HA is one of the most stable and less-soluble calcium phosphate bioceramics with Ca/P ratio of 1.67 [91]. The pure HA powder is white, whereas naturally occurring HA can also have brown, yellow, or green colorations, comparable to the discolorations of dental fluorosis. In biological systems, HA occurs as the principal inorganic

constituent of normal (bone, teeth, fish enameloid, and some species of shells) and pathological (dental and urinary calculus and stones) calcifications. The mechanical properties of HA depend on porosity, density, sinterability, crystal size, phase composition, and so on. The bending, compressive, and tensile strength values of HA ceramics lie in the range of 38–250, 120–150, and 38–300 MPa, respectively [95].

Young's modulus of dense HA ceramics varies from 20 to 120 GPa, depending on the residual porosity and impurities. Weibull's modulus of dense HA ceramics lies in the range 5–18, characteristic of brittle materials. The Vicker's hardness of dense HA ceramics is 3–7 GPa. The mechanical properties of HA bioceramics strongly depend on the microstructure and sintering ability; densely sintered bodies with fine grains are tougher and stronger than porous ones with larger grains [96].

2.8.3.2 Biological Properties of Hydroxyapatite

Both calcium and phosphate ions are present in HA; hence, no studies have noted any negative local or systemic toxicity. A carbonated nutrient apatite layer at the time of implant allows freshly formed bone to attach to HA directly. [108] Osteoclast cell attachment, growth, and development are stimulated by the HA surface. Moreover, mediators with the capability to interact with and concentrate bone organogenesis proteins (BMPs) in situ can be delivered via HA scaffolds [92].

Apatite's connection to biological tissues is critical for restoration. Mineralization and tissue interaction concepts are evolving due to changes in manufacturing technologies, scale, and resource nature. The scaffold was the first step in the bone tissue regeneration procedure. This physiological procedure initiates biological methods for producing densely packed materials with hybrid compositions by modeling and formulating molecules with the ability to randomly self-organize into higher form structures [94-95].

Recognizing the host responses to HA in vivo is critical. In general, a biomaterial's action mechanisms are bioactive, bioinert, biotolerant, and/or resorbable. These changes in awareness have taken place as a result of alterations in material characteristics and manufacturing techniques, as well as a better understanding of material interactions with tissues. The

developed wilderness of nanotechnology has outcomes in slashing HA production that are much more bioactive or bioresorbable[97].

2.8.4 Zinc oxide Nanoparticle (ZnO)

Zinc is an essential inorganic component which is widely used for drug, biological sciences, and manufacturers. An adult's average consumption from 8 to 15 mg/day, with nearly 5-6 mg/day lost through urine and sweat. It is also a necessary component of bones, enzymes, and many usable proteins. Zinc is required for the of living beings and bacteria growth, so even though zinc oxide nanoparticles are harmful to many viruses, and bacteria. People with a genetic deficiency of the soluble protein zinc suffer from enterodermatitis, which is a hereditary disease such as rough and scaly skin [98].

Because even though there are conflicting reports about nanomaterials due to their accidental use as well as decommissioning, a few metallic nanoparticles are useful to living creatures. Even before minerals and vitamins are consumed in large quantities, they can be problematic. Despite reports of DNA-damaging potential, the mutagenic potential of zinc oxide throughout bacteria has not yet been deeply investigated [99]. The chemical structure of zinc oxide shown in figure (2-12).

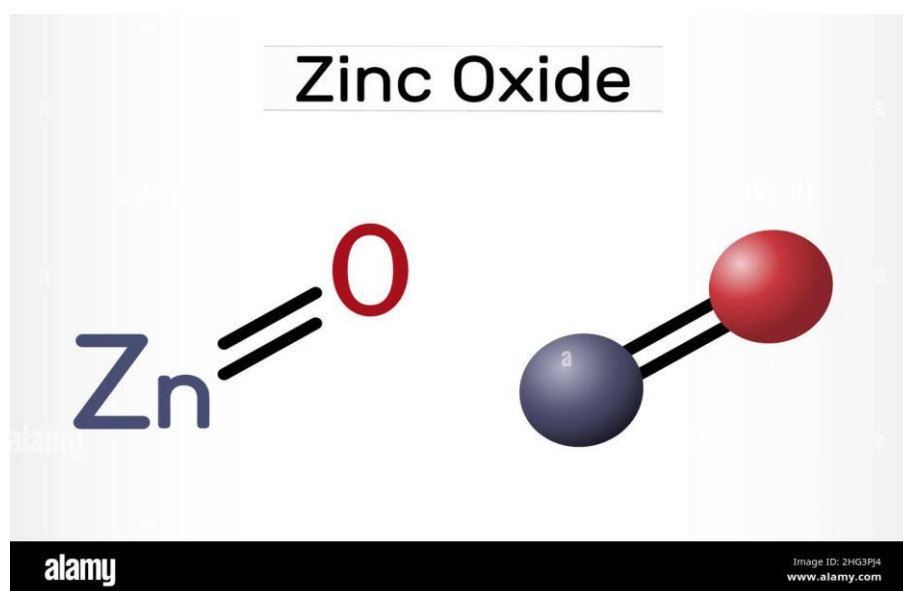


Figure (2-19) Chemical Structure of ZnO Nanoparticle [97]

2.8.4.1 Zinc Oxide as Antibacterial

Bacterial infectious diseases are widely acknowledged as a significant public health concern internationally. New bacterial genetic changes, antimicrobial resistance, and so on are on the rise, necessitating the creation of more powerful antimicrobial agents. Zinc oxide has been well-known for its anti-bacterial properties. It was used during the Ancient Egyptians' reign, and history findings reveal that zinc oxide was used in many topical applications for the treatment of injuries and skin eruptions as early as the 1920s. It is still used in sun screen moisturiser, as a supplement, photosensitive material, LED, transparent transistors, solar cells, memory chips, skincare, and catalysis [100]

Although a huge amount of ZnO is manufactured each year, only a small amount is used in medical science. [66] Zinc oxide is regarded as safe by the United States Food and Drug Administration (FDA) (21 CFR 182.8991). It has photooxidizing properties against bioactive molecules. Zinc oxide nanoparticles are one such inorganic metal oxide that meet all of the previous needs and can thus be safely utilized as drugs, packaging preservatives, and antibacterials. It freely disperses into food, killing microbes while protecting humans from illness. According to European Union Regulation 450/2009/EC, "active packaging" is defined as a substance that, in interactions with food, has the capacity to modify the contents of the food or its surroundings [101].

As a consequence, it is widely used as a fixative and is integrated into polymeric packaging to protect food from microbe destruction. In vitro, ZnO nanoparticles were found to be antibacterial against *Salmonella typhi* and *Staphylococcus aureus*. Zinc oxide nanoparticles had the strongest toxic effects against microbial cells of any metallic nanoparticles researched thus far. SEM and TEM illustrations have also shown that zinc oxides first damage the cell walls of microbes. They disrupt the metabolic functions of microbes, causing them to die. The properties of ZnO nanoparticles are determined by particle size, concentration, and particulate shape. ZnO nanoparticle bioavailability research has also been investigated [69], for example, analyzed the performance of long-term zinc oxide nanoparticle exposure on oral bioavailability and zinc metabolic activity in mice aged from 1 to 8 weeks. When rats were exposed to between 50 and 500 mg/kg of zinc oxide nanoparticles in their diet, their study found minimal toxicity. ZnO nps reduced body mass but increased

the mass of the pancreas, nervous system, and lungs at a maximum dosage of 5000 mg/kg [102].

The particle size has a huge effect on the absorption and dispersion of zinc oxide nanoparticles. Zinc oxide nanoparticles have been found to be more efficient through liver and kidney oral bioavailability than orally injected rats. Because zinc oxide nanoparticles are non-toxic in low concentrations, they encourage enzyme systems in humans and plants while also trying to suppress illnesses [102].

2.8.5 Glutaraldehyde

GA is a colorless, oily liquid with a sharp, pungent odor. Glutaraldehyde is used for industrial, laboratory, agricultural, medical, and some household purposes, primarily for disinfecting and sterilization of surfaces and equipment. For example, it is used in oil and gas recovery operations and pipelines, waste water treatment, x-ray processing, embalming fluid, leather tanning, paper industry, in fogging and cleaning of poultry houses, and as a chemical intermediate in the production of various materials. It may be used in select goods, such as paint and laundry detergent.

Glutaraldehyde is a 5 carbon dialdehyde as shown in Figure (2-13), empirical formula C₅H₈O₂ molecular weight 100.12. Despite being introduced in 1908, it remains somewhat of a chemical enigma as studies continue in an attempt to obtain a full understanding of its chemical structure. In its simplest form, glutaraldehyde exists as a monomeric dialdehyde, CHO (CH₂)₃ CHO. However, it can also occur as a dimer, trimer, and polymer and it is these forms that have made it a controversial chemical [103].

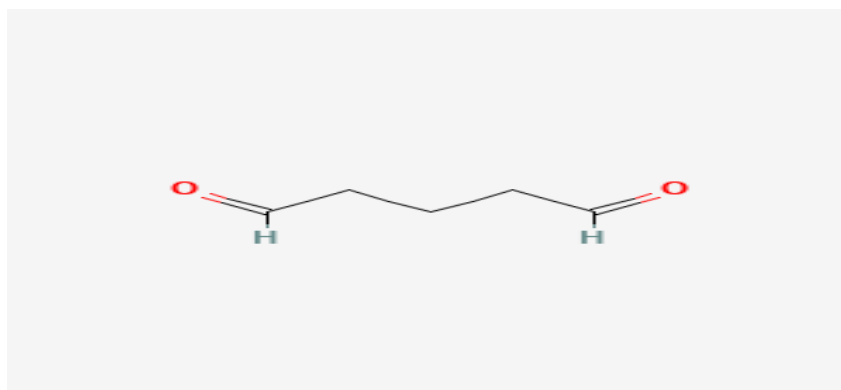


Figure (2-18) Chemical Structure of Glutaraldehyde [103]

2.9 Literature Survey

L - H He et.al, (2009) prepares biodegradable blend films composed of chitosan and PEG with various composition ratios. The chemical structure of the blend films was characterized with FTIR and X-ray, which showed no chemical bond formations but certain interactions probably coming from the hydrogen bonds. Morphologies of these blend films were viewed using AFM and SEM, suggesting that pure chitosan film had a smooth surface structure and the blend films surface showed a plenty of holes with varying size. Through the DMA measurement, it was found that there existed differences in the peak area and position of the blend films, and the peak at the glass transition temperature became significantly weaker and was markedly wider with the increasing content of PEG. The obtained results showed that the crystallinity of chitosan was suppressed and partially destroyed, and this should have an influence on the thermal behaviors and dynamic mechanical properties of the blend films [104].

Mohammad Shakir, et al (2014) A nanocomposite involving nano-hydroxyapatite/chitosan/polyethylene glycol (n-HAP/CS/PEG) scaffold has been successfully synthesized by co-precipitation approach at room temperature. The FTIR spectra of n-HAP/CS and n-HAP/CS/PEG scaffolds indicated significant intermolecular interaction between the various components of both the nanocomposites. The results of XRD, TEM and TGA/DTA suggested that the crystallinity and thermal stability of the n-HAP/CS/PEG scaffold have decreased and increased respectively, relative to n-HAP/CS scaffold. The comparison of SEM images of both the scaffolds indicated that the incorporation of PEG influenced the surface morphology while a better in-vitro bioactivity has been observed in n-HAP/CS/PEG than in n-HAP/CS based on SBF study, referring a greater possibility for making direct bond to living bone if implanted. Furthermore, MTT assay revealed superior non-toxic nature of n-HAP/CS/PEG to

murine fibroblast L929 cells as compared to n-HAP/CS. The comparative swelling studies of n-HAP/CS/PEG and n-HAP/CS scaffolds revealed a better swelling rate for n-HAP/CS/PEG. Also n-HAP/CS/PEG showed higher mechanical strength relative to n-HAP/CS supportive of bone tissue ingrowths [105].

Fereshteh Mohammad Ghorbani et al (2015) Chitosan (Cs), and poly(ϵ -caprolactone) (PCL), were both blended with zinc-doped hydroxyapatite nanoparticles (n Zn,HA) and electrospun into nanofibrous scaffolds using formic acid/acetic acid. The rationale behind this study was to demonstrate that presence of small quantities of Zn^{2+} ions doped in HA nanoparticles can improve biocompatibility of PCL/Cs blends. SEM observation revealed that average fiber diameter was increased from about 136 nm for a PCL/Ch blend, to around 210 nm for PCL/Ch/nZnHA nanocomposite. PCL/Ch/nZnHA scaffolds offered higher elastic modulus (about 3-fold) and tensile strength (nearly 1.5-fold) than the corresponding PCL/Cs scaffolds. In-vitro biocompatibility studies using human adipose derived stem cells (hAD-MSCs), demonstrated that the presence of only 5 wt% nZnHA in PCL/Cs/nZnHA nanocomposites enhanced hAD-MSCs' attachment compared to PCL/Cs and PCL/Cs/nHA. Finally, hAD-MSCs proliferation occurred at significantly higher rates of 1.5, 1.3 and 1.2 times on PCL/Cs/nZnHA scaffold compared to PCL, PCL/Cs and PCL/Cs/nHA, respectively [106].

Safa Taherkhani and Fathollah Moztarzadeh (2016) prepared nanocomposite scaffolds of poly(ϵ -caprolactone) (PCL) and starch with a range of porosity from 50 to 90%w by a solvent-casting/salt-leaching technique, and their physical and mechanical properties were investigated. X-ray diffraction patterns and Fourier transform infrared spectra confirmed the presence of the characteristic peaks of PCL in the fabricated scaffolds. Microstructure studies of the scaffolds revealed a uniform pore morphology and structure in all of the samples. The experimental measurements showed that the average contact angle of the PCL/starch composite was 88.0561.778. All of the samples exhibited compressive stress/strain curves similar to those of polymeric foams. The samples with 50, 60, 70, and 80 wt % salt showed compressive-load-resisting capabilities in the range of human cancellous bone. With increasing

porosity, a significant decrease in the mechanical properties of the scaffolds was observed [107].

Arundhati Bhowmick et al (2016) have developed hybrid nanocomposites of chitosan, poly (ethylene glycol) and nano hydroxyapatite-zinc oxide with interconnected macroporous structures for bone tissue engineering. These nanocomposites were characterized by different spectroscopic and analytical techniques. The percentage of porosities and tensile strength of these materials were found to be similar to that of the human cancellous bone. Moreover, these hybrid materials exhibited bio-degradability, neutral pH (7.4) and erythrocyte compatibility. Addition of nano-hydroxyapatite-zinc oxide into the nanocomposites increased antimicrobial activity and protein adsorption ability. The water uptake ability was found to increase with increasing the proportion of poly(ethylene glycol). Finally, osteoblast-like MG-63 cells were grown, attached and proliferated with these nanocomposites without having any negative effect and showed good cytocompatibility [108].

Akakuru and Isiuku (2017) prepares chitosan and hydrogels of the chitosan and crosslinked with varying amounts of glutaraldehyde to achieve different crosslink densities between 0.75 and 1.50. The materials were characterized in terms of the dependence of their swellabilities on time and pH. FTIR analysis was also carried out on the hydrogels and the results obtained show a band at 3451 cm^{-1} , attributed to O-H stretching of the chitosan. The crosslinked hydrogels also showed an N-H bending vibration at 1635 cm^{-1} which has a reduced intensity and has moved to a lower wavenumber when compared to the N-H bending vibration of the uncrosslinked chitosan hydrogels at 1652 cm^{-1} . The swelling studies showed that the extent of swelling of the hydrogels was dependent on the crosslink density (CD), increasing as CD increased. Uncrosslinked chitosan hydrogel had maximum swelling of 162.71% while that for the crosslinked chitosan hydrogels with CD of 0.75, 1.00 and 1.50 were 119.87%, 93.21% and 87.65% respectively. In all cases, their crosslinked counterparts had decreased swellabilities suggesting that, the crosslinked chitosan hydrogels can be used for a more controlled delivery of drugs and as efficient materials for tissue engineering [109].

Kumar (2018) studies the synthesis of highly effective, porous, biocompatible, and inert scaffold by using ceramic nanoparticles and

natural polymer for the application in tissue engineering. Freeze-drying method was used to fabricate nano-TiO₂ doped chitosan sample scaffold. The TiO₂ nanoparticles have a great surface area and inert properties while chitosan is highly biocompatible and antibacterial. The physiochemical properties of TiO₂ nanoparticles and scaffold are evaluated by XRD and FTIR. The mechanical properties are examined by stable microsystem (Texture Analyzer). The in-vitro degradation of scaffold is calculated in PBS containing lysozyme at pH 7.4. The growth factor and drug-loaded composites can improve osteogenesis and vascularization [92].

Agustina et al, (2019) prepared films using chitosan, nanocellulose and glutaraldehyde were carried out as an effort to obtain alternative biodegradable plastics. Chitosan has low mechanical, therefore nanocellulose is added from pineapple leaf fibers and glutaraldehyde additives. This research was conducted to obtain the optimum glutaraldehyde additive variable that functions as a crosslinker. chitosan used was 2% (w/v solution) and nanocellulose 3% (w/w chitosan) based on optimum results from previous research. The method used a casting method. Variable of glutaraldehyde added by 0%, 0.5%, 1%, 2%, and 3% (w/w chitosan). Tensile strength, elongation, functional groups, and absorbance were used to characterize film. The results showed that the results of FT-IR were a spectrum of chitosan and indicated the crosslinking between chitosan and glutaraldehyde. The tensile strength values change with the addition of glutaraldehyde at 0.5% and 1% the tensile increase and at 3,2% respectively the tensile decrease. The optimum value of adding glutaraldehyde is 1% based on the results of tensile strength and the lowest absorbance [110].

Esra Cansever Mutlu(2019) fabricated a blends of chitosan/poly(ethylene glycol)/hyaluronic acid. It conserves microscale particle structure even after incorporating zinc oxide (ZnO), the zeolite Mobil Composition of Matter No. 41 (MCM41) and penicillin G during this technique. Three different electrospray (ESP) blend compositions (ESPI, ESPII and ESPIII) have been produced in order to improve both antibacterial activity against to both gram-positive and gram-negative bacteria and biocompatibility. Results of FTIR spectroscopy and microscopy verified with SEM, EDS and AFM analyses. Hyaluronic acid surface has been specified definitely through ZnO-based ESPI surface composed of heterogeneously dispersed

microparticles. Surface structures of ESPII and ESPIII have more homogeneously dispersed microparticles as hill–valley surface by the aid of MCM 41-PEN. ESPI has good antibacterial activity against both gram-positive (*S. aureus* and *S. epidermidis*) and gram-negative bacteria (*E. cloacea*). Each electrospay film displayed good biocompatibility against to mouse fibroblast cell line L929 (ATTC number CCL-1)[111].

Ishraq (2020) was worked on studying for development of Chitosan and polyvinyl alcohol blend scaffolds crosslinked with natural crosslinked and reinforced with Nano hydroxyapatite with different concentrations by solvent casting and electrospinning technique. The results demonstrated that the scaffolds prepared have high degradation rate, and after addition natural crosslinking and Nano hydroxyapatite powder the degradation rate was decreased. Mechanical test results of blend showed as the concentration of natural crosslinking and Nano hydroxyapatite powder increased, the values of properties increased [92].

Rifat Ara Masud (2020) The antibiotic gentamicin was loaded into a novel bionanocomposite of chitosan-zinc oxide (ZnO) nanoparticles, poly (ethylene glycol) (PEG) cross-linked with sodium tri polyphosphate (STPP), and its wound healing efficiency was investigated in an attempt to enhance wound healing by controlling the release of drugs. ZnO nanoparticles with an average particle size of about 50 nm were prepared by a co-precipitation method and incorporated into a chitosan/PEG bionanocomposite to enhance antimicrobial properties of the composite. The size, morphology, elemental analysis, micro structure, swelling properties, cytocompatibility, antimicrobial properties, and wound healing properties of both nanoparticles and bionanocomposites were evaluated. Cytotoxicity analysis was carried out on Vero cells and BHK 21 cells, and both results confirmed the biocompatibility of the bionanocomposite. In vitro analysis demonstrated the enhanced antibacterial activity of drug-loaded bionanocomposites on *E. coli* and *S. enterica* because of the combined effect of the drug and ZnO nanoparticles. In vivo analysis of drug-loaded bionanocomposites showed better healing properties than commercial hydrogel wound dressing without any scar formation. Prepared bionanocomposite showed high biocompatibility with excellent antibacterial activities. Overall, the performed studies confirmed chitosan/poly (ethylene glycol)-zinc oxide based release system can be a potential

candidate for wound dressing applications with sustained drug release [112].

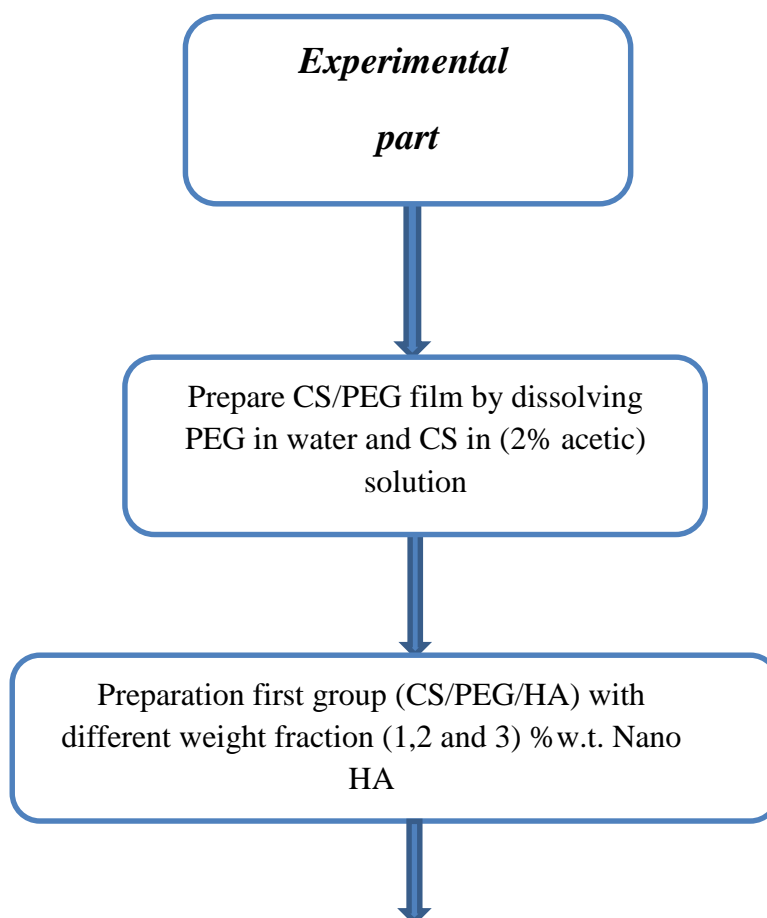
Neacsu *et al.* (2020) developed of a biomimetic composite based on naturally derived biomaterials. This freeze-dried scaffolds based on chitosan (CS), chitosan + gelatin (CS_Gel) and of the final inorganic-organic composite HAp(ESM)_CS_Gel_BA, using the interwoven hierarchical structure of eggshell membrane as bio-template. The bone regeneration capacity of the scaffold is enhanced with the help of added tricalcium phosphate from bovine Bone ash. With the addition of Gelatin (Gel) as organic matrix, the obtained composite is characterized by the ability to stimulate the cellular response and might accelerate the bone healing process. The experimental results showed highlight an original biocomposite scaffold obtained from naturally derived materials, in a nontoxic manner [113].

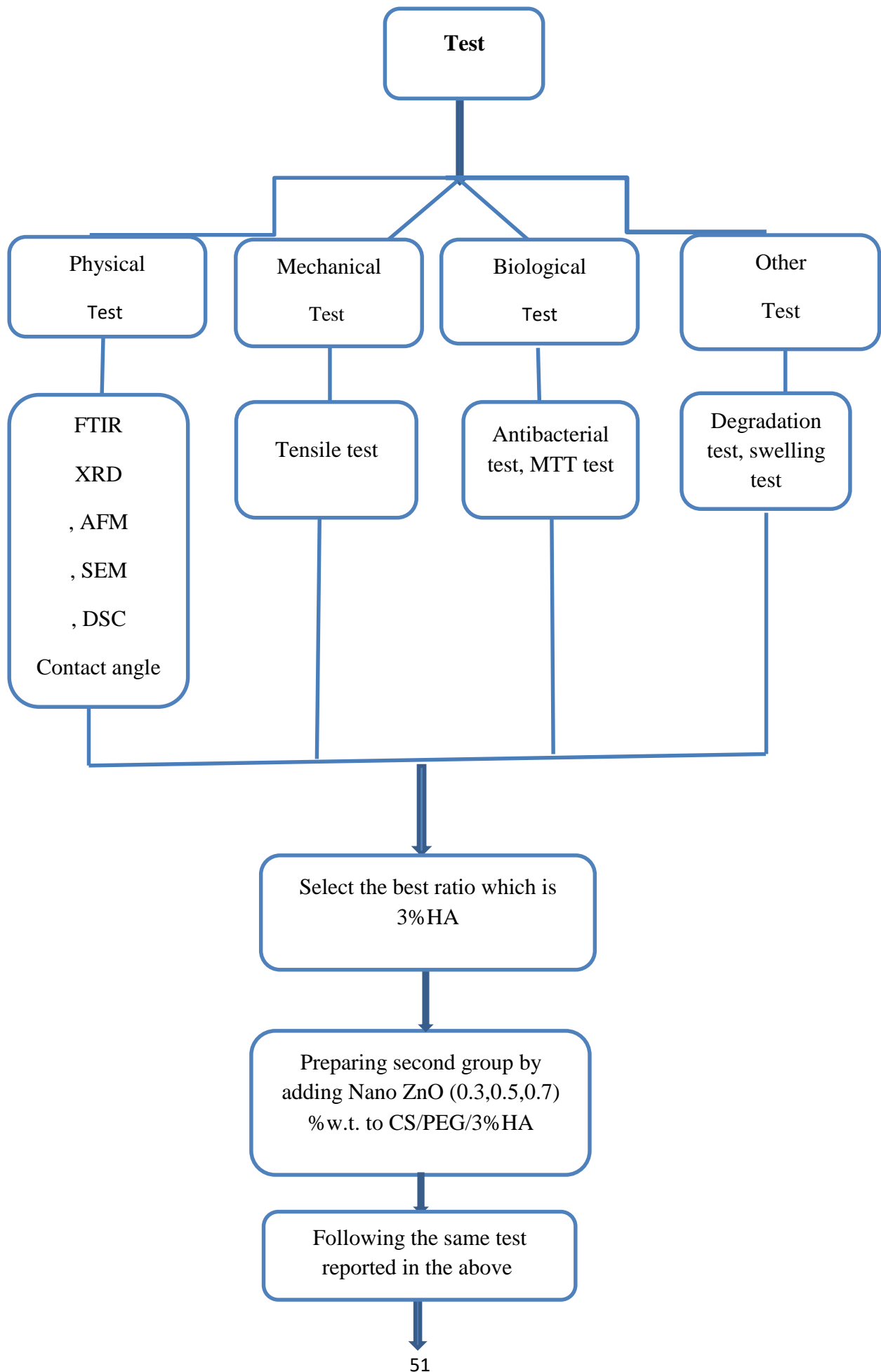
Chapter Three

3.1 Introduction

The current chapter entails all of the significant details about the methodology of the study, beginning with material selection and description and concluding with sample preparation. Furthermore, this chapter describes all of the tests that are performed on prepared samples. In this work, there are two basic parts that have been followed in the manufacture of bone scaffold, first is the part of is blend, nanocomposite and hybrid films (CS/PEG/HA/ZnO) for the manufacture of special bone scaffolds that help in the regeneration and construction of the damaged bone.

Nano powders (HA and ZnO) materials are used as reinforced material to get polymeric nanocomposite materials which are done to enhance some required properties of the composites. Second part of the work includes crosslinked the film above with glutaraldehyde(GA) to enhanced the mechanical, wettability properties for bone scaffold. Research plane that was carried out is shown in Figure (4-1).





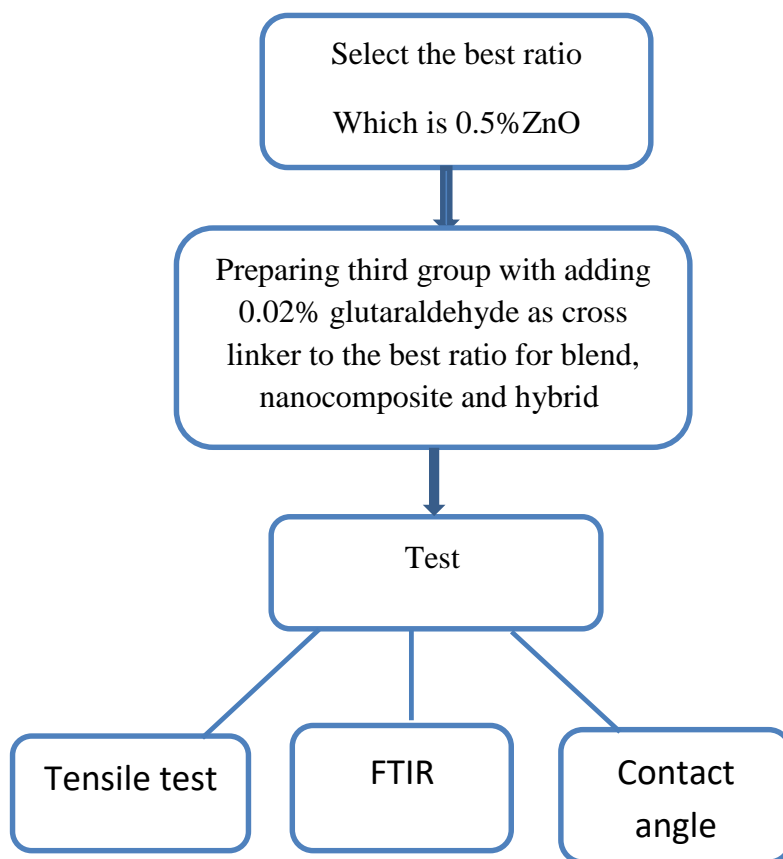


Figure (3-1): Research plan

3.2 Materials

3.2.1 Chitosan

The powder of chitosan CS was procured from a central drug house, in India with the properties listed in Table (3-1).

Table (3-1): Chitosan Properties

Property	Data
Chemical formula	$(C_6H_{11}NO_4)_n$
Deacetylation degree	$\geq 75\%$
viscosity	20-300 cps
Color	Off-white to yellow powder

3.2.2 Polyethylene glycol

polyethylene glycol (PEG) was procured from (Himedia , India), with the properties listed in Table(3-2).

Table (3-2): PEG Properties

Property	Data
Chemical formula	$[H(OCH_2CH_2) OH]_n$
Color	White
Molecular weight	4000g/mol

3.2.3 Glacial acetic acid

Glacial acetic acid from alpha chemical, India, with the properties listed in Table (3-3)

Table (3-3): Glacial Acetic Acid Properties

Property	Data
MW	6005
Purity	99%

3.2.4 Nano Hydroxyapatite

Nano hydroxyapatite HA obtained from N&R INDUSTRIES, INC. With the properties listed in Table(3-4)

Table (3-4): Nano Hydroxyapatite Properties

Property	Data
Product name	Nano Hydroxyapatite
Chemical formula	$\text{Ca}_5(\text{OH})(\text{PO}_4)_3$
Purity	99%
Average Particle Size	20nm
Color	White

3.2.5 Nano Zinc Oxide

ZnO nanoparticle was purchased from US Research Nanomaterial, Inc. With the properties listed in Table (3- 4).

Table (3-5): Nano ZnO Properties

Property	Data
Product name	Nano Zinc Oxide
Chemical formula	$\text{Ca}_5(\text{OH})(\text{PO}_4)_3$
Purity	99%
Average Particle Size	10-30 nm

3.2.5 Glutaraldehyde

was supplied by Qualikems, India. With the properties listed in Table (3- 4).

Table (3-6): Glutaraldehyde Properties

Property	Data
Chemical formula	$\text{C}_5\text{H}_8\text{O}_2$

Color	Yellow
Appearance	Liquid

3.3 Film formation

1- Chitosan powder was dissolved in 2% acetic acid mixed by magnetic stirred at 40 °C, for 1hr.

2- PEG granules or flakes that have been dissolved using distilled water by continuous stirring for 15 minutes at room temperature.

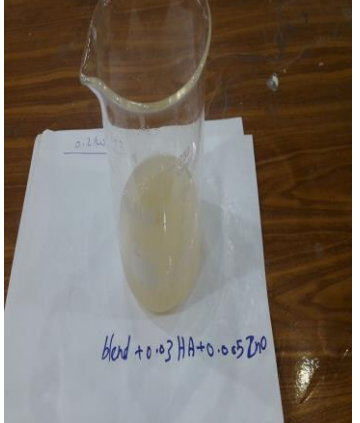
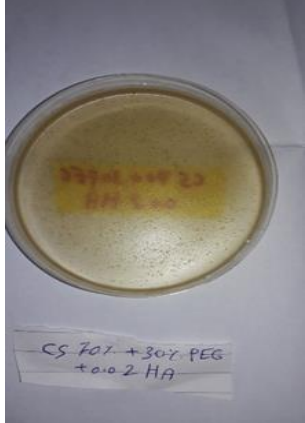
3-Three percent of chitosan and poly ethylene glycol (PEG) (90%:10%,80%:20%,70%:30%) will blended by stirred at 25 °C for half of hour and casted into a Petri dish. It is left at room temperature for one and half day to dry.

4- Prepare Nanocomposite film reinforced with (1,2 and 3) w.t.% HA, the nanoparticles were dispersed in distilled water by ultrasonic dispersion device for 15 min and a temperature of 40 °C. Then, poured gradually into CS/PEG (70%:30%) blend while the blend on stirrer. The blend was mixed for 30 min then casting it in a petri dish and left for 72 hr to dry then it is going to be ready for tests.

5-To prepare blend with Nano HA and ZnO, repeat the above steps from 1 to 4 and dispersion of about (0.03%, 0.05%, 0.07%) of ZnO particle in distilled water for 15 minutes at 40°C and 35 energy the sonication, nanoparticle was gradually poured out to the blend while the CS/PEG/HA (70:30:3) blend on magnetic stirred mixed for 45 min and the blend was poured into Petri dish and left for 72 hr to dry.

6- To prepare cross-linked film, repeat all step from 1 to 5 (for preparing the blend, nanocomposite, hybrid) adding 0.02% from glutaraldehyde gradually to the best ratio of three films (blend(CS/PEG), Nanocomposite film(CS/PEG/HA), Hybrid film(CS/PEG/HA/ZnO) mixed for 10 min, then cast the blend into petridesh and left dry for 3 days.

Table (3-7): Images for Solution and Dry Films Used in Research

Sample	Solution blends	Dry films
Chitosan+PEG blend		
Chitosan +PEG+HA film (Nanocomposite film)		
Chitosan+PEG+HA+ZnO (Hybrid film)		
Chitosan+PEG+HA+ZnO+GA (Cross-linked film)		

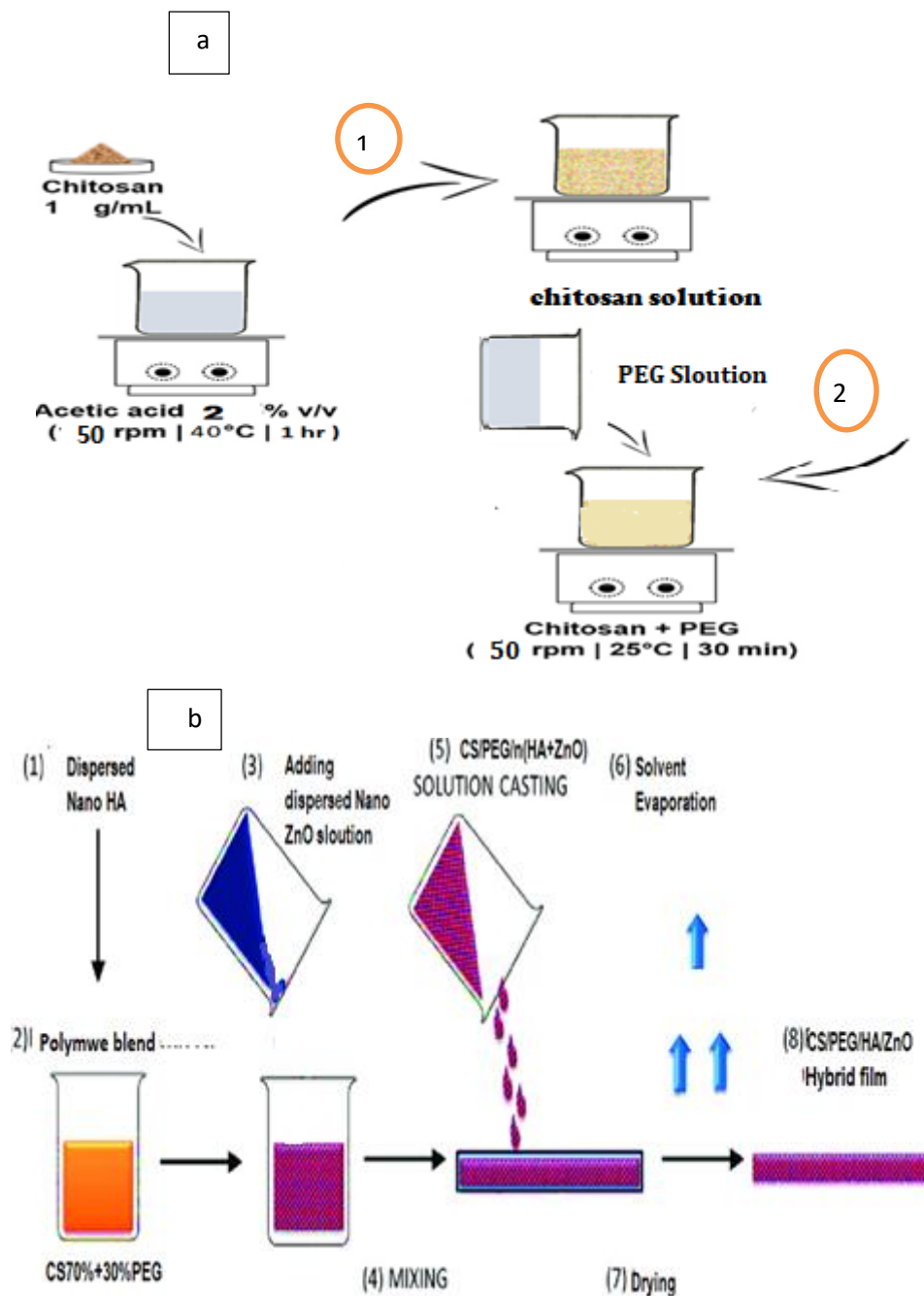


Figure (3-2): Schematic diagram of Film Preparation Process a) CS/PEG film b) Hybrid film [114].

3.4 Test

3.4.1 Infrared Fourier transform spectrometer (FTIR) Test

This method is used to characterize complex blends using the FTIR analysis equipment Type (IR Affinity-1), as shown in Figure (3-3). Blend

films were measured among 400 and 4000 cm^{-1} in transmission mechanism, either directly or by embedding the films in KBr pellets.



Figure (3-3): FTIR device

3.4.2 Field Emission SEM (FESEM)

The Field Emission Scanning Electron Microscope (FESEM) as shown in Figure (3-4) and image objects up to 500000 times more effectively than a standard scanning electron microscope (SEM) due to its significantly brighter electron source and thinner beam size. The capacity to conduct high-resolution imaging with relatively low accelerating voltages is a second feature of the FESEM. This improves the ability to observe very small surface details. This experiment was carried out in the labs of the Engineering Department at the University of Tehran.



Figure (3-4): SEM device

3.4.3 Contact Angle Test

The experiment was performed to determine how the addition of PEG and nanoparticles affects wettability. The contact angle ranges from 0 to 180 degrees' as shown in Figure (3-5). This device calculates the left and right contact angles and relates them. It also figures out their average values and shows them on a real-time data graph. It can also record video of how the contact angles change.

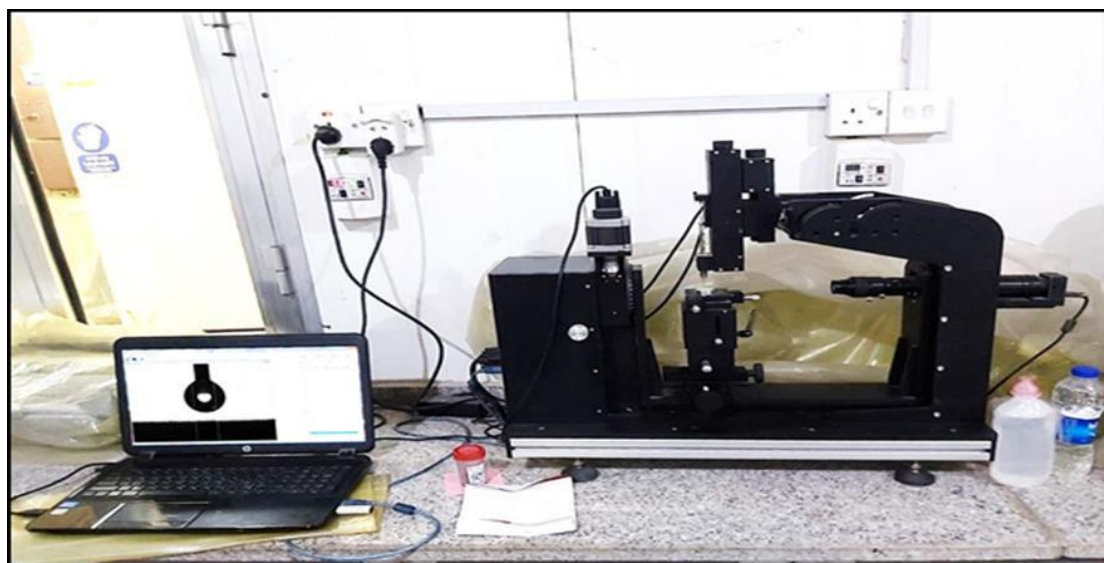


Figure (3-5):Contact Angle device

3.4.4 Degree of Swelling Test

the test was done using ASTD 570. A small piece of the film is put in the sachet and immersed in the PBS solution about 1 hour. After that, the Residual solution or solution left after immersion is disposed of and the swelling capacity is calculated using Equation (1). The final results are the average of all the samples that were tested. "This test was done in the laboratories of the Faculty of Materials Engineering Department of Polymer Engineering and Petrochemical Industries. which can calculate in following equation [115]:

$$\text{Degree of swelling (\%)} = \frac{W_s - W_d}{W_s} \times 100 \% \dots\dots\dots (3-1)$$

Where W_s (g) and W_d (g) are the weights of dried film and swollen film after immersion respectively.

3.4.5 In Vitro Degradation Test:

The samples are put in the tea-bag, immersed in small bottles containing 20 ml of a solution of PBS (Buffer Silene Phosphate) for five days. The samples are taken out, washed with distilled water, then dried in ovens for 4 hours at a temperature of 40°C, then the dissolution rate is measured using the following equation [116]:

$$w1 - \frac{w2}{w1} \times 100\% \dots \dots \dots (3-2)$$

Where W_1 : Where W_1 the dry weight before degradation (g) and W_2 the dry weight after degradation (g) at the specified time.



Figure (3-6): Degradation Method

3.4.6 Differential Scanning Calorimetry Test (DSC)

Differential scanning calorimetry measurements (DSC) measurement were carried out according to ASTM D3418-03 under a nitrogen gas atmosphere. The prepared samples with a weight of $(8-10) \pm 0.5$ mg was put in aluminum crucible and heated from room temperature up to 160°C at a rate of 10°C/min as shown in figure (3-7).



Figure (3-7): DSC device

3.4.7 Anti-bacterial Test

Determination of antibacterial activity was achieved using the Agar Well Diffusion Method, must be prepared the Muller Hinton agar in advance and the positive and negative bacteria were selected. In this test (Escherichia coli, staphylococcus aureus), several holes or gaps were made in the agar layer, then solution drops or a solid film were placed. The bacteria were distributed on the plate and placed in an incubator for 24 hours at a temperature of 37 °C. The antibacterial activity against E-Coli and S. aureus microorganism was assessed by measuring the diameter of the inhibition zone and recorded in mm.

3.4.8 X-Ray Diffraction Analysis

It is a rapid analytical technique, primarily used for phase identification of crystalline materials, the XRD test are used to characterize the nanoparticles of HA and ZnO , the device type SHIMDZU, 6000, as shown in figure (3-7).Japan automated powder diffractometer. With an X-ray current of 30 mA, the diffract grams were taken in the 2 range from 0 to 80 degrees.



Figure (3-8): X-Ray Device

3.4.9 Tensile test

A mechanical tester was used to perform the tensile test. The ASTM Standard Sheet (D882-01)[117], "Standard Test Protocol for Tensile Properties of Thin Plastic Film," where a film was 80 mm in length and 10 mm wide. using a strain rate of 5 mm/min



Figure (3-9): Tensile device**3.4.10 Atomic Force Microscope (AFM) test**

The thin film's surface morphology was further investigated using traditional tapping mode probes with constant magnitude (200 mV) AFM according to ASTM E 2865. The rotated tapping method with an etched silicone probe was used, with a frequency response of 55 kHz. Figure (3-10) depicts the AFM.

**Figure (3-10): AFM device****3.4.11 MTT assay**

In vitro, cell culture test was used to allow MG-63, Hdfn grow on the selected samples which is nanocomposite sample. The MTT assay was used to test the nanocomposite -cytotoxicity, which is based on the fact that living cells convert the yellowish MTT solution to a dissolved purple formazan particle. These samples were first placed in a 96_well polystyrene cell culture plate. as shown in Figure (3- 11) .Thereafter, a media (Dulbecco s Modified Eagle Medium + antibiotic +fetal bovine serum) was added to all the samples for 2 hours before adding MG-63 ,HdFn cells in order to improve the wettability of the samples. After been soaked in the medium for 2 hours, 100 μ L MG-63 and HdFn cell suspension containing 5×10^4 cells were seeded on rectangular specimens with dimensions (0.5 mm \times 0.5mm \times 250 μ m) . The sample were keep at 37 $^{\circ}$ C in a humidity environment of(5% CO₂)for one day .After that , the culture media changed with 100 μ L of 10% FBS , medium being refreshed every 3 days,10 μ L of sterilized MTT solution was added and the

specimens were incubated for further 24h ,and then 100 μ L of isopropanol was added to the sample in the 96 well plate. The last column of the cell culture plate was left without samples, i.e., only media and cells as a control. this test was done with different culture time for (1,2and 3) days as achieved according to ISO 10993. The cell viability is measured as follow

$$Viab. \% = \frac{OD570e}{OD570b} \times 100\% \text{ -----(3-3) [118].}$$

Viab. %: The percentage of living cells

OD570_e : is the calculated mean value density of the sample.

OD570_b : is calculated mean value density of the control sample.

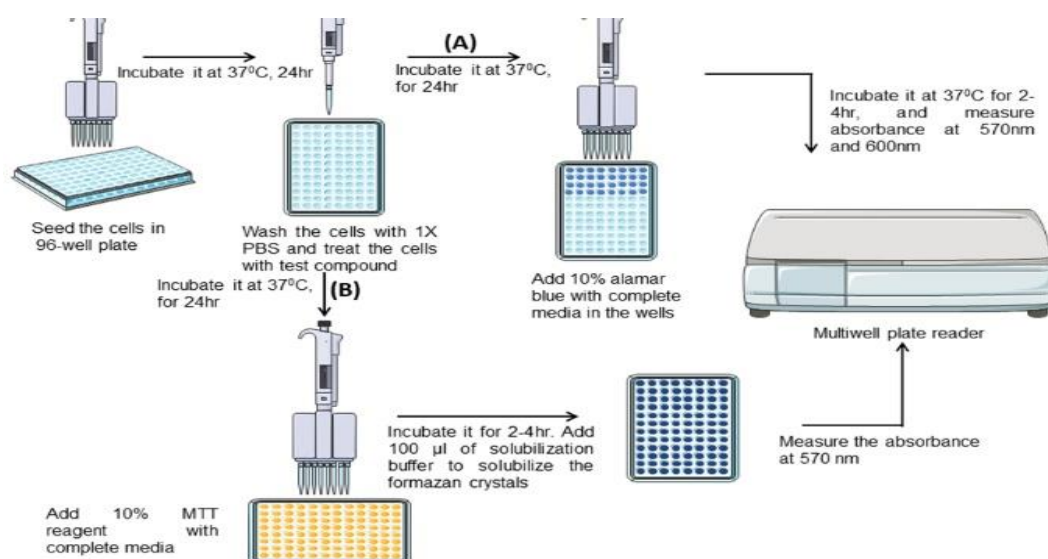


Figure (3-11): MTT Assay Procedure [118]

Chapter Four

4.1 Introduction

This chapter covers the detailed discussion for all the results which were obtained from the experimental work. As well as covers at the mechanical and physical tests that include DSC, FTIR, AFM and FE-SEM test and their results which are represented in tables, figure and pictures. These results are for blend and nanocomposite materials. Moreover, the results include vitro degradation rate, swelling degree, contact angle, tensile strength and in vitro biological activity included the anti-bacterial test to study the anti-bacterial activity of this nanocomposite materials prepared in this study and MTT to explicate the response of the fabricated bone scaffold biologically for bone tissue engineering.

4.2 Characteristics of Materials Used in This Study

4.2.1 FTIR Results of Neat Chitosan and Neat PEG

FTIR was used for fully characterization neat Chitosan. The FTIR spectrum of neat Chitosan in the wave number ($400\text{-}4000\text{ cm}^{-1}$) is shown in Figure (4-1) which exhibited many bands such as the bands at peak at 3425 cm^{-1} for O-H stretching, the CH_2 stretching at 2885 cm^{-1} , C=O at 1658 cm^{-1} , and NH at 1419 cm^{-1} While the IR spectrum of neat PEG showed in Figure (4-2) which exhibited a peak at 3464 for O-H and C-H₂ stretching at 2885 cm^{-1} , C-O-C cm^{-1} at 1111 cm^{-1} , and C-O at 840 cm^{-1} . Table (4-1) listed all transmissions bands of CS and PEG.

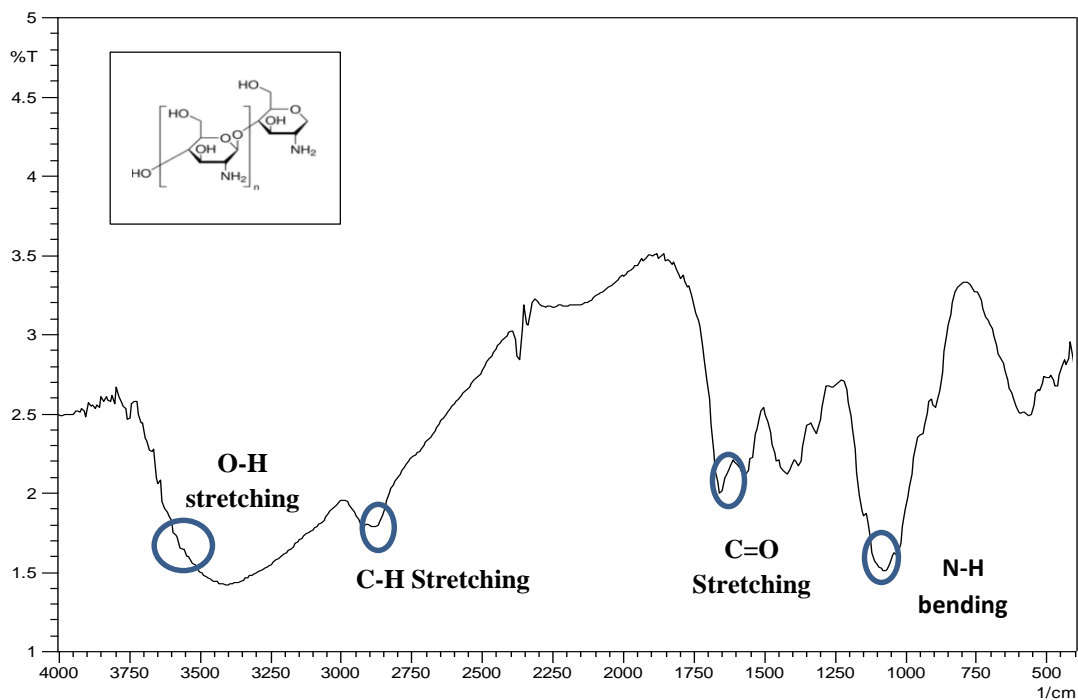


Figure (4-1): FTIR for Neat Chitosan

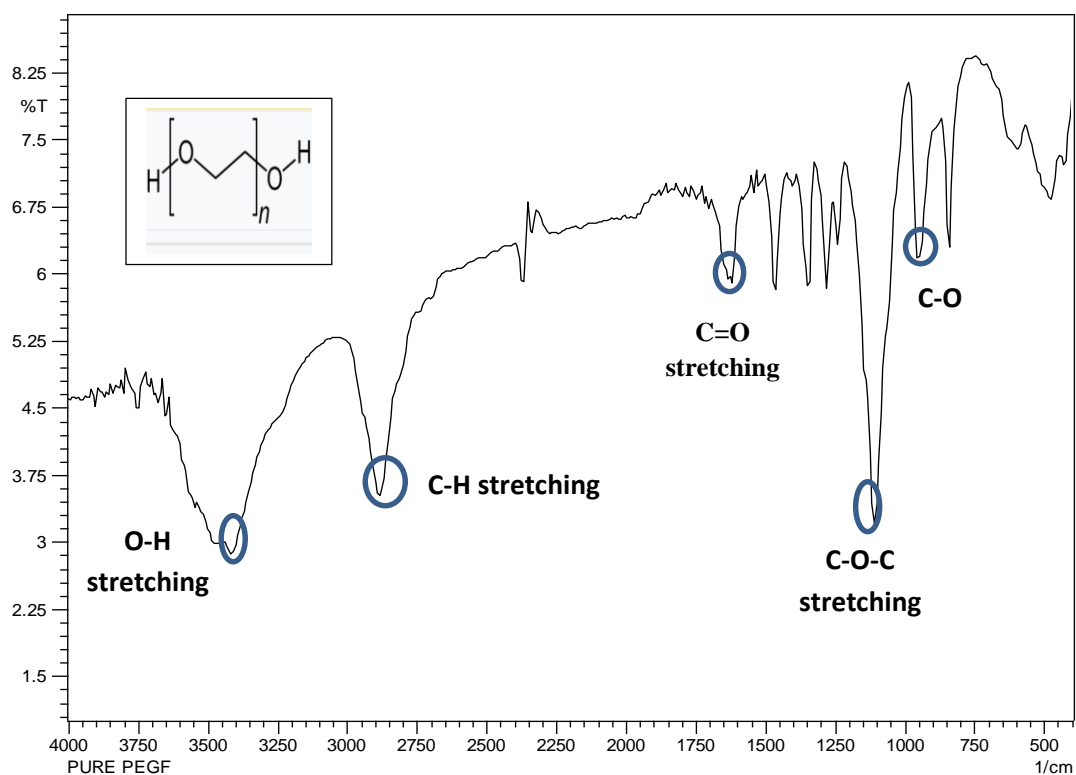


Figure (4-2): FTIR for Neat PEG

Table (4-1): Show FTIR for Neat CS and PEG

Type of bands	PEG standard cm^{-1} [119]	Neat PEG (Exp.)	CS standard cm^{-1} [105]	Neat CS (Exp.)
OH	3430	3464-3417	3440	3425
C-H stretching	2882	2885	2930–2860	2885
C=O(amid)	1620	1620	1636	1658
N-H (Amide II)	-----	-----	1420	1419
C-O-C	1114	1111	-----	-----
C-O	840	840	-----	-----

4.2.2 FTIR for Blend and Nano Composite

4.2.2.1 FTIR for Blend (CS/PEG) and Nanocomposite (CS/PEG) +HA w.t %

FTIR aimed to detect the hydrogen bonding interaction between functional groups in small molecules and also in macromolecules. As they cause to shift in the absorbance bands or increased the intensity of absorbance bands, also create a broadening of the particular bands of functional groups, it indicates the behavior of these groups in polymer blend [111].

The IR spectrum of the CS/PEG blend shows in Figure (4-3) and listed in Table (4-2) revealed to the O-H band shifted to 3419 cm^{-1} while C=O shifted to 1619 cm^{-1} , and for The blend with Nano HA the O-H peak shifted to 3425 cm^{-1} and CH_2 stretching also was shifted to 2893 cm^{-1} while C=O shifted to 1622 cm^{-1} , Moreover, phosphate stretching PO_4 vibration in HA at 1111 cm^{-1} The shift in band O-H suggested strong

hydrogen bonding and excellent HA distribution in the matrix [111,120] .

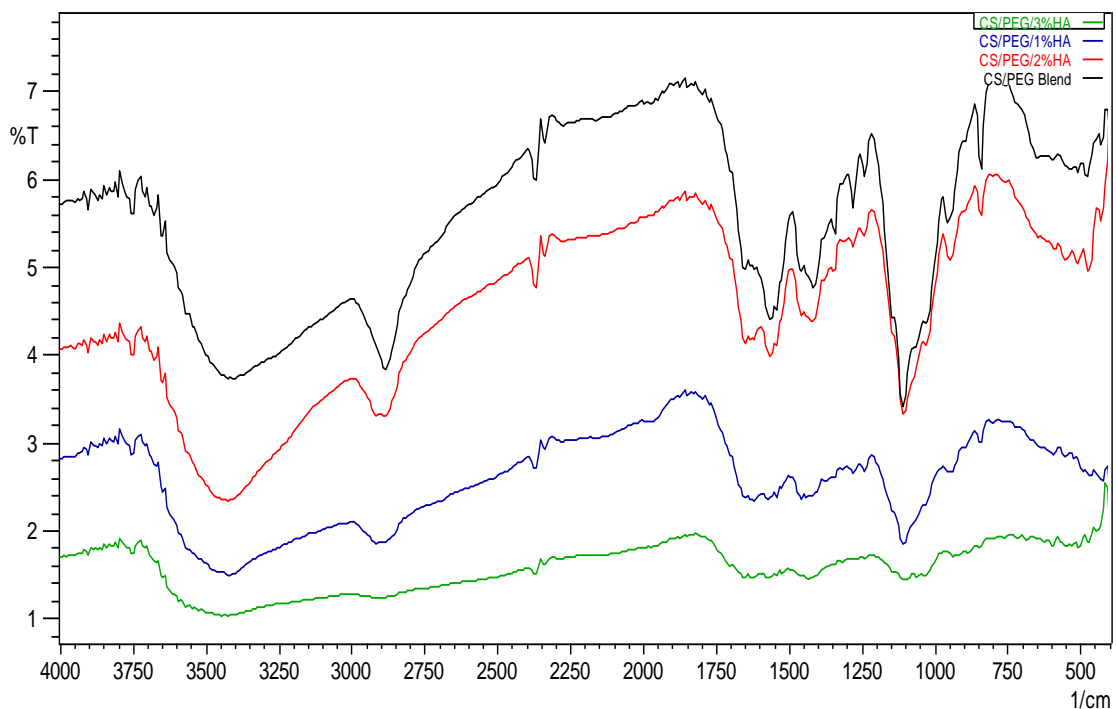


Figure (4-3): FTIR for Blend(CS/PEG) and (CS/PEG)+ HA% Nano Composite

4.2.2.2 FTIR for Hybrid Nanocomposite (CS/PEG/3%HA) +ZnO w.t%

The IR spectra of Hybrid Nanocomposite (CS/PEG/3%HA) +ZnO % as a function of different weight fraction of ZnO shows in Figure (4-4) and listed in Table (4-2) revealed to a prominent band at 3425 cm^{-1} for O-H, the CH_2 stretching at 2885 cm^{-1} , The C=O band shifted to $1651, 1620, 1635\text{ cm}^{-1}$ for (0.3, 0.5 and 0.7) w.t% ZnO, respectively. The transmission bands at 655 and 578 cm^{-1} for Zn-O. Furthermore, the transmission bands shifted from 563 to 578 and 570 cm^{-1} with increased the percent of ZnO because of the NH_2 group's connection to the Zinc Oxide nanoparticles [121]. The ZnO nanoparticles and the chitosan's (NH^{3+}) exhibit electrostatic interaction [108,121].

Finally, the addition of ZnO to the blend slightly increased the absorption intensities in the bands (C=O) at 1651 cm^{-1} [122].

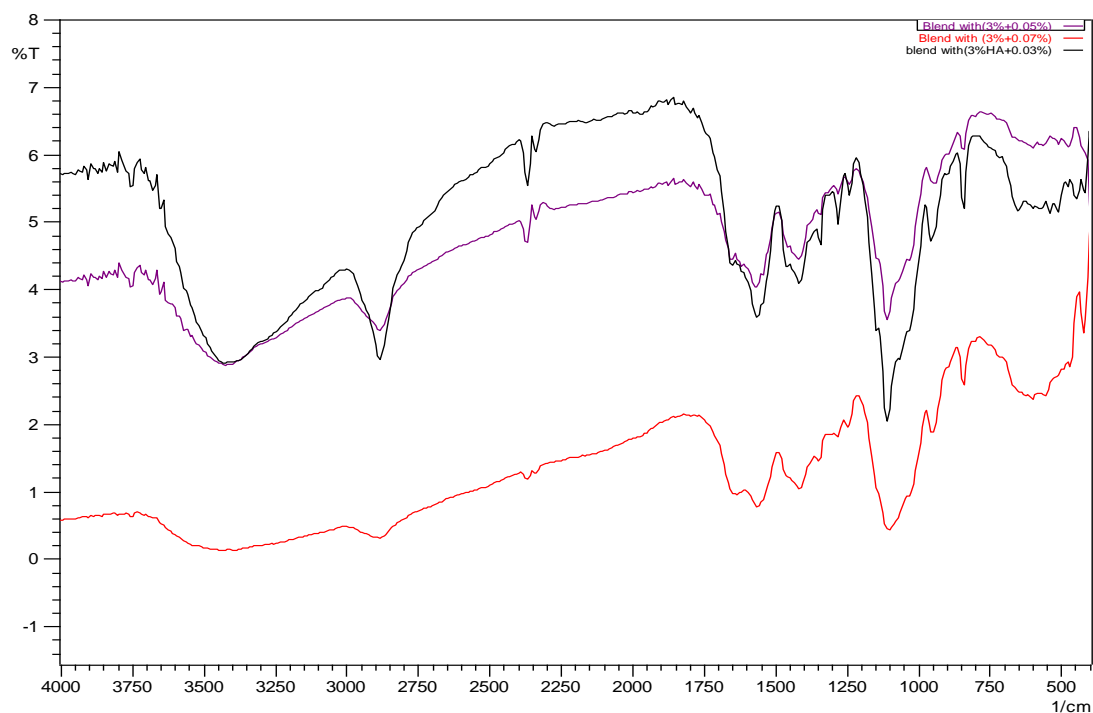


Figure (4-4): FTIR of Hybrid Nanocomposite

Table (4-2): FTIR Bands for Hybrid Nanocomposite

Type of bands	Blend CS/ PEG	Blend with Nano 1% HA	Blend with Nano 2% HA	Blend with Nano 3%HA	Blend with Nano 3%HA+ 0.3%Zn O	Blend with Nano 3%HA+0. 5%ZnO	Blend with Nano 3%HA+0 .7 %ZnO
OH	3419	3417	3425	3425	3425	3425	3425
C-H stretching	2885	2893	2893	2893	2885	2885	2885
C=O Amide I	1619	1620	1622	1620	1651	1620	1635
NH Amide II	1419	1442	1419	1435	1419	1419	1419
P-O stretching	-----	1111	1111	1111	1111	1111	1103
Zn-O	-----	-----	-----	-----	655-578	648-563	655-570

4.3 X-Ray Diffraction Test

4.3.1 X-Ray Diffraction of HA- Nanoparticles

The X-ray diffraction pattern Nano Hydroxyapatite at room temperature which were used in this study can be seen in Figure (4-5), and the peaks characteristic listed in Table (4-3) correspond to standard XRD peaks of hydroxyapatite (based on ICDD9–432) published in literature [123].

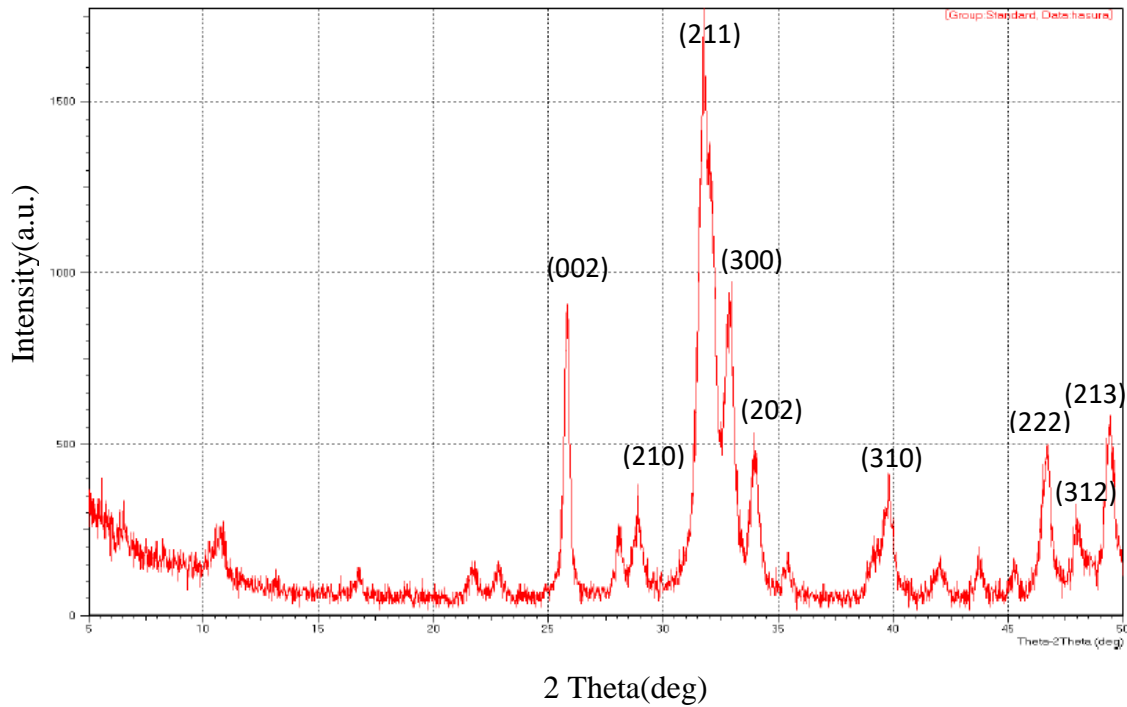


Figure (4-5) X-Ray Diffraction for HA-Nanoparticles

Table (4-3) XRD for Nano-HA

Peak no.	2Theta(deg)	d (Å°)	I/I ₁
1	10.8633	8.13770	8
2	16.7855	5.27755	3
3	21.8378	4.06664	5
4	22.8604	3.88699	6
5	25.8230	3.44737	38
6	26.5716	3.35192	3

7	28.1009	3.17288	9
8	28.9347	3.08332	13
9	30.9022	2.89134	3
10	31.9173	2.80167	100
11	32.9100	2.71939	53
12	34.0194	2.63320	22
13	35.5074	2.52619	4
14	39.1545	2.29887	8
15	39.8373	2.26103	20
16	42.0425	2.14739	6
17	43.7664	2.06672	5
18	45.2806	2.00107	3
19	46.7014	1.94344	27
20	48.1091	1.88981	11
21	49.4393	1.84204	30

4.3.2 The X-Ray Diffraction of ZnO- Nanoparticles

Figures (4-6) and Table (4-4) show the XRD analysis of zinc oxide nanoparticles at ambient temperature used in this study. All indexed peaks coincide well with those of ZnO (JCPDS Card No.36-1451), this means that a synthetic ZnO nanoparticles have a single crystallinity and relate to wurtzite hexagonal structures. The peaks that's appeared in the sample's XRD data were sharp and intense, indicating that the ZnO nanoparticles were crystalline [124].

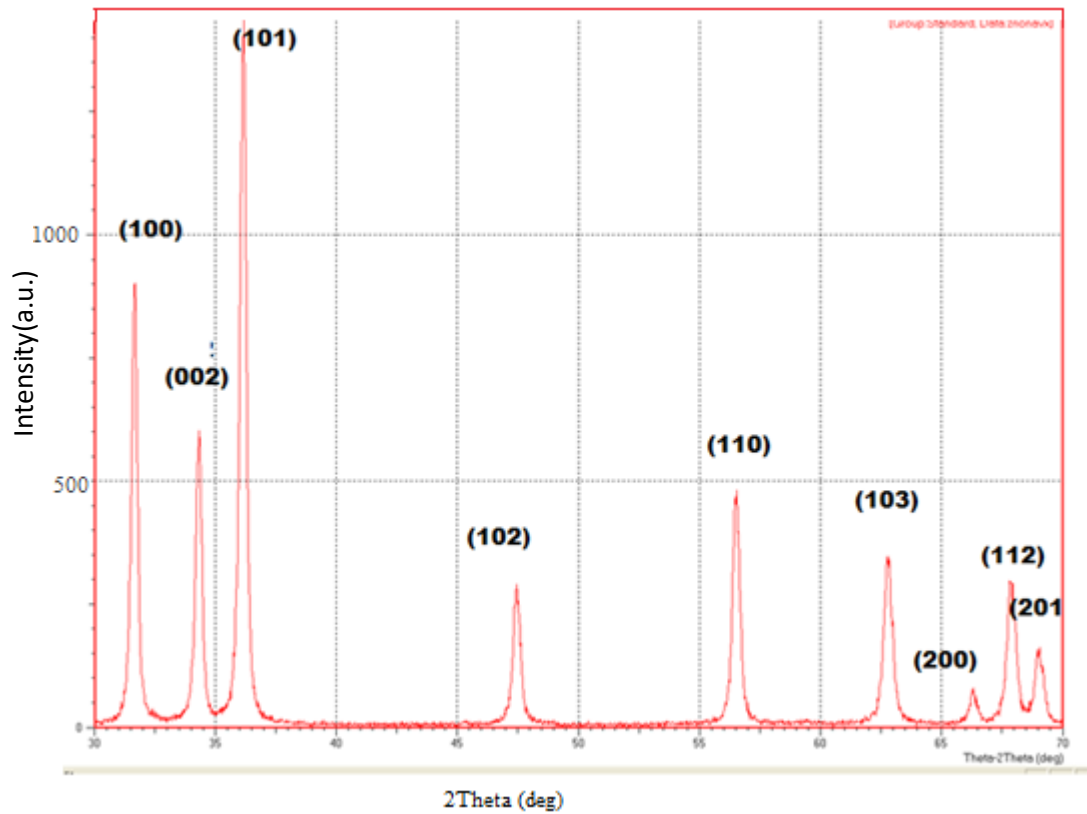


Figure (4-6): X-Ray Diffraction for ZnO-Nanoparticles

Table (4-4) the XRD for ZnO-Nanoparticles

Peak no.	2Theta (deg)	d (Å ^o)	I/I ₁
1	31.699	2.82049	57.1
2	34.382	2.60626	41.6
3	36.182	2.48062	100
4	47.459	1.91416	21
5	56.463	1.62841	29.1
6	62.216	1.47933	25.1
7	66.216	1.41024	3.8
8	67.805	1.38101	20.3

9	68.924	1.36130	10
10	72.472	1.30313	1.6
11	76.786	1.24031	3
12	81.258	1.18297	1.5
13	89.415	1.09497	5.8

4.4 Wettability test

Table (4-5) and Table (4-6) illustrate how adding PEG and various weight fractions of Nano HA effect on the wettability of chitosan film. It is observed that the contact angle decreased with the addition of PEG because PEG is a hydrophilic polymer and has a functional group, which increased the functional groups of chitosan and increased the chances of creating hydrogen bonding between blend and SPF solution, which increased the hydrophilic behavior of polymer [125].

Due to the small particle size of Nano HA (20nm), which does not obstruct the flow of SPF solution within the constructed scaffold, this discrimination of contact angle is also improved with higher amounts of additional Nano HA particles [125].

It is widely assumed that bone-like HA is required for the growth and repairs of the bone-tissue face and the apatite surface can be replicated in vitro at biological temperatures in phosphate buffered saline [126].

overall, reducing contact angle suggests increasing hydrophilicity, which enhances the absorption capacity of the material [81,127].

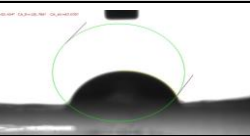
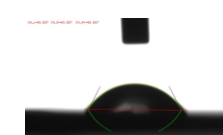
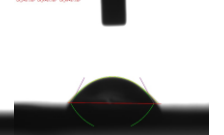
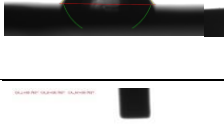
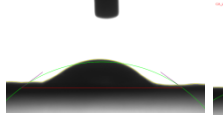
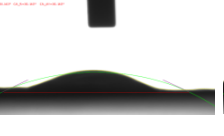
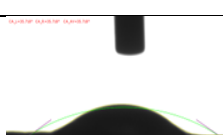
According to the findings of this study, HA loading increased the wettability, thus enhanced the absorption ability of the CS/PEG film, which concenter advantageous for the growth of bone cells on the surface [126]

As shown in Table (4-5) and Table (4-6) the contact angle is decrease due to addition different weight fraction of ZnO nanoparticles. Therefore, when ZnO comes into contact with aqueous medium, many Zn-OH groups form and act as apatite nuclei, activating the formation of bone apatite on the

(CS/PEG/HA) surface in SBF. Recently, Zn is an essential trace element having stimulatory effects on bone formation in vitro and in vivo [99,128].

Zn^{2+} was also found to increase bone protein, calcium content, and alkaline phosphatase rat in vitro [99]. ZnO in the cement can react with water or acid and release a lot of Zn^{+2} , which may help facilitate more rapid new bone formation and thus accelerate bone defect repair [96].

Table (4-5) Contact Angle Image for Blend and Nanocomposite

Time (sec)	0	30	60
Sample			
CS			
Blend(70%CS/ 30%PEG)			
CS/PEG+1% HA			
CS/PEG+2% HA			
CS/PEG+3% HA			
CS/PEG+3% HA+0.3%ZnO			
CS/PEG+3% HA+0.5%ZnO			

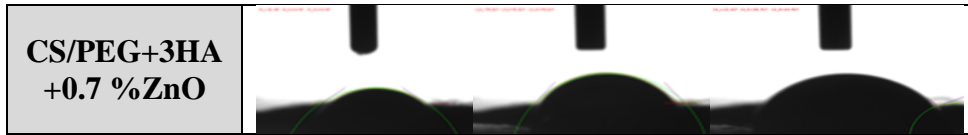


Table (4-6) Contact Angle for Hybrid Nanocomposite

Time (sec)	Contact Angle (°)							
	CS	CS/PEG	(CS/PEG)+ x %HA			(CS/PEG+3% HA)+ x %ZnO		
			1%H A	2%H A	3%H A	0.3%ZnO	0.5%ZnO	0.7%ZnO
0	94	71	70	64	38	35	30	26
30	92	65	64	59	33	32	28	22
60	81	57	59	55	31	30	24	20

4.5 Degree of Swelling Test

The behavior of swelling for the scaffold is one of the important factors that reflected the ability of the scaffold to qualify for in-vitro cell culture study and determined the infiltration and proliferation of cells for osteogenesis and chondrogenesis [125].

The relationship of swelling degree of the blend (CS/PEG) and Nanocomposite in phosphate buffer saline solution (PBS) with different weight fraction of HA nanoparticles is revealed in Figure (4-7) The (CS/PEG) blend has a higher swelling degree due to the nature of PEG being a hydrophilic polymer and soluble in water. Then, the ability of chitosan to up take a high ratio of water increased when blended with it (increased the hydrophilic groups (-OH)) [125]. Furthermore, it supports in the absorption of the cell culture, allowing nutrients to move through easily [130].

The swelling rate decreased with increased the percentage of HA (w.t %) because The number of hydrophilic groups (-OH) decreased due to the consumption of these groups in hydrogen bonding with HA nanoparticles. Despite that, there was no high difference in the swelling rate when adding HA to (CS/PEFG) blend therefore, the swelling rate remain high value that was sufficient to grow living cells [105,125]. This result is a good agreement with other literature [125,108]

When ZnO nanoparticle is added to the nanocomposite, as shown in the Figure (4-8), the swelling rate also gradually decreases, and the best ratio among them was 0.5w.t% of ZnO (365) %. This is because nanoparticles

are getting in between the polymer chains and occupying space, which makes it harder for the PBS liquid to absorb [105].

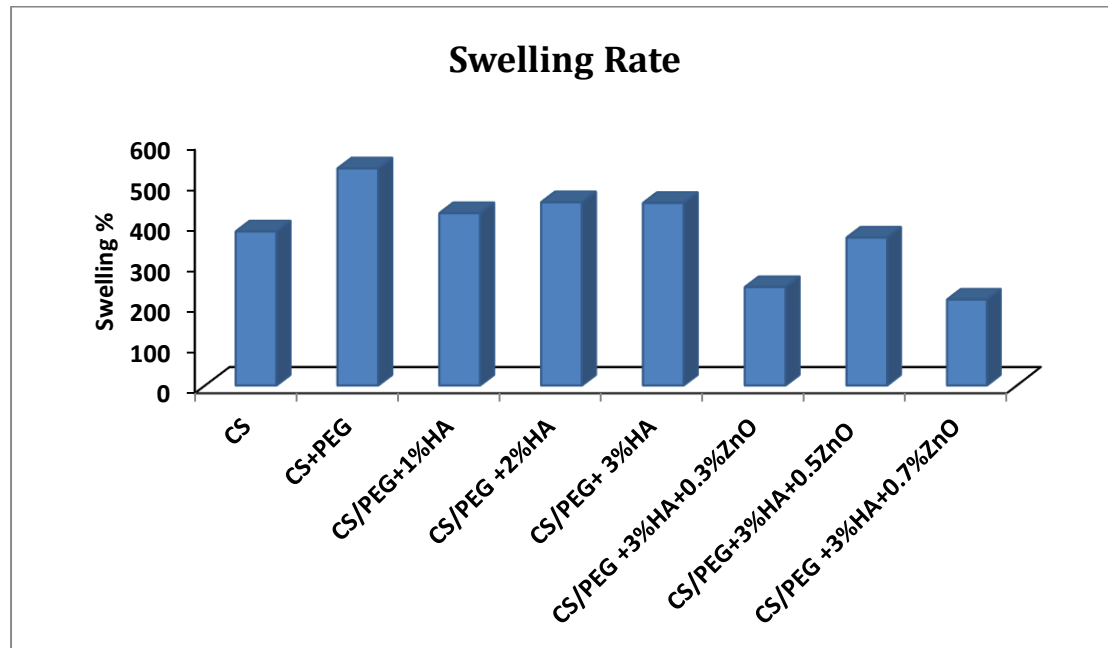


Figure (4-7) Swelling Rate for CS, (CS/PEG) Blend, Hybrid Nanocomposite in PBS

4.6 DSC Analysis

Thermal behavior of chitosan, PEG, the blend CS / PEG, Nanocomposites reinforced with (1,2 and 3) % .w.t HA and Hybrid nanocomposite film (CS: PEG:3%HA: (0.3,0.5,0.7) % .w.t ZnO) are analytic by DSC and exhibit endothermic peaks shown in Figures (4-8) and (4-9). The major characteristic of the chitosan curve is endothermic peak at about 84°C, which relates to film dehydration [131]. Despite the existence of crystalline regions in chitosan, T_m was not revealed due to its rigid-rod polymer structure with strong molecular bonding. Many natural polymers, including cellulose and chitin derivatives, exhibit this behavior [131]. It noticed the curve of neat PEG had melting temperatures (T_m) which was 63.57 °C.

Moreover, the T_m of blend CS/ PEG was dropped to 55.90 °C which It is generally accepted that the T_m corresponding to PEG component of the blend films would decrease owing to the increasing of lattice defects resulted from the partial miscibility of the noncrystalline phase [132].

Additionally, The T_m of nanocomposite increased with the addition of different weight fraction of HA and ZnO nanoparticles (as shown in Table (4-7) It has been postulated that adding nanoparticles has improved the scaffold's thermal stability, possibly as a result of interactions between the four components of the hybrid CS/PEG/n-HAP/n-ZnO [105] and also, due to uniform distribution of nanoparticles within the polymeric matrix chains that restricted the motion of molecules chains [133].

Moreover, the sharp peaks in blend and nanocomposite appropriated to the melting transition of polyethylene glycol segments [135]. The percentage of crystallinity can be determined by divided crystallization lenthalpy (ΔH) by integrating the area under endothermal peak and dividing it with ΔH° , the crystallization enthalpy of the theoretical 100% of PEG. The formula was shown in equation (4-1).

$$X_c = \Delta H / (1-\emptyset) \Delta H^\circ \text{ -----(4-1) [133]}$$

Where ΔH is the apparent enthalpy of fusion per gram of composite, ΔH° is the heat of fusion of a 100% crystalline PEG which is $(182.5) \text{ Jg}^{-1}$ [120] and \emptyset is the weight fraction of the CS and filler in the composites.

The degree of crystallization of the PEG component lowered noticeably as CS was incorporated, suggesting that CS molecules do inhibit the growth of PEG particles in the blend. The interaction between CS and PEG molecules lowered PEG's crystalline abilities, suggesting good interaction among blend substances and great dispersion of nanoparticles within the blend [125].

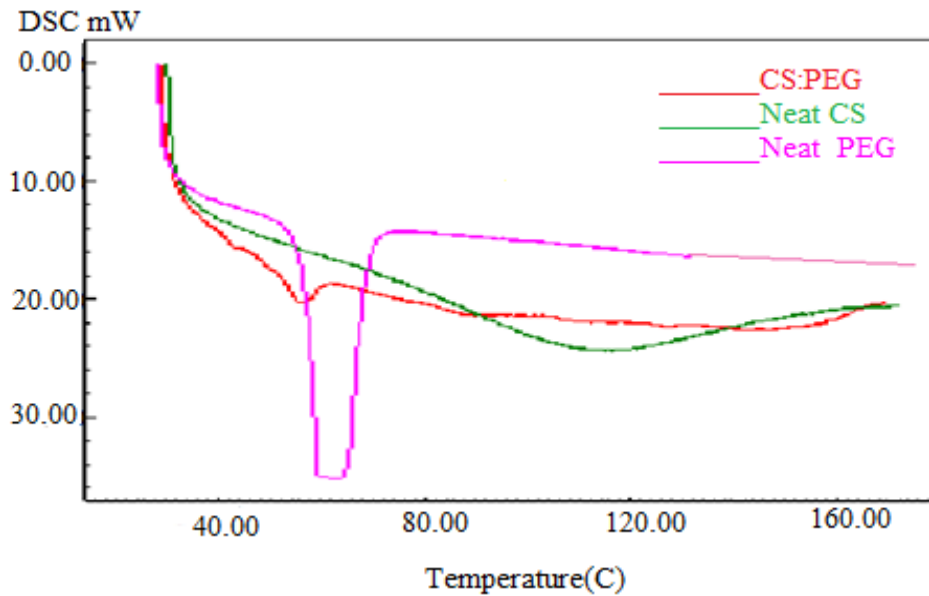


Figure (4-8) DSC for Melting Endotherm and in Nitrogen Atmosphere of Neat CS, PEG, and Blend CS/PEG

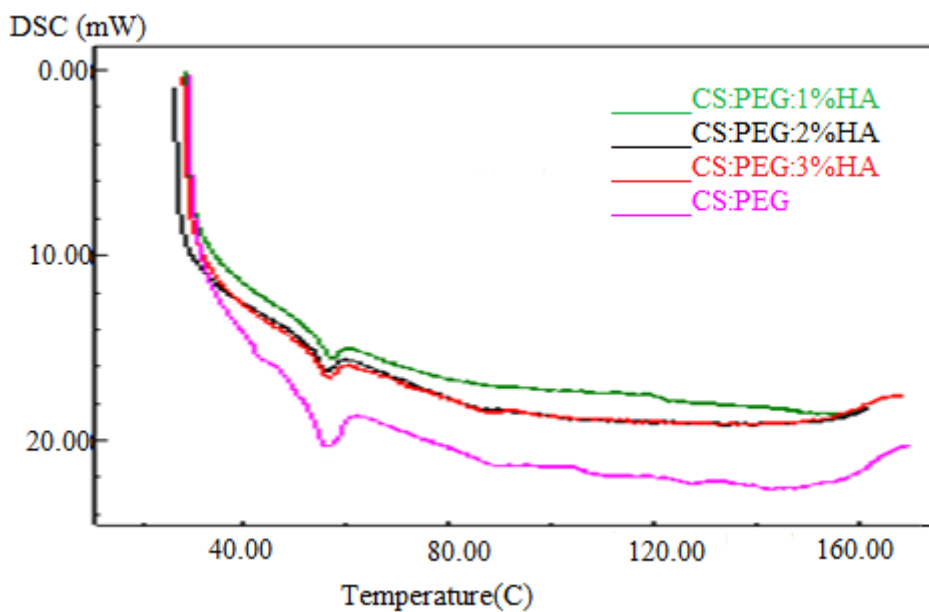


Figure (4-9) DSC for Melting Endotherm at Nitrogen Atmosphere of Blend CS/PEG and Nanocomposite as a Function of HA w.t%

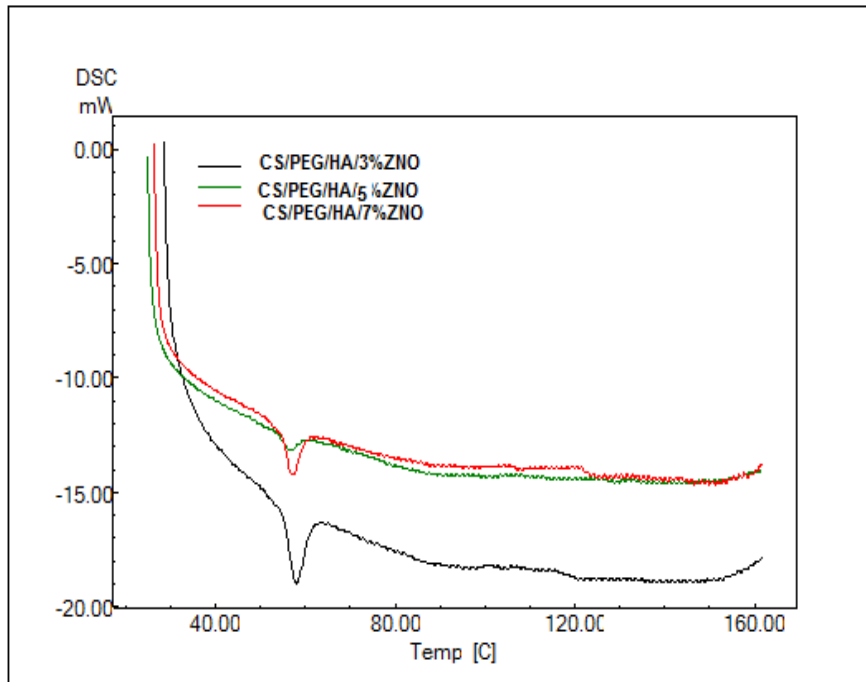


Figure (4-10) DSC for Melting Endotherm at Nitrogen Atmosphere of Hybrid Nanocomposite as a Function of ZnO w.t%

Table (4-7) DSC for Melting Endotherm at Nitrogen Atmosphere for CS/PEG, Nanocomposite film and Hybrid Nanocomposite film

<i>Sample</i>	<i>T_m</i> °C	<i>ΔH</i> J/g	<i>X_{c,PEG}</i> (%)
CS	----	----	----
PEG	63.57	200	109
CS/PEG	55.90	18	33
CS/PEG/1%HA	56	10	11
CS/PEG/2%HA	56.44	9	13
CS/PEG/3%HA	56.60	9.5	15
CS/PEG/3%HA/0.3%ZnO	57	12.02	21.9
CS/PEG/3%HA/0.5%ZnO	57.14	12.5	22.8
CS/PEG/3%HA/0.7%ZnO	57.99	13	23.7

4.7 Tensile test:

4.7.1 Effect Addition PEG and Different Percent of Nano-Hydroxyapatite on Tensile Strength and Elastic Modulus of CS

Figures (4-11) and (4-12) show the effect of blending PEG and addition different weight fractions of hydroxyapatite on the tensile strength and elastic modulus of chitosan (CS).

Furthermore, the tensile strength and elastic modulus of CS increased with the blend of PEG to the CS due to good interaction between the CS and PEG due to created hydrogen bonding between them that behave as physical cross-links sites [120], and the tensile strength increased with increased the percentage of hydroxyapatite due to good adhesion between the blend and reinforcement phase and also due to the nature of particles of hydroxyapatite that is a ceramic material has a high mechanical properties which enhances the tensile strength and elastic modulus of the polymer [126, 134 and 135].

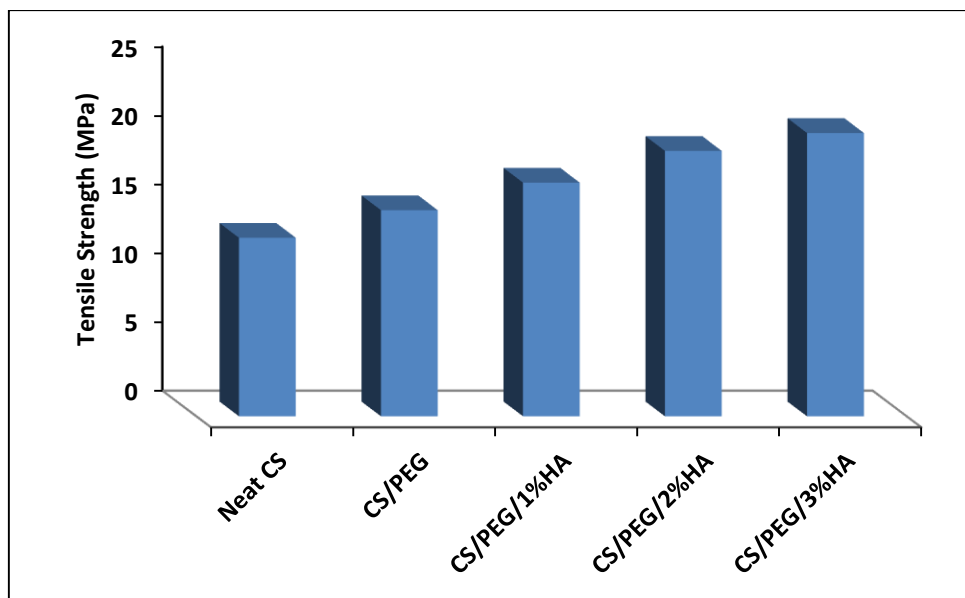


Figure (4-11) Tensile Strength for CS, Blend (CS/PEG) and Nanocomposite as a Function of Different Percent of HA Nanoparticles

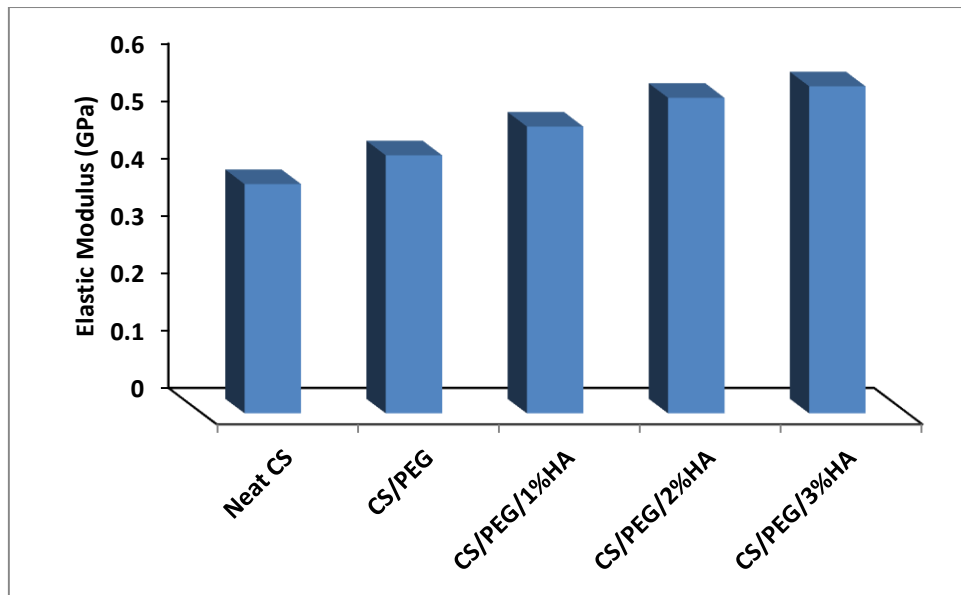


Figure (4-12) Elastic modulus for CS, Blend (CS/PEG) and Nanocomposite as a Function of Different Percent of HA Nanoparticle

4.7.2 Effect Addition PEG and Different Percent of Nano-Hydroxyapatite on elongation of CS

Figure (4-13) exhibit the effect of PEG and nanoparticles of hydroxyapatite on the elongation of CS. From the figure, the elongation increased with PEG addition due to the role of PEG that is used as a plasticizer polymer and also due to creating a hydrogen bond with CS which enhances the elongation of CS [120]. However, the elongation decreased with increased percent of HA because the nanoparticles restricted the motion of the polymer chains as well as there was some agglomerates of nanoparticles which behaved as a defects restricted the elongations [135].

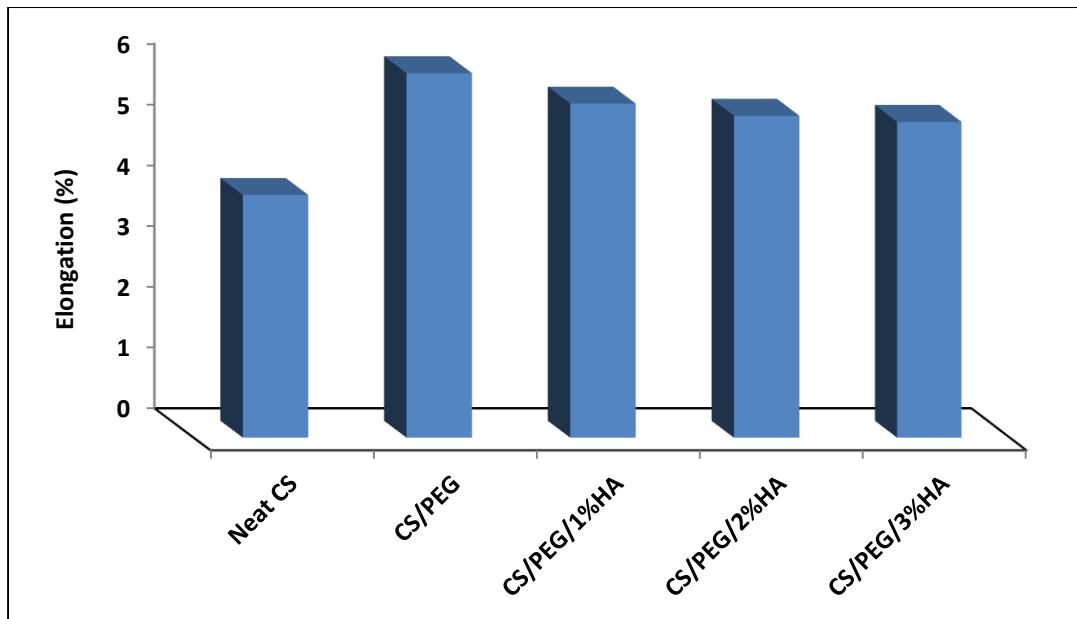


Figure (4-13): Elongation for CS, Blend (CS/PEG) and Nanocomposite as a Function of Different Percent of HA Nanoparticle

4.7.3 Effect Addition Different Percent of Nano- ZnO on Tensile Strength and Elastic Modulus of Nanocomposite (CS/PEG/3%HA)

The effect of the addition ZnO on the tensile strength of nanocomposite material is revealed in Figures (4-14) and elastic modulus shown in Figure (4-15). They increased with the increased of the percentage of nanoparticles of ZnO due to the uniform distribution of ZnO within the matrix thus getting good adhesion between ZnO and Polymer which permit to translate of the load from matrix to nanoparticles which had high mechanical properties which supported the tensile strength and elastic modulus of hybrid nanocomposite [134,135] However when increased the percentage of ZnO over 0.5% the tensile strength and elastic modulus decrease due to agglomerate the ZnO that causes to diminution them [134,135].

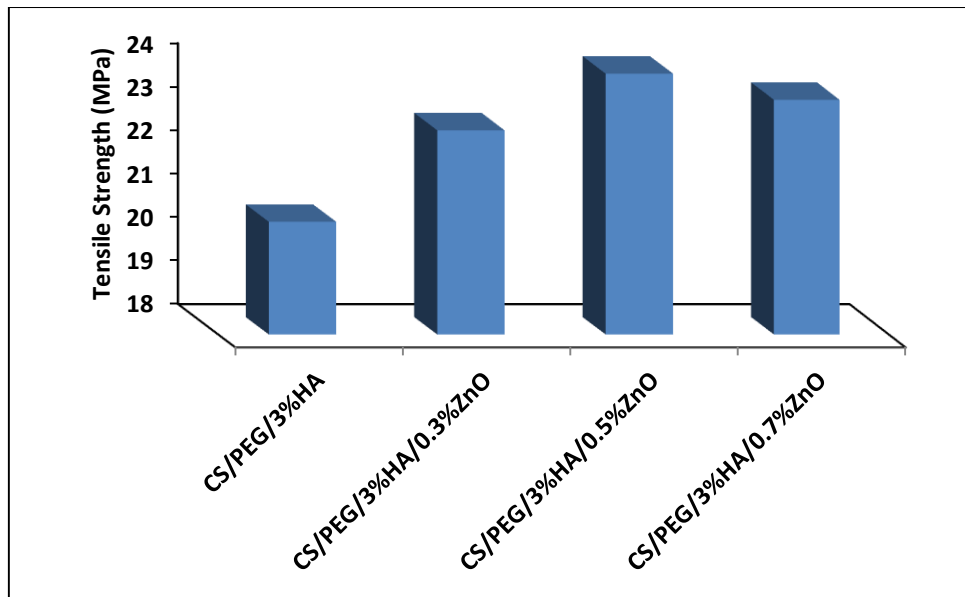


Figure (4-14): Tensile Strength for Hybrid Nanocomposite as a Function of Different Percent of ZnO Nanoparticles

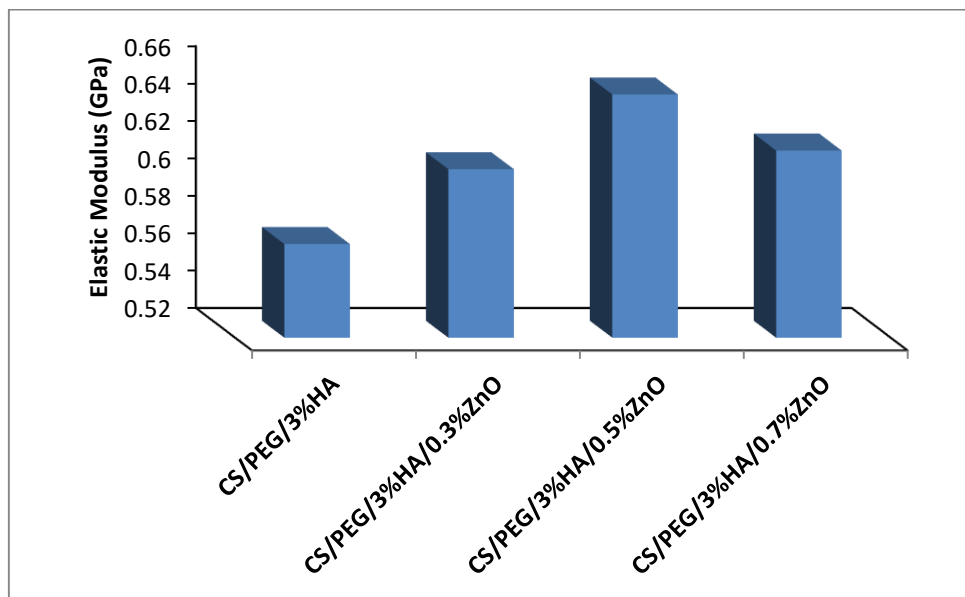


Figure (4-15): Elastic Modulus for Hybrid Nanocomposite as a Function of Different Percent of ZnO Nanoparticles

4.7.4 Effect Addition Different Percent of Nano- ZnO on Elongation of Nanocomposite (CS/PEG/3%HA)

The elongation at the break of the hybrid nanocomposite shows in Figure (4-16). The elongation decreased with increased the weight fraction of ZnO w.t% because these nanoparticles were dispersion within the matrix of

polymer and hind the motion of the chain thus they decreased the elongation [134,136].

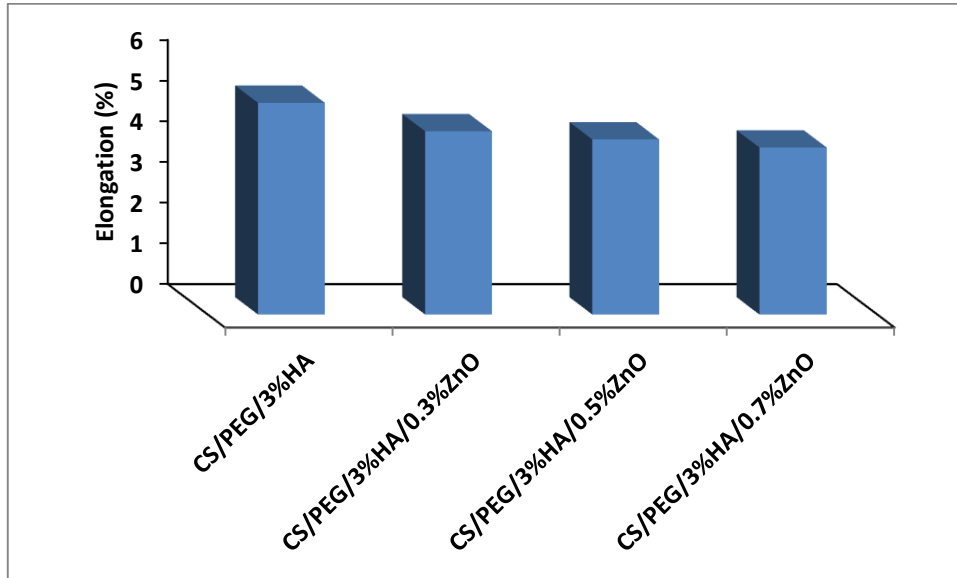
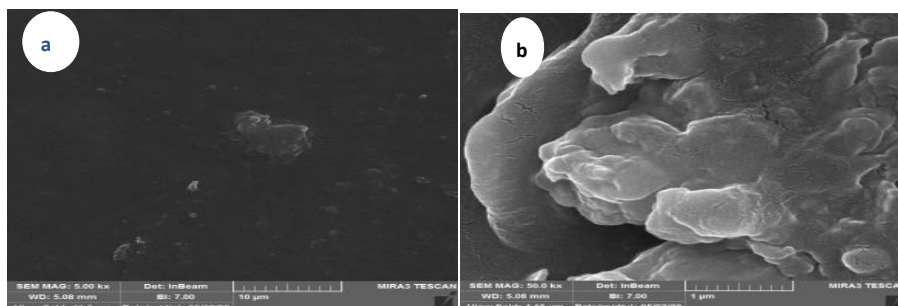


Figure (4-16) Elongation for Hybrid Nanocomposite as a Function of Different Percent of ZnO Nanoparticles

4.8 Morphology Test

A scanning electron microscope can provide information on the morphology and structure of the neat polymer and composite material. It is a device to show the distribution of reinforced phase, particularly for Nanomaterials [134].

Figure (4-17) shows a micrograph of the CS/PEG blend at 10kx, 50kx, 100kx, and 200kx magnifications that reveals a homogeneous structure and the absence of defects and voids. In addition, it contained some small holes and a rough surface as a result of the inclusion of PEG, which promotes the adherence and ingrowth of live cells since PEG changes the morphology of the surface and then develops the surface contact [105].



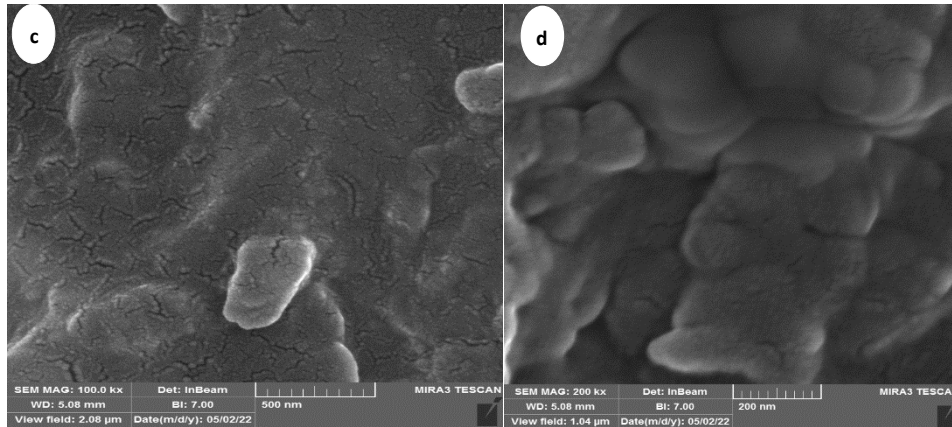


Figure (4-17): FE- SEM of Blend 70CS:30PEG at Magnification a- 5kx b- 50kx c- 100kx d- 200kx

Figure (4-18) displays 50kx, 100kx, and 200kx FE-SEM images of Nanocomposite film. It found that Nano-HA was well distributed throughout the matrix (CS/PEG) and there are good interactions and adhesion among CS/PEG/HA.

Moreover, the uniform distribution of HA was produced from good dispersion of nanoparticles during mixing and dispersion by ultrasonic and also due to create hydrogen bonding between matrix and HA which led to good embedded the HA within the matrix and then enhance the transfer of load from matrix to reinforced particles [134]. Furthermore, the HA particles distribute all over the matrix as small hills that support the Nano-roughness which led to stimulating the growth of fibroblast and osteoblast cells.

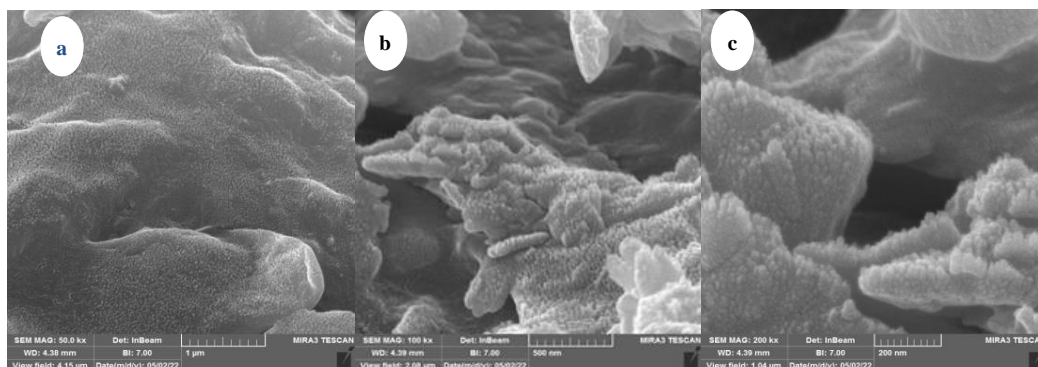


Figure (4-18) FE-SEM of Nanocomposite CS/PEG/3% HA at Magnification a- 50kx b- 100kx c- 200kx

Figure (4-19) displays 30kx, 50kx, and 100kx FE-SEM images of hybrid Nanocomposite film. The ZnO and Ha nanoparticles uniform distributed within the blend (CS/PEG) and dispersion along the surface of polymeric

materials. Moreover, there are some porous which enhance the growth and adhesion living cells on these surface. Additionally, this images are similar the images in literature [108].

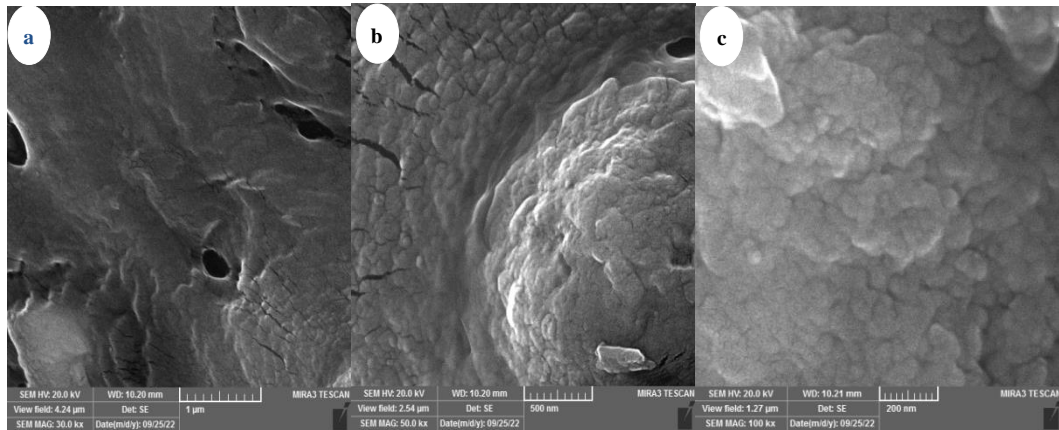


Figure (4-19): FE-SEM of Hybrid Nanocomposite CS/PEG/3%HA/0.5%ZnO at Magnification a- 30kx b- 50kx c- 100kx

4.9 AFM Test

To study the effect of adding polyethylene glycol and nanoparticles on the nature of the polymeric surface, a three-dimensional topography images of surfaces of neat chitosan, (CS/PEG)blend and nanocomposites shown in the Figure (4-20), and the Table (4-8) also shows the parameters of roughness, The results indicated that Chitosan film has the roughness surface with average S_a (18.4nm) and S_q (24nm) and the surface roughness increased by adding 30%PEG and became S_a (19)nm and S_q (25)nm due to the role of PEG which used as plasticizer that increased the ductile of CS which causes to increase the roughness of CS[132].

When adding hydroxyapatite nanoparticles, the surface roughness S_a , S_q decreases with the increase in the percent of HA, moreover, when adding zinc oxide nanoparticles, the roughness is decreased with increased the ZnO w.t%, because these Nanoparticles (HA and ZnO) dispersion between the polymeric chains and filled the voids which decreased the surface roughness [134].

Skewness (S_{sk}), the other surface variable, describes the symmetrical variation of nanostructures on surfaces from its average plane [111]. When S_{sk} is below 0, height distribution of surface nanoparticles skewed below

the mean plane, also if $S_{sk} < 0$ it can be bear surface with holes, if $S_{sk} > 0$ it can be flat surface with peaks, S_{sk} greater than 1 indicate extremely holes and peak on the surface. So as shown in Table below by adding Nano HA, ZnO, The S_{sk} is higher than zero so it indicated that the surface was flat surface with peak and there is good distribution of nanoparticles [111], which is clear from 3D image that clarify the uniform distribution of the hill along the surface [93].

Kurtosis (S_{ku}), gives the sharpness of the surface. When S_{ku} is above 3, it shows that all nanoparticles have sharper surface. From Table (4-7) the S_{ku} is more than 3 therefore the sharpness of surfaces was increased with the increase the addition of nanoparticles (especially HA had needle shape) which enhances the adhesion and growth of living cells on the scaffold thus gives a rapid and complete growth rate [111]. Moreover, the S_{ds} which is the density of summits was decreased with blended PEG with CS. However, it increased with reinforced this blend with HA and ZnO nanoparticles that referred to increase the asperities which also supported the adhesion process of living cells on the surface of scaffold [137].

Another parameter of roughness is the surface bearing index (S_{bi}) which is a function of the mechanical properties. From Figure (4-21) surface bearing index is increased with blend CS with PEG and reinforced with nanoparticles (HA, ZnO) w.t% that supported the results of the tensile test that referred to improve the mechanical properties of CS [137].

Finally, the core fluid retention index (S_{ci}) was increased as blend PEG with the CS that indicated to increase the fluid absorption due to nature of PEG is a hydrophilic material increased the absorption of the fluid. However, this parameter was decreased with increased he percent of nanoparticles (HA, ZnO) w.t%, it indicates to decreased the fluid absorption that accepted with the results of swelling test which is previous interpreted to penetration of nanoparticles between the polymeric the chains that leded to decreased the spaces among the chains thus it decreased the amount of absorption fluid [134,136].

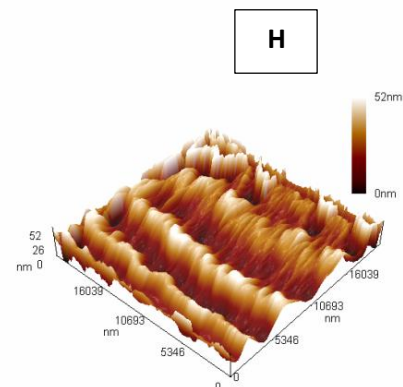
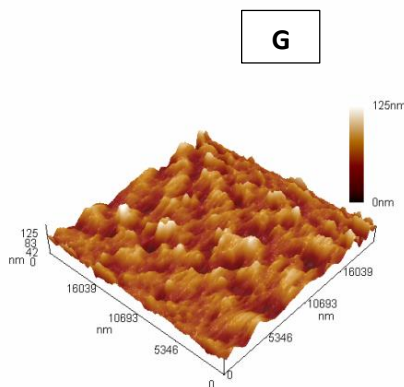
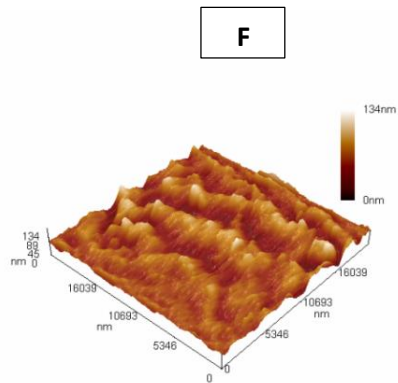
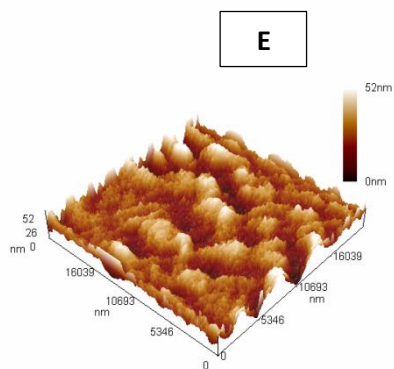
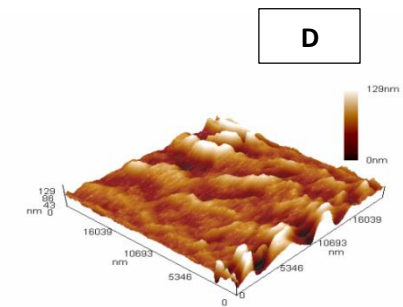
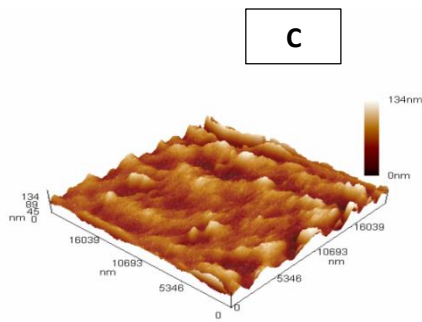
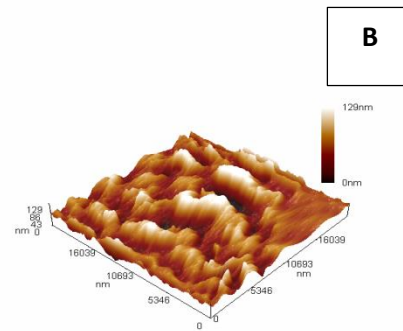
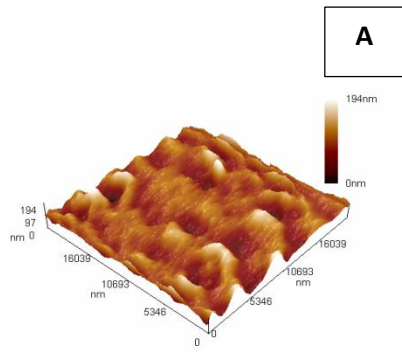


Figure (4.20): 3D AFM Image of A- Neat CS B-CS/PEG Blend C- (CS/PEG)+1%HA D- (CS/PEG)+2%HA E-(CS/PEG)+3%HA F- (CS/PEG/3%HA)+0.3%ZnO G) (CS/PEG/3%HA)+0.5%ZnO H) (CS/PEG/3%HA)+0.7%ZnO

Table (4-8) Shows the Parameters of Roughness of AFM Test

Sample	S _a (nm)	S _q (nm)	S _{bi}	S _{ci}	S _{sk}	S _{ku}	S _{ds}
CS	18.4	24	0.438	1.60	0.136	3.94	0.110
CS/PEG	19	25	0.454	1.63	0.0145	3.33	0.0153
CS/PEG/1%HA	17	23	0.495	1.61	0.0506	3.51	0.0166
CS/PEG/2%HA	16	21	0.738	1.59	0.0672	3.86	0.0197
CS/PEG/3%HA	14	18	0.867	1.57	0.0698	4.35	0.0254
CS/PEG/3%HA/0.3%ZnO	13	16	1.08	1.55	0.0774	3.43	0.0318
CS/PEG/3%HA/0.5%ZnO	11	14	1.63	1.53	0.0821	3.65	0.0394
CS/PEG/3%HA/0.7%ZnO	10	13	1.38	1.53	0.106	4.63	0.0436

4.10 Degradation Test

Degradation rate is the most important factor for degradable polymeric scaffold. When scaffold has an appropriate rate of degradation, it will encourage cells to grow and stimulate new tissue creation. Neat CS, CS/PEG blend, nanocomposite film(CS/PEG/HA), Hybrid nanocomposite film(CS/PEG/HA/ZnO). It has been shown from the Figure (4-21) that the blend CS/PEG have the highest degradation rate. The addition of PEG increased the degradation potential for all given times, which can be clarified by a rise in the porosity of the CS/PEG as compared to CS due to the presence of PEG which is hydrophilic in nature [84].

Indeed, these results show that the addition of a plasticizer improves the degradation of biofilms. These results are in agreement with those obtained by Stefani et al., [83].

The ionic interaction between the PBS solution and the functional groups of the chitosan in the composite was essential for the chitosan to degrade and eventually decrease the absorption of the solution. However, a maximum of degradation ratio was reached on the 1th day, followed by a steady decline in degradation rate until the 5th and lost its initial shape after 5th days figure (4-21). Degradation rate of composite scaffolds is decreased with increased (HA and ZnO)w.t% nanoparticles more than neat

scaffolds. The decreasing in degradation rate of this scaffolds due to the higher chemical stability of nanoparticles and uniformly distributed throughout of scaffolds, this led to resisting the PBS solution seepage into the scaffold architecture. Increase the concentration of nanoparticle in the nanocomposite scaffolds also decreased the degradation rate [138].

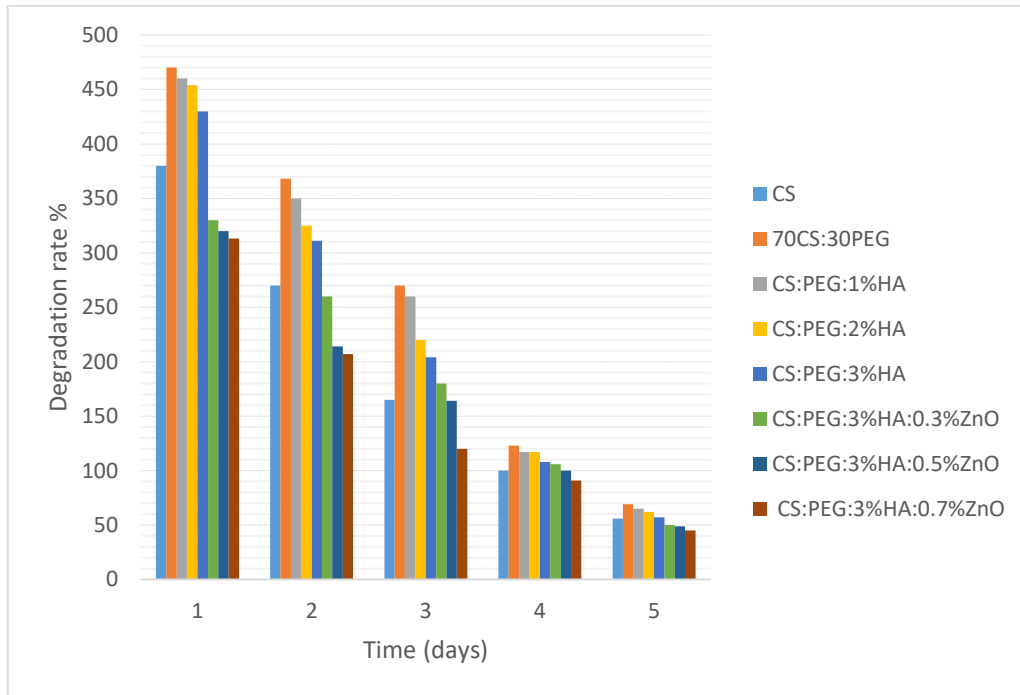


Figure (4-21): Degradation Rate for CS, CS/PEG Blend, Nanocomposite with Ha w.t.% and Hybrid Nanocomposite

4.11 Antibacterial Test

4.11.1 Antibacterial for Neat Chitosan, CS/PEG Blend and Nano composite

The test of antibacterial must be carried out on the bone scaffold to evaluate the ability of the prepared scaffold to resist bacterial infection. Figures (4-22) and (4-23) show the inhabitation zone against the E-Coli (Negative gram) and S.aureus (Positive gram). The neat Chitosan exhibited the highest inhibition zone because is an antibacterial polymer due to the positive charge of amino groups that don't interact with the membranes of bacteria [139].

The inhibition zone was decreased when adding PEG (blend CS/PEG) because the PEG doesn't have antibacterial properties so, it reduces the

inhibition zone [131,140]. Moreover, the inhibition of the blend decreased with the addition of nanoparticles hydroxyapatite due to some agglomerations of HA during the preparation process of the film which affects the antibacterial activity of HA. However, when increased the percentage of HA , the inhibition zone increases due to the Hydroxyapatite Nanoparticles are antibacterial particles that deactivate the bacterial grovel and spores so that the efficiency of bactericidal became higher [141] .

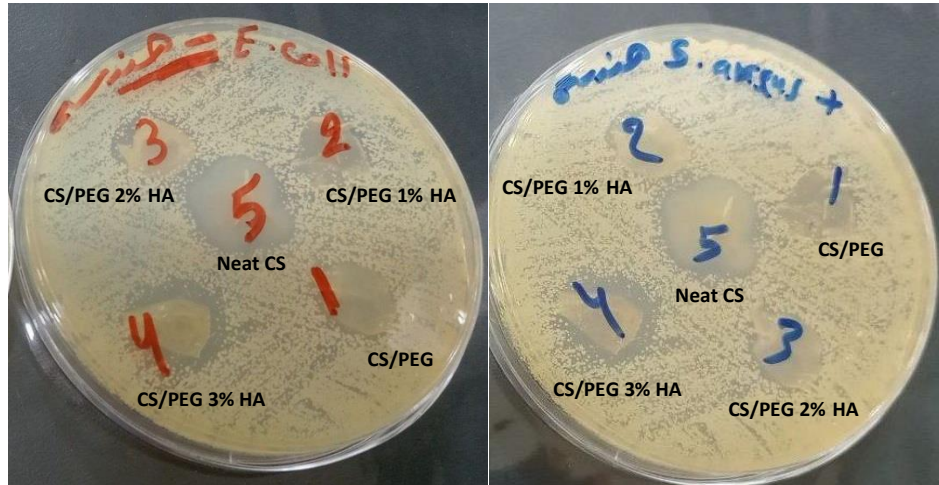


Figure (4-22) Illustrated The Inhibition Area of Neat CS, CS/PEG Blend, and Polymer Blend Nano Composites for E. coli and Staphylococcus Colony.

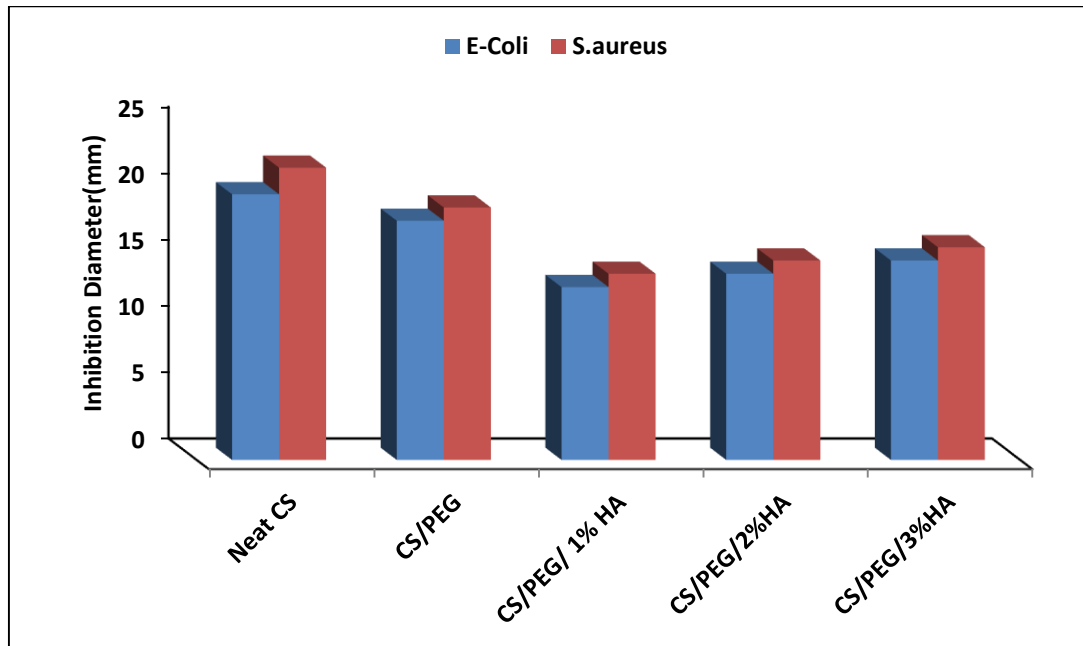


Figure (4- 23): Inhibition Diameter of Neat CS, CS/PEG Blend, and Nanocomposites as a Function of HA-Nanoparticles Content in Composite.

4.11.2 Antibacterial for Hybrid Nanocomposite

The bactericidal activity of three distinct nanocomposite films was investigated Figures (4-24) and (4-25). Among the *S. aureus*, and *E. coli*. According to results, all the films show inhibitory effect against these bacteria. Furthermore, they have inhibition zone more than inhibition zone at nanocomposite reinforced with just Nanoparticles of HA due to synergetic effect of HA and ZnO nanoparticles against these bacteria due to these nanoparticles are antibacterial materials [131].

Moreover, the inhibition behavior of ZnO is believed to have antibacterial properties that may result from its ability to completely cover its surface with oxygen from ZnO, which would be disrupting the bacteria's membrane [142].



Figure (4-24): Illustrated The Inhibition Area of Hybrid Nanocomposites for *E. coli* and *Staphylococcus* Colony.

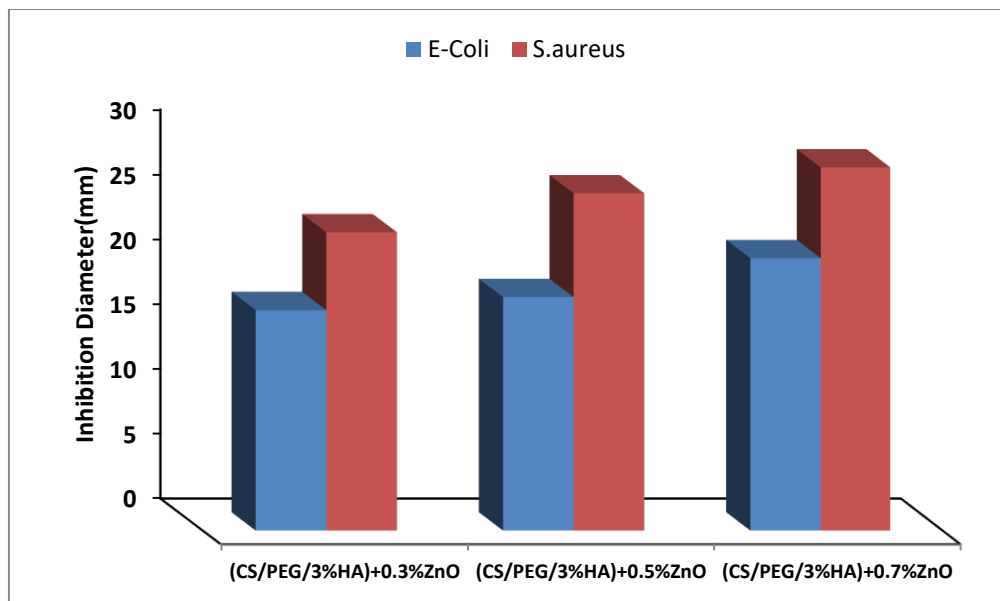


Figure (4-25): Inhibition Diameter of Hybrid Nanocomposites as a Function of ZnO-Nanoparticles Content in Composite.

4.12 MTT assay

The MTT test was performed on a hybrid nanocomposite film to evaluate the cytotoxicity of the fabricated composites as well as their biocompatibility, which is an important factor for applications in tissue engineering for bone, a scaffold cannot be used effectively unless it can be made biocompatible with human bone cells [122]. In vitro, MTT assay was carried out by implanting two types of cells, human osteoblastic (MG-63) cells and Human Dermal Fibroblast normal (HdFn) cells. The MTT assay studies revealed higher cell proliferation in nanocomposite film (70CS:30PEG :3%HA:0.5%ZnO). The results of HdFn cells showed that Cell viability obtained a high percentage on the first day(24hr.), reaching 97%, a good percentage that supports cell adhesion and growth on the scaffold, as well as supports the fact that the scaffold is safe and for 48 hr.the cell viability record 90% and still within the acceptable and biocompatible, as well as at 72hr. the percentage reaches approximately 85%, and this is normal, because the cells have absorbed most of the nutrients through the time, in other side the evaluation of the improved scaffolds' biocompatibility revealed that they were cytocompatible and had no detrimental effects on osteoblast-like MG-63 cells. [131] MG-63 cell viability remains stable at 80% in 24,48 hr. and 75% at 72 hr. the same

state in HdFn due to consumption of nutrients. These results suggest the films' excellent biocompatibility and may remain optimistic for their potential usage in biological applications. (Level of significance $p < 0.05$), which greatly helped to increase cell viability proven that these nanocomposites can effectively increase the number of human osteoblastic MG 63 cells [143]. also This shows that the recently made scaffolds aid in the growth, adhesion, and proliferation of osteoblast-like cells.

To obtain further information on cellular adhesion, optical microscopy was used to observe the distribution of MG-63 cell line.

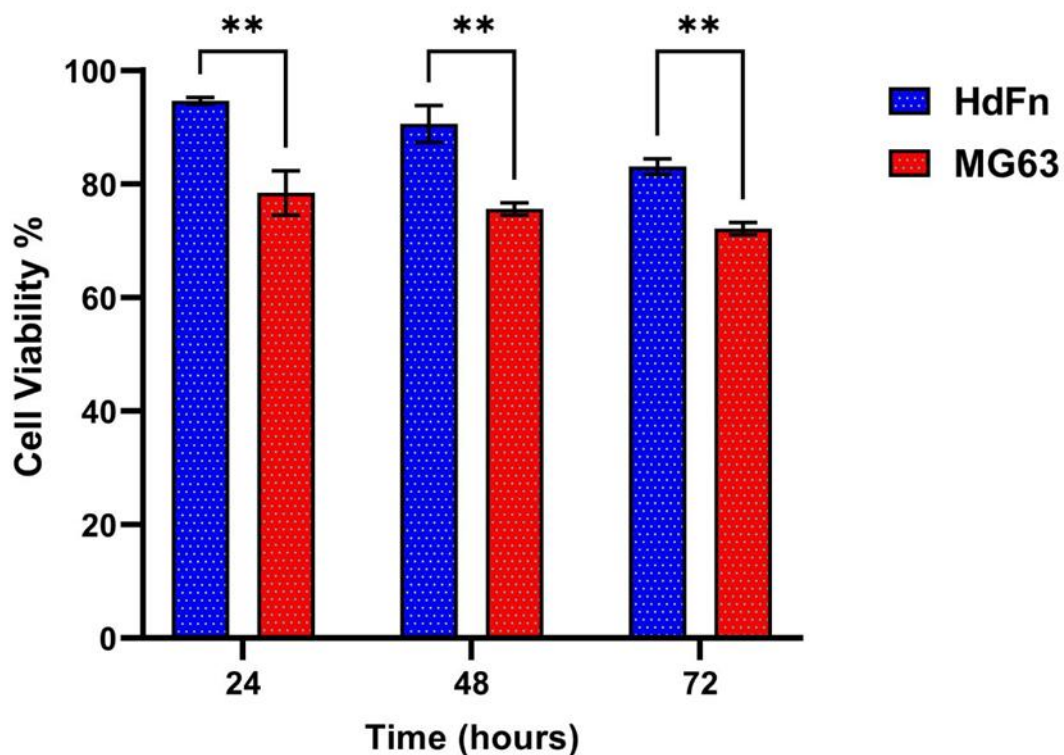


Figure (4-26): Inverted Cell Viability of MG-63, HdFn cells grown over (a)24 hr. (b) 48hr. (c) 72 hr.

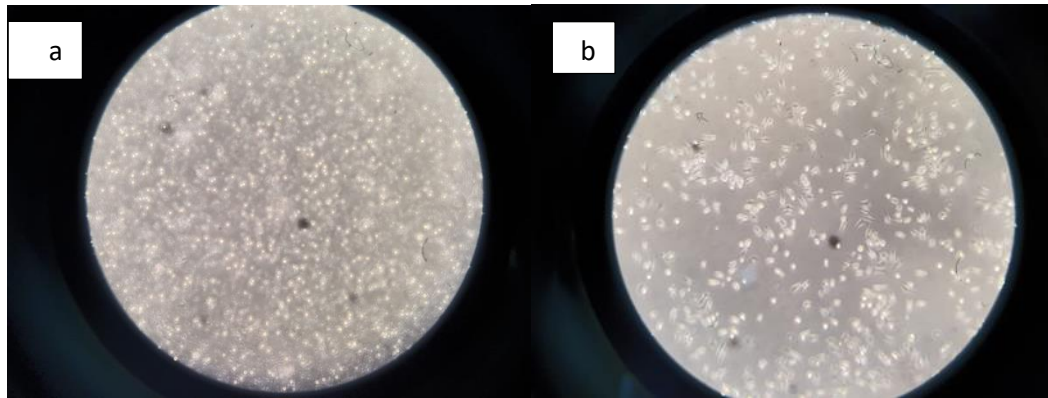


Figure (4-27): Optical Microscopy Image was Used to Observe The Distribution of MG-63 Cell Line (a)after 24hr, (b)after 72 hr.

4.3 Tests for Cross-linked Blend, Nanocomposite and Hybrid Nanocomposite Film

4.3.1 FTIR for Cross-linked Blend, Nanocomposite, Hybrid nanocomposite (CS/PEG/HA/ZnO/GA)

The FTIR spectrum of the cross-linked Chitosan/PEG presented in Figure (28-4) the O-H stretching bands shifted to 3417 cm^{-1} , and C=O amind I at 1635 cm^{-1} which has increased intensity and has moved to a higher wavenumber when compared with the C=O bending vibration of uncross linked blend CS/PEG at 1619 cm^{-1} . And for Nanocomposite (CS/PEG/HA/GA) the O-H peak at 3425 cm^{-1} and CH_2 stretching was shifted to 2870 cm^{-1} while C=O at 1620 cm^{-1} .

The IR spectra of cross-linked Hybrid Nanocomposite (CS/PEG/3%HA/0.5%ZnO) +0.02%GA shows in Figure (4-30) and listed in Table (4-9) there's shifting at 3417 cm^{-1} for O-H compare with uncross linked hybrid film, The NH band shifted to 1411 cm^{-1} , respectively. This can be attributed to the effective crosslinking of chitosan with glutaraldehyde, which occurred at the amino groups of chitosan [109]

Table (4-9): FTIR for CS/PEG Blend, Nanocomposite, Hybrid Cross-linked with GA

Type of Band	Cs/PEG/GA	Cs/PEG/HA /GA	Cs/PEG/HA/ ZnO/GA
OH	3417	3425	3417
C_H stretching	2885	2870	2885
C=O (Amind I)	1635	1620	1620
N-H (Amind II)	1419	1419	1411
P-O	-----	1111	1111
Zn-O	-----	-----	563-648

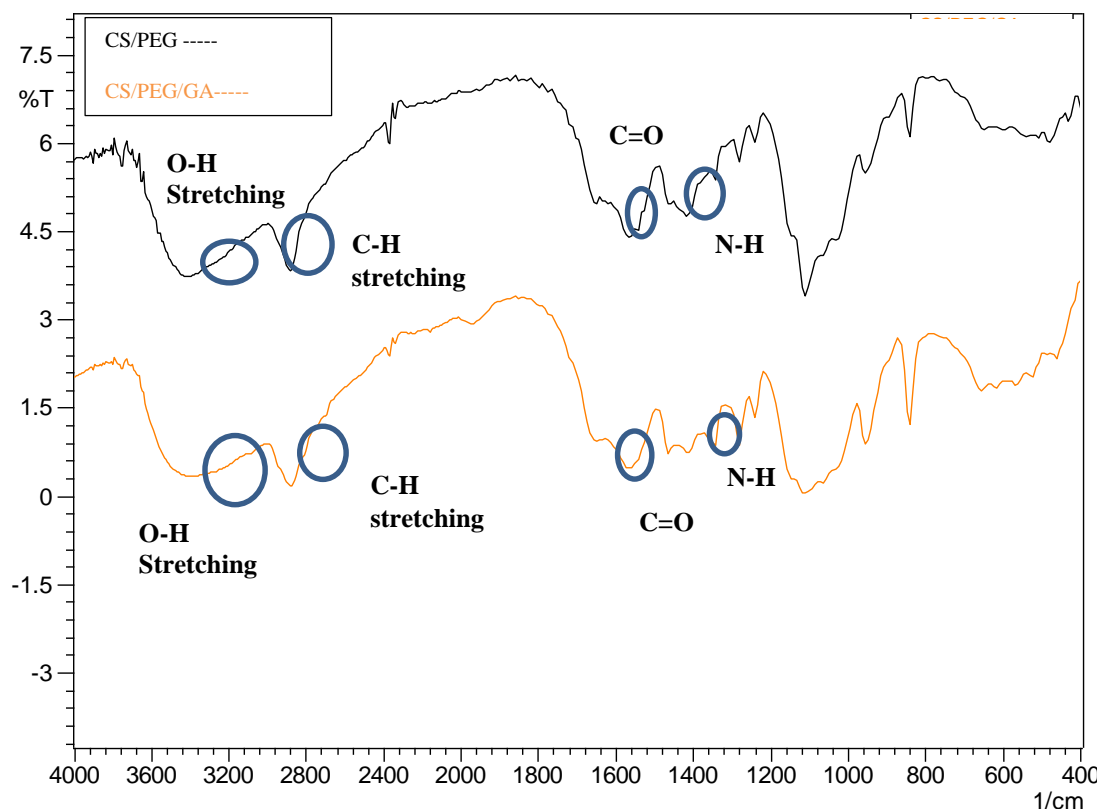


Figure (4-28): FTIR for Cross linked and Uncross linked CS/PEG Blend

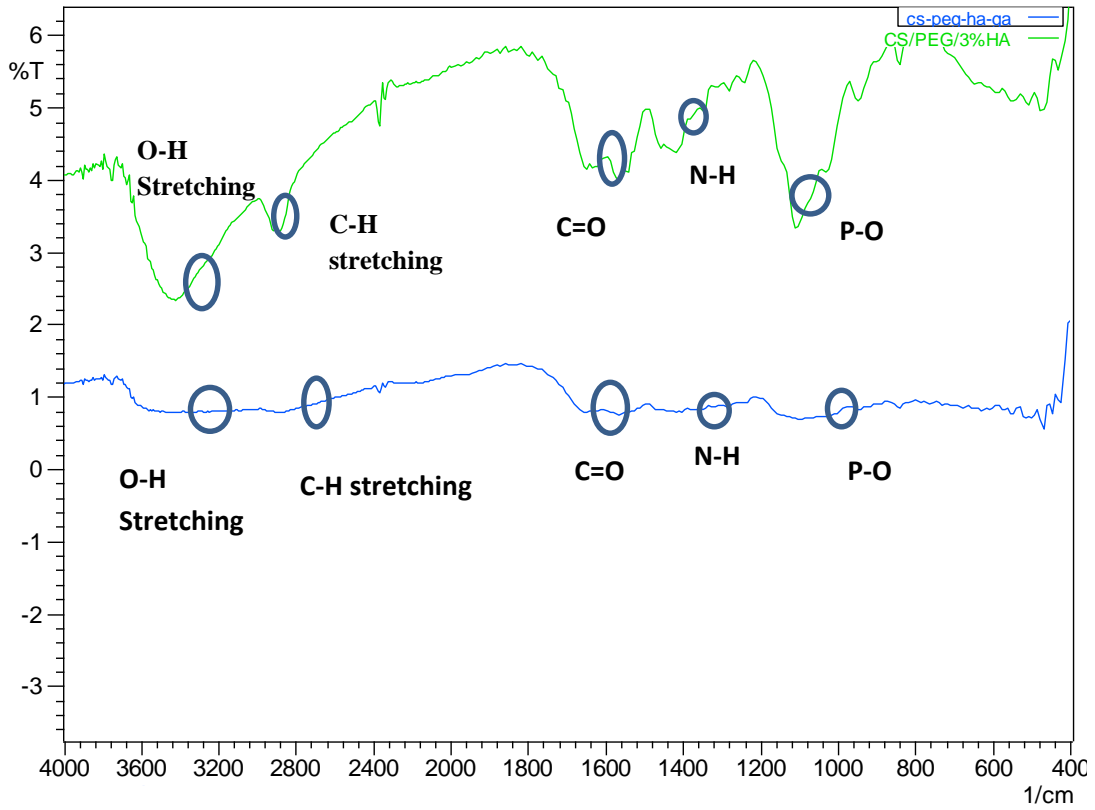


Figure (4-29): FTIR for Cross linked and Uncross linked Nanocomposite CS/PEG /3%HA

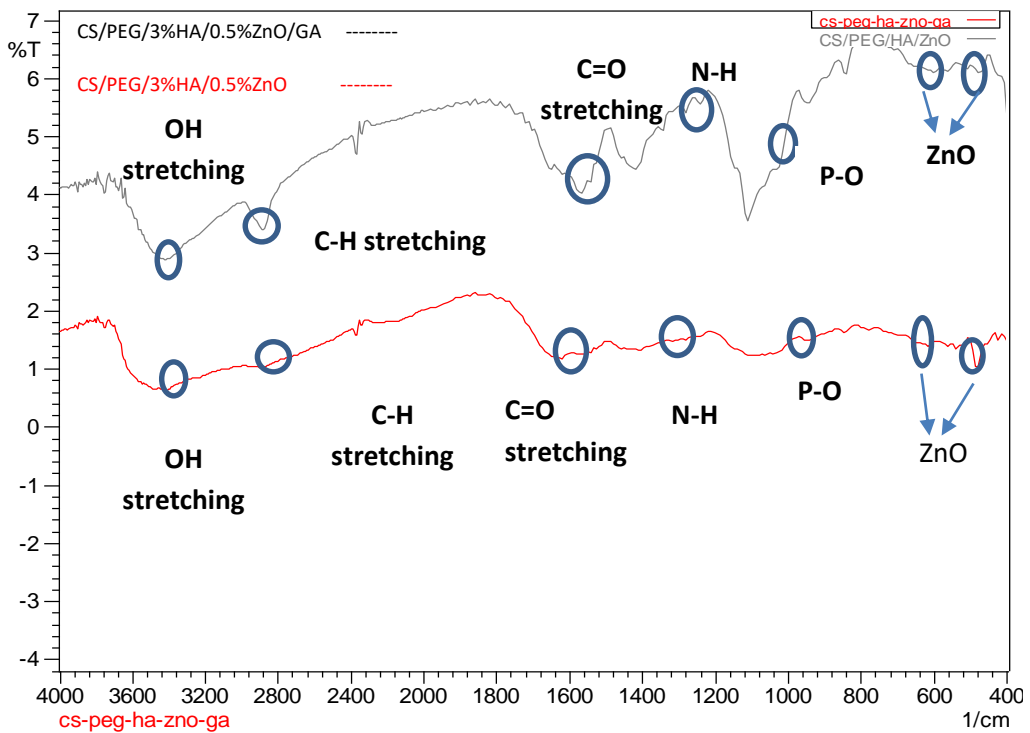


Figure (4-30): FTIR for Cross-linked and Uncross-linked Hybrid Nanocomposite

4.3.2 Wettability for Cross-linked Blend, Nanocomposite with HA, Hybrid nanocomposite

To evaluate the effect of the crosslinking process on change in hydrophilicity/hydrophobicity of the scaffolds, the contact angles were measured at various time intervals (0s, 30s and 60s). The contact angles for blend CS/PEG/GA significantly decreased after crosslinking, which indicated that the crosslinked blend were hydrophilic [144].

As shown in Table (4-10) contact angle increase when adding crosslinker glutaraldehyde for Nano composite film with 3%HA the contact angle increased to 42° also adding the crosslinker to Nanocomposite blend with 0.5% increased to 73° at 0 second compare with crosslinked blend and nanocomposite film.

Moreover, the blend crosslinked with GA showed higher wettability compared to its nanocomposite and hybrid nanocomposite, demonstrating that the developed film's surface wettability was reduced by the GA's moderate hydrophobic nature. Furthermore, the values show in Table (4-10)

Table (4-10): Contact angle for CS/PEG blend, Nanocomposite Nanocomposite as a Function of HA 3%, Hybrid nanocomposite (0.5%ZnO) Cross-linked with GA

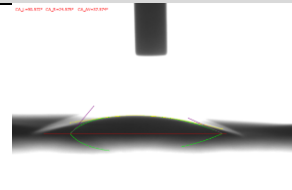
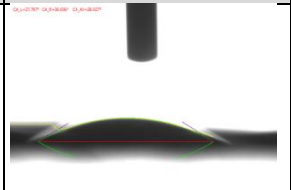
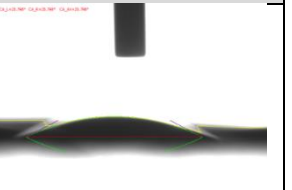
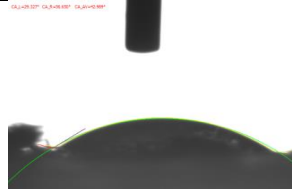
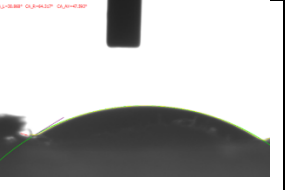
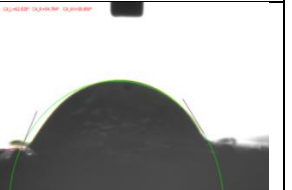
Sample	Time(Sec)		
	0	30	60
CS/PEG/ 0.02%GA			
CS/PEG/ 3%HA/0. 02%GA			
CS/PEG/ 3%HA/0. 5%ZnO/0 .02%GA			

Table (4-11): Contact Angle for(CS/PEG) blend, Nanocomposite as a Function of HA w.t% film, Hybrid film(3%HA,0.5%ZnO) Cross-linked with GA

Time (sec)	Contact Angle(°)		
	CS/PEG/0.02 %GA	CS/PEG/3%HA/0.0 2%GA	CS/PEG/3%HA/0.5% Zno/0.02%GA
0	30	42	73
30	27	48	66
60	25	45	58

4.3.3 Tensile Test for Cross-linked with GA

4.3.3.1 Effect Addition GA on Tensile Strength of Blend, Nano composite and Hybrid Nanocomposite

Figure (4-29) depicts the blend(CS/PEG), Nanocomposite(CS/PEG/HA), Hybrid(CS/PEG/HA/ZnO) cross-linked with glutaraldehyde. However, Chitosan induces crosslinking between glutaraldehyde and amine groups (NH₂) Since free amino groups in chitosan are very active to cross-linking between aldehyde groups, whenever activated, the aldehyde molecule attaches to (amine groups) and bonds between CS/PEG, bringing CS/PEG matrix closer [145].

Moreover, the addition of glutaraldehyde by 0.02% reducing tensile strength of blend compare with uncrosslinked film because films become brittle, chitosan glutaraldehyde has a variety of drawbacks, including brittleness. Although if the linkages that form become closer as glutaraldehyde is added [145-146].

However, compared to uncrossed films, tensile strength decreased after the addition of filler (3, and 0.5 wt%) of HA, ZnO because of significant reactions between the nanoparticle, glutaraldehyde and matrix, so that limited the movement of the matrix and reduced tensile. They serve as stress concentrators, preventing stress applied to the films from passing from the matrix to the filler, which causes the films to fail earlier [147].

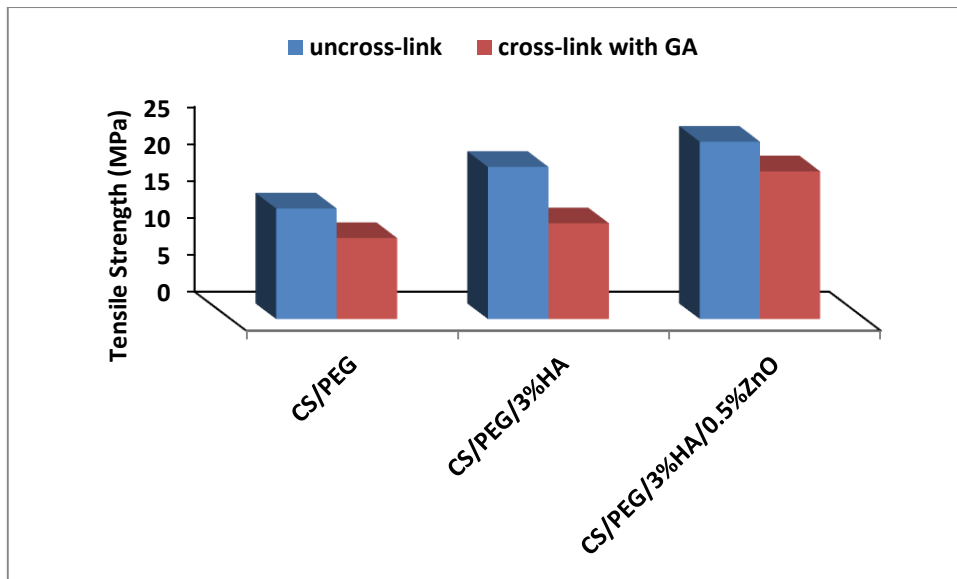


Figure (4-31): Tensile Strength for Crosslinked Blend, Nanocomposite as a Function of HA w.t%, Hybrid Nanocomposite

4.3.3.2 Effect Addition GA on Elastic Modulus of Blend, Nano composite and Hybrid Nanocomposite

Figure (4-30) the addition of glutaraldehyde decreased the elastic modulus in the blend. Made the film more brittle, which limited the motion of the polymer and therefore reduce elastic modulus [147].

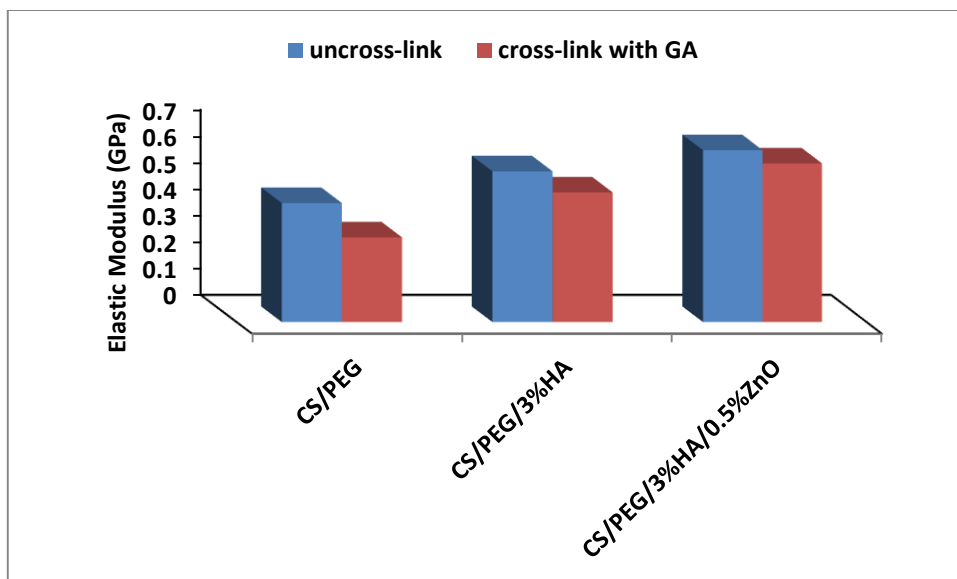


Figure (4-32): Elastic Modulus for Cross-linked Blend, Nanocomposite, Hybrid Nanocomposite

4.3.3.3 Effect Addition of GA on Elongation of Blend, Nanocomposite and Hybrid Nanocomposite

As shown in Figure (4-31) the addition of glutaraldehyde decreased the elongation value comparing with uncross- linked films. This decreasing in elongation values indicated that the addition of chitosan and glutaraldehyde into chitosan matrix resulted in strong interactions between them, limiting composite movement and thus reducing elongation [145-147].

There was a decreasing of Elongation after addition glutaraldehyde in hybrid film revealed that a cross-linked structure had formed, limiting the motion of the polymer chain [147].

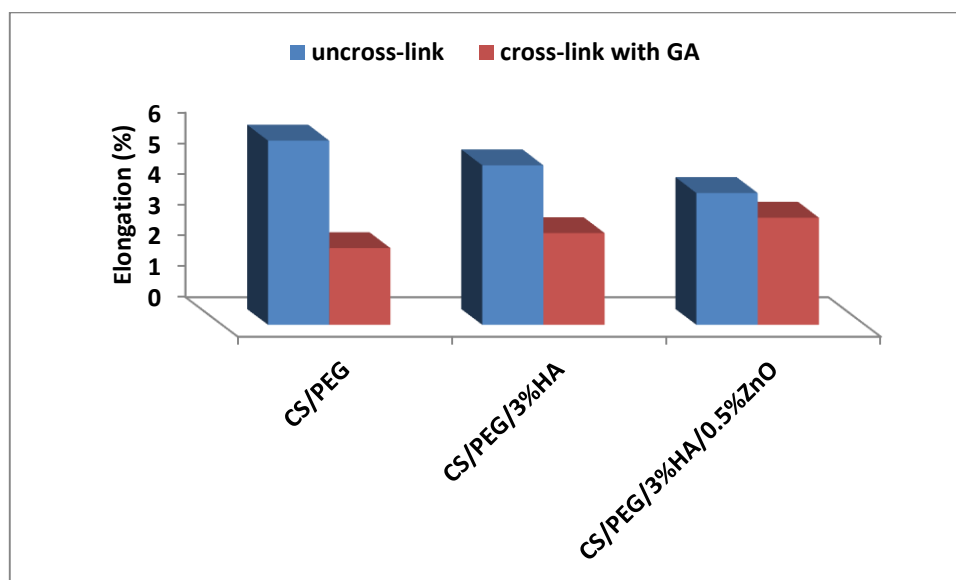


Figure (4-33): Elongation for Crosslinked Blend, Nanocomposite, Hybrid Nanocomposite

Chapter Five

5.1 Conclusions

1-FTIR results show that there's a good interaction between the components and there is not chemical bond between the components of the blend. The FTIR spectra exhibited the formation of hydrogen bonds between chitosan and polyethylene glycol as well as the formation of a hydrogen bond between the blend (CS/PEG) and nanoparticles of hydroxyapatite HA and ZnO .

2-The contact angle of the nanocomposite decreased with increased the weight fraction of HA and ZnO, which make the film more hydrophilic and enhanced the water absorption ability of the CS/PEG scaffold, which may be advantageous for bone cell growth on the surface.

3- SEM outcomes found that Nano-HA,ZnO was uniformly distributed throughout the matrix (CS/PEG) and that there was good adhesion among CS/PEG/HA/ZnO.

4- The melting temperature blend CS/ PEG was increased with the addition of different weight fraction of HA and ZnO nanoparticles due to incorporation of Nanoparticles has increased the thermal stability of scaffold.

5- The swelling rate of CS increased when blended with PEG, while adding HA, ZnO nanoparticles decreased the swelling rate.

6- the results of degradation rate show that the addition of PEG as a plasticizer improves the degradation of biofilms due to PEG increase the porosity and hydrophilic of the CS/PEG blend. While the degradation rate decreased with addition the Nano HA and ZnO, which can give suitable time to bone tissue to repair and cell to growth to complete the regeneration process.

7- the tensile strength and elastic of modulus increased with increased the percentage of hydroxyapatite due to the nature of particles of hydroxyapatite that is a ceramic material has a high mechanical properties, tensile strength and elastic modulus increased with increased the percentage of nanoparticles of ZnO .

9- According to AFM results, the roughness decreases as the nanoparticle concentration increases (HA, ZnO wt.%) additionally, kurtosis(S_{ku}) indicated the sharpness of surfaces were increased with the increase the addition nanoparticles, which enhance the adhesion and growth of living cells on the scaffold.

10- In antibacterial test, show the inhibition zone against the E-Coli (Negative gram) and S.aureus (Positive gram). The neat Chitosan exhibited a high inhibition, while The inhibition zone was decreased when adding PEG (blend CS/PEG),

Moreover, the inhibition zone increases due to addition the Hydroxyapatite HA and ZnO nanoparticles which had antibacterial properties.

11-MTT study shows higher cell viability this indicate that the scaffold able to proliferate human osteoblastic MG 63 cells significantly also that the newly developed scaffolds benefit for the osteoblast-like cells growth, attachment and proliferation.

12-gluteraldehyde causes decreasing in mechanical, physical which could be badly effect on the prepared scaffold.

5.2 Recommendations for Further Studies

1- The use of different types and systems of reinforcing materials (particles) such as (TiO₂, graphene oxide, carbon nanotube) at different weight fraction.

2-Preparation of Chitosan Scaffolds by using another technique such as freeze-drying and sol-gel.

3-Using other polymers to blend with chitosan for bone regeneration such as alginate, hydrogels, Polycaprolactone (PCL)

4-Study the effect of crosslinking by using another types of cross linkers such as genipin.

References

References

- [1] Zhang, D., Wu, X., Chen, J., & Lin, K. (2018). The development of collagen based composite scaffolds for bone regeneration. *Bioactive materials*, 3(1), 129-138.
- [2] E. Hernlund, A. Svedbom, M. Ivergård, J. Compston, C. Cooper, J. Stenmark, E. V. McCloskey, B. Jönsson & J.A. Kanis (2013). Osteoporosis in the European union: medical management, epidemiology and economic burden., *Archives of osteoporosis*, 8(1), 1-115.
- [3] Kumar, G., & Narayan, B. (2014). Morbidity at bone graft donor sites. *Classic Papers in Orthopaedics*, 503-505.
- [4] Henkel, J., Woodruff, M. A., Epari, D. R., Steck, R., Glatt, V., Dickinson, I. C., ... & Hutmacher, D. W. (2013). Bone regeneration based on tissue engineering conceptions—a 21st century perspective. *Bone research*, 1(1), 216-248.
- [5] E.J. Sheehy, D.J. Kelly and F.J. O'Brien, (2019) "Biomaterial-based endochondral bone regeneration: a shift from traditional tissue engineering paradigms to developmentally inspired strategies", *Mater Today Bio* ,3, 100009.
- [6] Zadpoor, A. A. (2015). Bone tissue regeneration: the role of scaffold geometry. *Biomaterials science*, 3(2), 231-245.
- [7] Fausto, S., Di Carlo Marco, C. M., Sonia, F., Alessandro, C., and Marwin, G. (2018). The impact of different rheumatic diseases on health-related quality of life: a comparison with a selected sample of healthy individuals using SF-36 questionnaire, EQ-5D and SF-6D utility values. *Acta Bio Medica: Atenei Parmensis*, 89(4), 541.
- [8] Khademhosseini, A., & Langer, R. (2016). A decade of progress in tissue engineering. *Nature protocols*, 11(10), 1775-1781.
- [9] Nan Su, Jing Yang, Yangli Xie, Xiaolan Du, Hangang Chen, Hong Zhou, and Lin Chen (2019). Bone function, dysfunction and its role in diseases including critical illness.
- [10] Paul T. Cowan and Preet Kahai (2022) "Anatomy, Bones", *Stroger Hospital of Cook County*.
- [11] Florencio-Silva, R., Sasso, G. R. D. S., Sasso-Cerri, E., Simões, M. J., & Cerri, P. S. (2015). Biology of bone tissue: structure, function, and factors that influence bone cells. *BioMed research international*.

Reference

- [12] Dinçel & Y. M. (2018). Bone graft types. *Bone Grafting-Recent Advances with Special References to Cranio-Maxillofacial Surgery*, 27-40.
- [13] U. Ranjan Dahiya, S. Mishra and S. Bano (2019). Application of Bone Substitutes and Its Future Prospective in Regenerative Medicine. in: *Biomater. Tissue Reconstr. or Regen.*, IntechOpen.
- [14] Reznikov, N., Shahar, R., & Weiner, S. (2014). Bone hierarchical structure in three dimensions. *Acta biomaterialia*, 10(9), 3815-3826.
- [15] Karpinski R, Jaworski L and Czubacka P (2017). The structural and mechanical properties of bone. *J Technol Exploit Mech Eng*, 3(1): 43e50.
- [16] Heyden RJ. (2019). Bone classification e anatomy and physiology. In: *Anatomy and physiology*, Rex Bookstore, Inc.
- [17] Rho JY, Kuhn-Spearing L and Zioupos P. (1998). Mechanical properties and the hierarchical structure of bone. *Med Eng Phys* 20(2): 92–102.
- [18] Hutmacher, D. W., Schantz, J. T., Lam, C. X. F., Tan, K. C., & Lim, T. C. (2007). State of the art and future directions of scaffold-based bone engineering from a biomaterials perspective. *Journal of tissue engineering and regenerative medicine*, 1(4), 245-260.
- [19] Hart, N. H., Nimphius, S., Rantalainen, T., Ireland, A., Siafarikas, A., & Newton, R. U. (2017). Mechanical basis of bone strength: influence of bone material, bone structure and muscle action. *Journal of musculoskeletal & neuronal interactions*, 17(3), 114.
- [20] Fazzalari, N. L. (2011). Bone fracture and bone fracture repair. *Osteoporosis international*, 22, 2003-2006.
- [21] Kohrt, W. M., Wherry, S. J., Wolfe, P., Sherk, V. D., Wellington, T., Swanson, C. M., and Boxer, R. S. (2018). Maintenance of serum ionized calcium during exercise attenuates parathyroid hormone and bone resorption responses. *Journal of Bone and Mineral Research*, 33(7), 1326-1334.
- [22] Hsieh, J. L., Shen, P. C., Wu, P. T., Jou, I., Wu, C. L., Shiau, A. L., & Chen, S. Y. (2017). Knockdown of toll-like receptor 4 signaling pathways ameliorate bone graft rejection in a mouse model of allograft transplantation. *Scientific reports*, 7(1), 1-9.

Reference

- [23] Jenffer Robinoson,(2020).Osteoprosis Guide:brittle bones, treatments and more.
- [24] Patel, H., Bonde, M., & Srinivasan, G. (2011). Biodegradable polymer scaffold for tissue engineering. *Trends Biomater Artif Organs*, 25(1), 20-29.
- [25] Mathew, A. P., Augustine, R., Kalarikkal, N. A. N. D. A. K. U. M. A. R., & Thomas, S. (2016). Tissue Engineering: Principles, recent trends and the future. *Nanomedicine and Tissue Engineering-State of the art and recent trends. Nanomed Tissue Eng*, 31-82.
- [26] Leijten, J., Seo, J., Yue, K., Trujillo-de Santiago, G., Tamayol, A., Ruiz-Esparza, G. U., & Khademhosseini, A. (2017). Spatially and temporally controlled hydrogels for tissue engineering. *Materials Science and Engineering: R: Reports*, 119, 1-35.
- [27] Place, E. S., George, J. H., Williams, C. K., & Stevens, M. M. (2009). Synthetic polymer scaffolds for tissue engineering. *Chemical society reviews*, 38(4), 1139-1151.
- [28] Franca N. Alaribe, Sello L. Manoto and Shirley C.K.M. Motaung, (2016). Scaffolds from biomaterials: advantages and limitations in bone and tissue engineering.*Biologia*, vol. 71, no. 4, p. 353—366.
- [29] Sengupta, D., & Heilshorn, S. C. (2010). Protein-engineered biomaterials: highly tunable tissue engineering scaffolds. *Tissue Engineering Part B: Reviews*, 16(3), 285-293.
- [30] J. Melke. et al. (2016). Silk fibroin as biomaterial for bone tissue engineering. *Acta Biomater*. 31 1-16.
- [31] Song, E., Kim, S. Y., Chun, T., Byun, H. J. and Lee, Y. M. (2006). Collagen scaffolds derived from a marine source and their biocompatibility. *Biomaterials*, 27(15), 2951-2961.
- [32] Levingstone, T. J., Thompson, E., Matsiko, A., Schepens, A., Gleeson, J. P., and O'Brien, F. J. (2016). Multi-layered collagen-based scaffolds for osteochondral defect repair in rabbits. *Acta biomaterialia*, 32, 149-160.
- [33] Osathanon, T., Linnes, M. L., Rajachar, R. M., Ratner, B. D., Somerman, M. J., & Giachelli, C. M. (2008). Microporous nanofibrous fibrin-based scaffolds for bone tissue engineering. *Biomaterials*, 29(30), 4091-4099.

Reference

- [34] Gamboa-Martínez, T. C., Gómez Ribelles, J. L., and Gallego Ferrer, G. (2011). Fibrin coating on poly (L-lactide) scaffolds for tissue engineering. *Journal of Bioactive and Compatible Polymers*, 26(5), 464-477.
- [35] Turco, G., Marsich, E., Bellomo, F., Semeraro, S., Donati, I., Brun, F., & Paoletti, S. (2009). Alginate/hydroxyapatite biocomposite for bone ingrowth: a trabecular structure with high and isotropic connectivity. *Biomacromolecules*, 10(6), 1575-1583.
- [36] J. Venkatesan, I. Bhatnagar, P. Manivasagan, K.H. Kang and S.K. Kim,(2015). Alginate composites for bone tissue engineering a review., *Int. J. Biol. Macromol*, 72 ,269-281.
- [37] K.M. Sajesh, R. Jayakumar, S.V. Nair and K.P. Chennazhi, (2013). Biocompatible conducting chitosan/polypyrrole–alginate composite scaffold for bone tissue engineering., *Int. J. Biol.Macromol*, 465-471.
- [38] Zhao, N., Wang, X., Qin, L., Zhai, M., Yuan, J., Chen, J., & Li, D. (2016). Effect of hyaluronic acid in bone formation and its applications in dentistry. *Journal of biomedical materials research Part A*, 104(6), 1560-1569.
- [39] M.N. Collins & C. Birkinshaw, (2013). Hyaluronic acid based scaffolds for tissue engineering—A review, *Carbohydr Polym*. 92(2), 1262-1279.
- [40] Varoni, E., Tschon, M., Palazzo, B., Nitti, P., Martini, L., & Rimondini, L. (2012). Agarose gel as biomaterial or scaffold for implantation surgery: characterization, histological and histomorphometric study on soft tissue response. *Connective tissue research*, 53(6), 548-554.
- [41] Dutra, N. L. S., de Brito, T. V., de Aguiar Magalhães, D., Sousa, S. G., Batista, J. A., Pereira, C. M. C., ... & dos Reis Barbosa, A. L. (2021). Sulfated polysaccharide extracted from seaweed *Gracilaria caudata* attenuates acetic acid-induced ulcerative colitis. *Food Hydrocolloids*, 111, 106221.
- [42] U A Stock, J P Vacanti (2001). Tissue engineering: current state and prospects.
- [43] Raghavendra, G. M., Varaprasad, K., & Jayaramudu, T. (2015). Biomaterials: design, development and biomedical applications. In *Nanotechnology applications for tissue engineering* , 63(4), 1279-1303.

Reference

- [44] Motamedian, S. R., Hosseinpour, S., Ahsaie, M. G., & Khojasteh, A. (2015). Smart scaffolds in bone tissue engineering: A systematic review of literature. *World journal of stem cells*, 7(3), 657.
- [45] M. Sai Bhargava Reddy, Deepalekshmi Ponnamma, Rajan Choudhary & Kishor Kumar Sadasivuni (2021). A Comparative Review of Natural and Synthetic Biopolymer Composite Scaffolds.
- [46] Lanza, R., Langer, R., Vacanti, J. P., & Atala, A. (Eds.). (2020). Principles of tissue engineering. Academic press.
- [47] Bittner, S. M., Guo, J. L., Melchiorri, A. & Mikos, A. G (2018). Three-dimensional printing of multilayered tissue engineering scaffolds. *Mater. Today* 21, 861–874.
- [48] Hutmacher, D. W., Schantz, J. T., Lam, C. X. F., Tan, K. C., & Lim, T. C. (2007). State of the art and future directions of scaffold-based bone engineering from a biomaterials perspective. *Journal of tissue engineering and regenerative medicine*, 1(4), 245-260.
- [49] Petite, H., Viateau, V., Bensaid, W., Meunier, A., de Pollak, C., Bourguignon, M., & Guillemain, G. (2000). Tissue-engineered bone regeneration. *Nature biotechnology*, 18(9), 959-963.
- [50] Müller, W. E., Wang, S., Tolba, E., Neufurth, M., Ackermann, M., Muñoz-Espí, R., & Wang, X. (2018). Transformation of amorphous polyphosphate nanoparticles into coacervate complexes: an approach for the encapsulation of mesenchymal stem cells. *Small*, 14(27), 1801170.
- [51] K.S. Ogueri, T. Jafari, J.L. Escobar Ivirico, C.T. Laurencin, (2019). Polymeric Biomaterials for Scaffold-Based Bone Regenerative Engineering. *Regen. Eng. Transl. Med.*, vol. 5, pp. 128–154.
- [52] Stratton, S., Shelke, N.B., Hoshino, K., Rudraiah, S. and Kumbar S.G. (2016). Bioactive Polymeric Scaffolds for Tissue Engineering. *Bioact. Mater.*, 1, 93–108.
- [53] Dhandayuthapani, B., Yoshida, Y., Maekawa, T., & Kumar, D. S. (2011). Polymeric scaffolds in tissue engineering application: a review. *International journal of polymer science*, 2011.

Reference

- [54] Ji, Y., Ghosh, K., Shu, X. Z., Li, B., Sokolov, J. C., Prestwich, G. D., ... & Rafailovich, M. H. (2006). Electrospun three-dimensional hyaluronic acid nanofibrous scaffolds. *Biomaterials*, 27(20), 3782-3792.
- [55] Ionela Andreea Neacsu, Adriana Petruta Serban and Adrian Ionut Nicoara, (2020). Biomimetic Composite Scaffold Based on Naturally Derived Biomaterials. *Polymers*, vol. 12, pp. 1-19.
- [56] Linhardt, A., König, M., Schöfberger, W., Brüggemann, O., Andrianov, A. K., & Teasdale, I. (2016). Biodegradable polyphosphazene based peptide-polymer hybrids. *Polymers*, 8(4), 161.
- [57] Jiang L and Zhang J. Biodegradable & biobased polymers. In: Myer K, editor. *Applied plastics engineering –handbook*. Oxford: William Andrew Publishing; 2011. p. 145–5
- [58] Chen, Y., Zhou, S., & Li, Q. (2011). Microstructure design of biodegradable scaffold and its effect on tissue regeneration. *Biomaterials*, 32(22), 5003-5014.
- [59] Göpferich, A. (1996). Mechanisms of polymer degradation and erosion. *The biomaterials: silver jubilee compendium*, 117-128.
- [60] Liao SS, Cui FZ, Zhang W and Feng QL. (2004). Hierarchically biomimetic bone scaffold materials: nano-HA/collagen/PLA composite. *J Biomed Mater Res B Appl Biomater* 69(2): 158–165
- [61] Zhang Li, Li Yubao, Yang Aiping, Peng Xuelin, Wang Xuejiang & Zhang Xiang (2005). Preparation and in vitro investigation of chitosan/nano-hydroxyapatite composite used as bone substitute materials.
- [62] Hutmacher DW. (2000). Scaffolds in tissue engineering bone and cartilage. *Biomaterials* .21(24): 2529–2543.
- [63] Schantz, J. T., Lim, T. C., Ning, C., Teoh, S. H., Tan, K. C., Wang, S. C., & Hutmacher, D. W. (2006). Cranioplasty after trephination using a novel biodegradable burr hole cover: technical case report. *Neurosurgery*, 58(1), ONS-E176.
- [64] Zhou, Y., Chen, F., Ho, S. T., Woodruff, M. A., Lim, T. M., & Hutmacher, D. W. (2007). Combined marrow stromal cell-sheet techniques and high-strength biodegradable composite scaffolds for engineered functional bone grafts. *Biomaterials*, 28(5), 814-824.

Reference

- [65] G. Bouet, D. Marchat, M. Cruel, L. Malaval and L. Vico, (2015). In vitro threedimensional bone tissue models: from cells to controlled and dynamic environment. *Tissue Eng. B Rev.* 21, 133–156.
- [66] O'brien, F. J. (2011). Biomaterials & scaffolds for tissue engineering. *Materials today*, 14(3), 88-95.
- [67] Roseti, L., Parisi, V., Petretta, M., Cavallo, C., Desando, G., Bartolotti, I., & Grigolo, B. (2017). Scaffolds for bone tissue engineering: state of the art and new perspectives. *Materials Science and Engineering: C*, 78, 1246-1262.
- [69] T. Gong, J. Xie, J. Liao, T. Zhang, S. Lin & Y. Lin, (2015). Nanomaterials and bone regeneration. 3 ,15029.
- [68] F. Matassi, L. Nistri, D. Chicon Paez, M. Innocenti, (2011). New biomaterials for bone regeneration, *Clin . Cases Miner. Bone Metab.* 8, 21–24.
- [70] Amini, A. R., Laurencin, C. T., & Nukavarapu, S. P. (2012). Bone tissue engineering: recent advances and challenges. *Critical Reviews™ in Biomedical Engineering*, 40(5).
- [71] B. Thavornyutikarn, N. Chantarapanich, K. Sitthiseripratip, G.A.Thouas and Q. Chen (2014). Bone tissue engineering scaffolding: computer-aided scaffolding techniques., *Prog. Biomater.* 3, 61–102.
- [72] S. Saravanan, R.S. Leena, N. Selvamurugan, (2016). Chitosan based biocomposite scaffolds for bone tissue engineering. *Int. J. Biol.Macromol.* 93 ,1354-1365
- [73] A.S. Siva and M.N.M. Ansari, (2015). A Review on Bone Scaffold Fabrication Methods., *Int. Res. J. Eng.Technol.* 2(6), 1232-1237.
- [74] Siemann, U. (2005). Solvent cast technology—a versatile tool for thin film production. In *Scattering methods and the properties of polymer materials* (pp. 1-14). Berlin, Heidelberg: Springer Berlin Heidelberg.
- [75] B. Subia, J.Kundu, S. C. Kundu,(2010). Biomaterial scaffold fabrication techniques for potential tissue engineering applications., *Tissue.Eng. InTech.*
- [76] X. Liu, P. X. Ma, (2004). Polymeric scaffolds for bone tissue engineering., *Ann. Biomed. Eng.* 32(3) ,477-486.

Reference

- [77] X. Wang, W. Li, V. Kumar, (2006). A method for solvent-free fabrication of porous polymer using solid-state foaming and ultrasound for tissue engineering applications, *Biomaterials*. 27(9) 1924-1929.
- [78] Sampath, U. G. T., Ching, Y. C., Chuah, C. H., Sabariah, J. J., & Lin, P. C. (2016). Fabrication of porous materials from natural/synthetic biopolymers and their composites. *Materials*, 9(12), 991.
- [79] Kumar, A., Yadav, N., Bhatt, M., Mishra, N. K., Chaudhary, P., & Singh, R. (2015). Sol-gel derived nanomaterials and its applications: a review. *Research Journal of Chemical Sciences*, 2231, 606.
- [80] M. Marcacci, S. Zaffagnini, E. Kon, G.M. Marcheggiani Muccioli, A. Di Martino, B. DiMatteo, T. Bonanzinga, F. Iacono, G. Filardo, (2013). Unicompartmental osteoarthritis: an integrated biomechanical and biological approach as alternative to metal resurfacing, *Knee Surg. Sports Traumatol". Arthrosc.* 21 ,2509–2517.
- [81] C. Lee Ventola, (2014). Medical applications for 3D printing: current and projected use *Pharmacol.. Ther.* 39 ,704–711.
- [82] Castro, N. J., O'brien, J., & Zhang, L. G. (2015). Integrating biologically inspired nanomaterials and table-top stereolithography for 3D printed biomimetic osteochondral scaffolds. *Nanoscale*, 7(33), 14010-14022.
- [83] A. Muxika, A. Etxabide, J. Uranga, P. Guerrero, K. De La Caba, (2017) Chitosan as abioactive polymer: processing, properties and applications, *Int. J. Biol. Macromol.* 105 , 1358–1368.
- [84] A. Baranwal, A. Kumar, A. Priyadharashini, G.S. Oggu, I. Bhatnagar, A. Srivastava, P. Chandra, (2018) Chitosan: an undisputed bio-fabrication material for tissue engineering and bio-sensing applications, *Int. J. Biol. Macromol.* 110, 110–123.
- [85] E. Fakhri, H. Eslami, P. Maroufi, F. Pakdel, S. Taghizadeh, K. Ganbarov, M. Yousefi, A. Tanomand, B. Yousefi, S. Mahmoudi and H.S. Kafil, (2020). Chitosan biomaterials application in dentistry., *Int. J. Biol. Macromol.* 162 ,956–974.
- [86] A. Muxika, A. Etxabide, J. Uranga, P. Guerrero, K. De La Caba, (2017) Chitosan as abioactive polymer: processing, properties and applications", *Int. J. Biol. Macromol.* 105 ,1358–1368.

Reference

- [87] K. Knop, R. Hoogenboom, D. Fischer and U. S. Schubert, (2010). Poly (ethylene glycol) in drug delivery: 730 pros and cons as well as potential alternatives, *Angew. Chem. Int. Ed.* 49 ,6288-6308.
- [88] H. Schellekens, W. E. Hennink, V. Brinks, (2013). The immunogenicity of polyethylene glycol: facts and fiction, *Pharm. Res.* 30 1729-1734.
- [89] Shakeel Ahmed, Saiqa Ikram (2016) Chitosan Based Scaffolds and Their Applications in Wound Healing .
- [90] Catauro, M., Bollino, F., Papale, F., Gallicchio, M., & Pacifico, S. (2015). Influence of the polymer amount on bioactivity and biocompatibility of SiO₂/PEG hybrid materials synthesized by sol-gel technique. *Materials Science and Engineering: C*, 48, 548-555.
- [91] Mohammad, Othman R and Yee-Yeoh F (2014). Nanoporous hydroxyapatite preparation methods for drug delivery applications. *Rev. Adv. Mater. Sci.* 38 138–47
- [92] I. A. R. Kadhim, (2020). Preparation and Properties of Natural Biopolymer for Bone Regeneration., University of Technology.
- [93] Iyyappan E, Wilson P and Sheela Kand Ramya R (2016) “Role of triton X-100 and hydrothermal treatment on the morphological features of nonporous hydroxyapatite nanorods” *Mater. Sci. Eng. C* 63 554–62
- [94] Giulia Molino, Maria Chiara Palmieri, Giorgia Montalbano, Sonia Fiorilli and Chiara Vitale-Brovarone (2020) "Biomimetic and mesoporous nano-hydroxyapatite for bone tissue application: a short review".
- [96] Bala Y , Seeman E (2015) “Bone's material constituents and their contribution to bone strength in health, disease, and treatment *Calcif Tissue*”.
- [97] Shavandi A, Bekhit A E-D A, Sun Z F and Ali A (2015). A review of synthesis methods, properties and use of hydroxyapatite as a substitute of bone. *Biomimetic, Biomater. Biomed. Eng.* 25 98–117
- [98] Khwaja Salahuddin Siddiqi, , Aziz Ur Rahman, Tajuddin Azamal Husen (2018) · Properties of Zinc Oxide Nanoparticles and Their Activity Against Microbes.

Reference

- [99] Maremanda KP, Khan S and Jena G (2014). Zinc protects cyclophosphamide-induced testicular damage in rat: involvement of metallothionein, tesmin and Nrf2” *Biochem Biophys Res Commun* 445:591–596
- [100] Kim, M. H., Seo, J. H., Kim, H. M., & Jeong, H. J. (2014). Zinc oxide nanoparticles, a novel candidate for the treatment of allergic inflammatory diseases. *European journal of pharmacology*, 738, 31-39.
- [101] Shahzadi, L., Chaudhry, A. A., Aleem, A. R., Malik, M. H., Ijaz, K., Akhtar, H., ... & Yar, M. (2018). Development of K-doped ZnO nanoparticles encapsulated crosslinked chitosan based new membranes to stimulate angiogenesis in tissue engineered skin grafts. *International journal of biological macromolecules*, 120, 721-728.
- [102] Singh, A., Singh, N. Á., Afzal, S., Singh, T., & Hussain, I. (2018). Zinc oxide nanoparticles: a review of their biological synthesis, antimicrobial activity, uptake, translocation and biotransformation in plants. *Journal of materials science*, 53(1), 185-201.
- [103] Migneault, I., Dartiguenave, C., Bertrand, M. J., & Waldron, K. C. (2004). Glutaraldehyde: behavior in aqueous solution, reaction with proteins, and application to enzyme crosslinking. *Biotechniques*, 37(5), 790-802.
- [104] He, L. H., Xue, R., Yang, D. B., Liu, Y., and Song, R. (2009). Effects of blending chitosan with PEG on surface morphology, crystallization and thermal properties. *Chinese journal of polymer science*, 27(04), 501-510.
- [105] Shakir, M., Jolly, R., Khan, M. S., Iram, N. E., Sharma, T. K., & Al-Resayes, S.I.(2015).Synthesis and characterization of a nano-hydroxyapatite/chitosan/polyethylene glycol nanocomposite for bone tissue engineering. *Polymers for Advanced Technologies*, 26(1), 41-48.
- [106] Ghorbani, F. M., Kaffashi, B., Shokrollahi, P., Seyedjafari, E., & Ardeshirylajimi, A. (2015). PCL/chitosan/Zn-doped nHA electrospun nanocomposite scaffold promotes adipose derived stem cells adhesion and proliferation. *Carbohydrate polymers*, 118, 133-142.
- [107] Taherkhani, S., & Moztarzadeh, F. (2016). Fabrication of a poly (ϵ -caprolactone)/starch nanocomposite scaffold with a solvent-casting/salt-leaching technique for bone tissue engineering applications. *Journal of Applied Polymer Science*, 133(23).

Reference

- [108] Bhowmick, A., Pramanik, N., Manna, P. J., Mitra, T., Selvaraj, T. K. R., Gnanamani, A., ... & Kundu, P. P. (2015). Development of porous and antimicrobial CTS–PEG–HAP–ZnO nano-composites for bone tissue engineering. *RSC advances*, 5(120), 99385-99393.
- [109] Akakuru OU and Isiuku BO, .Chitosan Hydrogels and their Glutaraldehyde-Crosslinked Counterparts as Potential Drug Release and Tissue Engineering Systems - Synthesis, Characterization, Swelling Kinetics and Mechanism., *Journal of Physical Chemistry & Biophysics*, vol. 7, no. 3, pp. 1-7, 2017.
- [110] Arianita, A., Amalia, B., Pudjiastuti, W., Melanie, S., Fauzia, V., & Imawan, C. (2019, October). Effect of glutaraldehyde to the mechanical properties of chitosan/nanocellulose. In *Journal of Physics: Conference Series* (Vol. 1317, No. 1, p. 012045). IOP Publishing.
- [111] Mutlu, E. C., Ficai, A., Ficai, D., Yildirim, A. B., Yildirim, M., Oktar, F. N., & Demir, A. (2018). Chitosan/poly (ethylene glycol)/hyaluronic acid biocompatible patches obtained by electrospraying. *Biomedical Materials*, 13(5), 055011.
- [112] Masud, R. A., Islam, M. S., Haque, P., Khan, M. N. I., Shahruzzaman, M., Khan, M., ... & Rahman, M. M. (2020). Preparation of novel chitosan/poly (ethylene glycol)/ZnO bionanocomposite for wound healing application: effect of gentamicin loading. *Materialia*, 12, 100785.
- [113] Neacsu, I. A., Serban, A. P., Nicoara, A. I., Trusca, R., Ene, V. L., & Iordache, F. (2020). Biomimetic composite scaffold based on naturally derived biomaterials. *Polymers*, 12(5), 1161.
- [114] S. Malathi, P. Balashanmugam, T. Devasena, S. Narayana Kalkura,(2021).Enhanced antibacterial activity and wound healing by a novel collagen blended ZnO nanoparticles embedded noisome nanocomposites.
- [115] A. C. Dumitru, F. M. Espinosa, R. Garcia, G. Foschi, S. Tortorella, F. Valle, M. Dallavalle, F. Zerbettod and F. Biscarini(2015). In situ nanomechanical characterization of the early stages of swelling and degradation of a biodegradable polymer.
- [116] Standard Test Method for in Vitro Degradation Testing of Hydrolytically Degradable Polymer Resins and Fabricated Forms for Surgical Implants, F1635-04a," Annual Book of ASTM Standard, 2004.

Reference

- [117] "Standard Test Method for Tensile Properties of Thin Plastic, D 882-01," Annual Book of ASTM Standard, 2010.
- [118] Kumbhar, S. G., & Pawar, S. H. (2016). Synthesis and characterization of chitosan-alginate scaffolds for seeding human umbilical cord derived mesenchymal stem cells. *Bio-Medical Materials and Engineering*, 27(6), 561-575.
- [119] Kenechukwu, F. C., Ibezim, E. C., Attama, A. A., Momoh, M. A., Ogbonna, J. D. N., Nnamani, P. O., ... & Uronnachi, E. M. (2013). Preliminary spectroscopic characterization of PEGylated mucin, a novel polymeric drug delivery system. *African Journal of Biotechnology*, 12(47), 6661-6671.
- [120] Zeng, M., Fang, Z., & Xu, C. (2004). Novel method of preparing microporous membrane by selective dissolution of chitosan/polyethylene glycol blend membrane. *Journal of applied polymer science*, 91(5), 2840-2847.
- [121] Avcu, E., Baştan, F. E., Abdullah, H. Z., Rehman, M. A. U., Avcu, Y. Y., & Boccaccini, A. R. (2019). Electrophoretic deposition of chitosan-based composite coatings for biomedical applications: A review. *Progress in Materials Science*, 103, 69-108.
- [122] Cansever Mutlu, E., Birinci Yıldırım, A., Yıldırım, M., Fıcaı, A., Fıcaı, D., Oktar, F. N., ... & Demir, A. (2020). Improvement of antibacterial and biocompatibility properties of electrospray biopolymer films by ZnO and MCM-41. *Polymer Bulletin*, 77, 3657-3675.
- [123] Shahabi, S., Najafi, F., Majdabadi, A., Hooshmand, T., Haghbin Nazarpak, M., Karimi, B., & Fatemi, S. M. (2014). Effect of gamma irradiation on structural and biological properties of a PLGA-PEG-hydroxyapatite composite.
- [124] Patra, P., Mitra, S., Debnath, N., Pramanik, P., & Goswami, A. (2014). Ciprofloxacin conjugated zinc oxide nanoparticle: A camouflage towards multidrug resistant bacteria. *Bulletin of materials science*, 37, 199-206.
- [125] Sura Kamel (2021). Enhancement of Polymeric Nano Composite Performance for Bone Cement Application., Ph. D, Babylon university.
- [126] Ba Linh, N. T., Min, Y. K., & Lee, B. T. (2013). Hybrid hydroxyapatite nanoparticles-loaded PCL/GE blend fibers for bone tissue engineering. *Journal of Biomaterials Science, Polymer Edition*, 24(5), 520-538.

Reference

- [127] M. Mahmud, R. Daik and Z. Adam, (2018). Influence of poly (ethylene glycol) on the characteristics of γ radiation-crosslinked poly (vinyl pyrrolidone)-low molecular weight chitosan network hydrogels. *Sains Malays.* 47 (6) 1189–1197.
- [128] Zhang Yanzhong, Hongwei O, Chwee TL, Seeram R, Zheng-Ming H. (2005). Electrospinning of gelatin fibers and gelatin/PCL composite fibrous scaffolds. *Journal of Biomedical Materials Research*;72B:156–65.
- [129] Venugopal, J. R., Low, S., Choon, A. T., Kumar, A. B., & Ramakrishna, S. (2008). Nanobioengineered electrospun composite nanofibers and osteoblasts for bone regeneration. *Artificial organs*, 32(5), 388-397.
- [130] P. T. S. Kumar, S. Srinivasan, V. K. Lakshmanan, H. Tamura, S. V. Nair, R. Jayakumar,(2011).Synthesis, characterization and cytocompatibility studies of α -chitin hydrogel/nano hydroxyapatite composite scaffolds., *Int. J. Biol. Macromol.* , 49, 20.
- [131] Nele-Johanna Hempe, Tra Dao,Matthias M. Knopp, Ragna Berthelsen and Korbinian Löbmann,(2020) .The Influence of Temperature and Viscosity of Polyethylene Glycol on the Rate of Microwave-Induced In Situ Amorphization of Celecoxib.
- [132] Zhang, X., Zhang, Z., Wu, W., Yang, J., & Yang, Q. (2021). Preparation and characterization of chitosan/Nano-ZnO composite film with antimicrobial activity. *Bioprocess and Biosystems Engineering*, 44, 1193-1199.
- [133] Peng, Z., Kong, L. X., and Li, S. D. (2005). Non-isothermal crystallisation kinetics of self-assembled polyvinylalcohol/silica nano-composite. *Polymer*, 46(6), 1949-1955.
- [134] Masar najim (2020). Characterization of Biomaterials and StructuralAnalysis of aKnee Joint Replacement Applications Ph. D, Babylon university.
- [135] Asra Ali Hussein “fabrication and characterization of advanced blend polymer nanocomposite for human bone structural application”, Ph.D., Babylon university ,2017
- [137] Sura Kamel Jebur(2021)” Comparing Study for PEDOT: PSS/Graphene and PEDOT: PSS/Graphene with Isopropyl Alcohol Nanocomposite Thin Films by Spin Coating Technique”, M.sc, Babylon university.

Reference

- [138] Peter, M., Binulal, N. S., Nair, S. V., Selvamurugan, N., Tamura, H., & Jayakumar, R. (2010). Novel biodegradable chitosan–gelatin/nano-bioactive glass ceramic composite scaffolds for alveolar bone tissue engineering. *Chemical engineering journal*, 158(2), 353-361.
- [139] Kammoun, M., Haddar, M., Kallel, T. K., Dammak, M., & Sayari, A. (2013). Biological properties and biodegradation studies of chitosan biofilms plasticized with PEG and glycerol. *International journal of biological macromolecules*, 62, 433-438.
- [140] Thura Abd (2020). Preparation a Biopolymer Blends for Wound Healing., Msc,babylone university.
- [141] Qahtan Adnan Hamad, (2015). Fabrication and Characterization of Denture Base Material by Hybrid Composites from Self Cured PMMA Resin, PhD Thesis University of Technology, Materials Engineering Department, 89.
- [142] Ehterami, A., Kazemi, M., Nazari, B., Saraeian, P., & Azami, M. (2018). Fabrication and characterization of highly porous barium titanate based scaffold coated by Gel/HA nanocomposite with high piezoelectric coefficient for bone tissue engineering applications. *Journal of the mechanical behavior of biomedical materials*, 79, 195-202.
- [143] Gamboa-Solana, C. D. C., Chuc-Gamboa, M. G., Aguilar-Pérez, F. J., Cauich-Rodríguez, J. V., Vargas-Coronado, R. F., Aguilar-Pérez, D. A., ... & Pacheco, N. (2021). Zinc oxide and copper chitosan composite films with antimicrobial activity. *Polymers*, 13(22), 3861.
- [144] Asto ES, Darjito D, Khunur MM. (2019) Effect of pH and Contact Time on Adsorption of Cu²⁺ Metal Ions Using Glutaraldehyde Cross-Linked Chitin”. *J Ilmu Kim Univ IOP Conf. Series: Journal of Physics: Conf. Series* 1317.
- [145] Khan, A., Khan, R. A., Salmieri, S., Le Tien, C., Riedl, B., Bouchard, J., ... & Lacroix, M. (2012). Mechanical and barrier properties of nanocrystalline cellulose reinforced chitosan based nanocomposite films. *Carbohydrate polymers*, 90(4), 1601-1608.
- [146] Arianita, A., Amalia, B., Pudjiastuti, W., Melanie, S., Fauzia, V.,and Imawan, C. (2019).Effect of glutaraldehyde to the mechanical properties of chitosan/nanocellulose. In *Journal of Physics: (Vol. 1317, No. 1, p. 012045)*.

Reference

[147] Sivaselvi, K., & Ghosh, P. (2017). Characterization of modified Chitosan thin film. *Materials Today: Proceedings*, 4(2), 442-451.

الخلاصة:

تؤثر عيوب أنسجة العظام على ملايين الأشخاص في جميع أنحاء العالم. تعتمد إصلاحات عيوب العظام على دمج أو استبدال التطعيم العظمي. العلاجات الحالية لعيوب العظام غير كافية وتفتقر إلى التكنولوجيا الموثوقة كما ان الطرق علاجية التقليدية والشائعة مثل تطعيم عظمي (allogeneic bone grafting) لم يحقق التأثير العلاجي المثالي. مما دفع الباحثين إلى استكشاف طرق جديدة لتجديد العظام للتغلب على الأمراض السريرية المختلفة مثل التهابات العظام وأورام العظام وفقدان العظام بسبب الصدمات (trauma). وفي العقود الأخيرة، طورت هندسة أنسجة العظام (BTE) وكانت رائدة في هذا المجال وتم تسلط الضوء على تصميم سقالات (BTE) وفقاً لبيولوجيا العظام وتوفر الأساس المنطقي لتصميم الجيل التالي من سقالات BTE التي تتوافق مع التئام العظام الطبيعي وتجديدها. لذلك تم تكريس الباحثين في مجال هندسة أنسجة العظام، وتركز الاهتمام على تطوير المواد المركبة للتطبيقات الطبية الحيوية لمعالجة مشاكل العظام. وعلى الرغم من استخدام مركبات البوليمر الصناعية والطبيعية، إلا أنه قد حلت البوليمرات الطبيعية محل البوليمرات الصناعية بسبب التوافق الحيوي المحسن والطبيعة الغير سامة لمنتجاتها القابلة للتحلل. وبذلك يتم استخدام سقالة بوليمرية قابلة للتحلل لتعزيز نمو الأنسجة وإعادة تشكيلها مع تشكل العظم الجديد، وسوف تتحلل الدعامة المؤقتة ويمتصها الجسم.

في الدراسة الحالية، تم تحسين الخواص البيولوجية والمورفولوجية والميكانيكية للشيتوزان (CS) المقوى ب هيدروكسي اباتيت (HA) وأكسيد الزنك (ZnO)، وتم تحقيق ذلك في ثلاث خطوات ، اذ تضمنت الخطوة الأولى: خلط البوليمر الطبيعي (الشيتوزان) مع بوليمر صناعي (بولي إيثيلين جلايكول) (PEG) كمادة ملدنة بنسب مختلفة (CS: PEG)، (70:30 ، 80:20,90:10)٪ على التوالي والتي تم تحضيرها بطريقة الصب . وبناءً على مرونة العينة، تم اختيار مزيج (70:30) ٪ وتقويته بثلاثة نسب وزنية مختلفة من جزيئات هيدروكسي اباتيت النانوية HA (1,2,3 %w.t) ، تم تقييم هذه المادة المركبة النانوية باستخدام فحص (FTIR)، و (DSC)، الفحص المجهر الإلكتروني و (FE- SEM)المجهر الإلكتروني لمسح الانبعاث الميداني ، الفحص المجهرى للقوة الذرية (AFM)، اختبارات الترطيب والانتفاخ والتحلل. ووجد أن نسبة (3%) من HA كانت الأفضل بسبب خواصها العالية من الخصائص الميكانيكية والفيزيائية والبيولوجية. اما الخطوة الثانية تضمنت اضافة ثلاثة نسب مختلفة من أكسيد الزنك النانوي (0.3,0.5,0.7 %ZnO) إلى المادة المركبة النانوية (nanocomposite) (70%CS/30%PEG/3%HA) لتحضير مادة مركبة نانوية هجينة (Hybrid nanocomposite)، و تم اجراء فحوصات المورفولوجية، والميكانيكية، وقابلية البلل، والانتفاخ، والتحلل، والنشاط المضاد للبكتيريا، والسمية الخلوية.

اذ أشارت نتائج FTIR لفيلم المادة المركبة نانوية إلى تداخلات جيدة وتكون رابطة هيدروجينية بين البوليمرين وأيضًا مع الجسيمات النانوية من HA و ZnO، وأظهر نتائج عينة FE-SEM ل (CS / PEG / HA) و (CS / PEG / HA / ZnO) الى مزيجًا جيدًا من CS و PEG مع تشتت جيد لجسيمات النانوية (HA,ZnO%) داخل Matrix. كما كشفت نتائج اختبار قابلية التبلل عن إضافة PEG والجسيمات النانوية من HA و ZnO إلى CS زيادة قابلية التبلل ل CS اذ انخفضت زاوية التلامس من 94° درجة CS النقي إلى 38° درجة عند (CS/PEG/3%HA) و 26° ل (CS/PEG/3%HA/0.5%ZnO) مما جعلت طبيعة سطح المركب النانوي الهجين أكثر حبا للماء مما يدعم التوافق الحيوي ونمو الخلايا الحية عليه.

بناءً على نتائج دراسات الانتفاخ، تمت زيادة نسبة الانتفاخ لمزيج CS / PEG في وسط الزرعة (محلول PBS)، مما يسمح للمواد الغذائية بالتدفق بسهولة أكبر من خلاله بينما انخفض معدل الانتفاخ للمركبات النانوية بشكل طفيف مع زيادة نسبة HA %. وأيضًا ينخفض الانتفاخ للمركب النانوي الهجين قليلاً ويبلغ معدل التناقص (3) % مع إضافة 0.5% من ZnO ويعود لدخول الجسيمات النانوية بين سلاسل البوليمر وتحتل المزيد من المساحات. علاوة على ذلك، زاد معدل التحلل السقالات (الدعامات) المركبة مع إضافة PEG، ومع ذلك، فقد انخفض بشكل طفيف مع إضافة الجسيمات النانوية (HA ZnO %) بسبب وجود الجسيمات النانوية التي عززت ثبات السقالات (Scaffold) ولكنها تظل قيمة التحلل بمقدار مقبول.

كما أظهرت نتائج AFM زيادة خشونة سطح CS بإضافة 30% PEG، لكن خشونة السطح انخفضت مع زيادة نسبة الجسيمات النانوية (HA,ZnO) لكنها لا تزال سطوح حادة تم الكشف عنها من قيمة (S_{ku}) أعلى من (3)، مما عزز التصاق الخلايا الحية. وايضا مع متغير آخر للخشونة وهو مؤشر تحمل السطح (S_{bi}) وهو دالة للخصائص الميكانيكية وتزداد قيمته مع مزيج CS و PEG وتقويتها بالجسيمات النانوية (HA,ZnO) %w.t وهذه النتائج ل (S_{bi}) التي دعمت نتائج اختبار الشد الذي أشار الى تحسين الخواص الميكانيكية لCS

ازدادت الخواص الميكانيكية (مقاومة الشد ومعامل المرونة) بزيادة نسبة (HA و ZnO %)، اذ ازدادت مقاومة الشد بنسبة 84%، وزادت مرونة المعامل بنسبة 62% مع إضافة جزيئات نانوية بنسبة 0.5% من ZnO والتي تدعم تجديد (ترميم) العيب العظمي. علاوة على ذلك، من الاختبار المضاد للبكتيريا تبين ان هناك خصائص مضادة للبكتيريا للمركب النانوي الهجين والتي تم تعزيزها بزيادة النسبة الوزنية من HA و ZnO , كما اشار اختبار MTT إلى أن السقالة (الدعامة) تعزز القابلية الحيوية لخلايا (HdFn, MG-63) والانتشار

في السقالات وبالتالي، يمكن أن يعمل هذا المركب النانوي الهجين كمرشح لاستخدامه في هندسة أنسجة العظام.

كانت الخطوة الثالثة هي إضافة الجلترالدهايد (GA) بنسبة (0.02%) باعتباره مادة مشبكة (Crosslinker) لأفضل نسبة من مزيج البوليمر (70%CS/30%PEG)، مركب نانوي مقوى بـ (70%CS/30%PEG/3%HA)، ومركب نانوي هجين (CS/PEG/3%HA/ZnO) لمعرفة تأثير Crosslinker على خصائص المركبات النانوية المحضرة.

اذ أظهرت النتائج ان المزيج البوليمري المتشابك مع GA له قابلية تبلل عالية مقارنةً بالمركب النانوي والمركب النانوي الهجين المتشابك مما يدل على زيادة زاوية التلامس بسبب استخدام GA كمشبك crosslinker. علاوة على ذلك، اذ تقل مقاومة الشد ومعامل المرونة والاستطالة مع إضافة GA مقارنة بالأفلام uncrosslinker بسبب الروابط المكونة تكون أكثر إحكاما مع إضافة الجلترالدهايد مما يؤدي إلى تقليل الخواص الميكانيكية.



جمهورية العراق

وزارة التعليم العالي والبحث العلمي

جامعة بابل

كلية هندسة المواد

قسم هندسة المواد البوليمرات والصناعات البتروكيمياوية

مواد متراكبة بوليمرية نانوية مطوره لتطبيقات اصلاح الانسجة العظمية

رسالة

مقدمة الى كلية هندسة المواد / جامعة بابل وهي جزء من متطلبات نيل

درجة الماجستير في هندسة المواد / البوليمر

من قبل الباحثة:

زهراء كريم ماشي هادي

(بكالوريوس في هندسة المواد, 2019)

بإشراف:

أ.د. مسار نجم عبيد